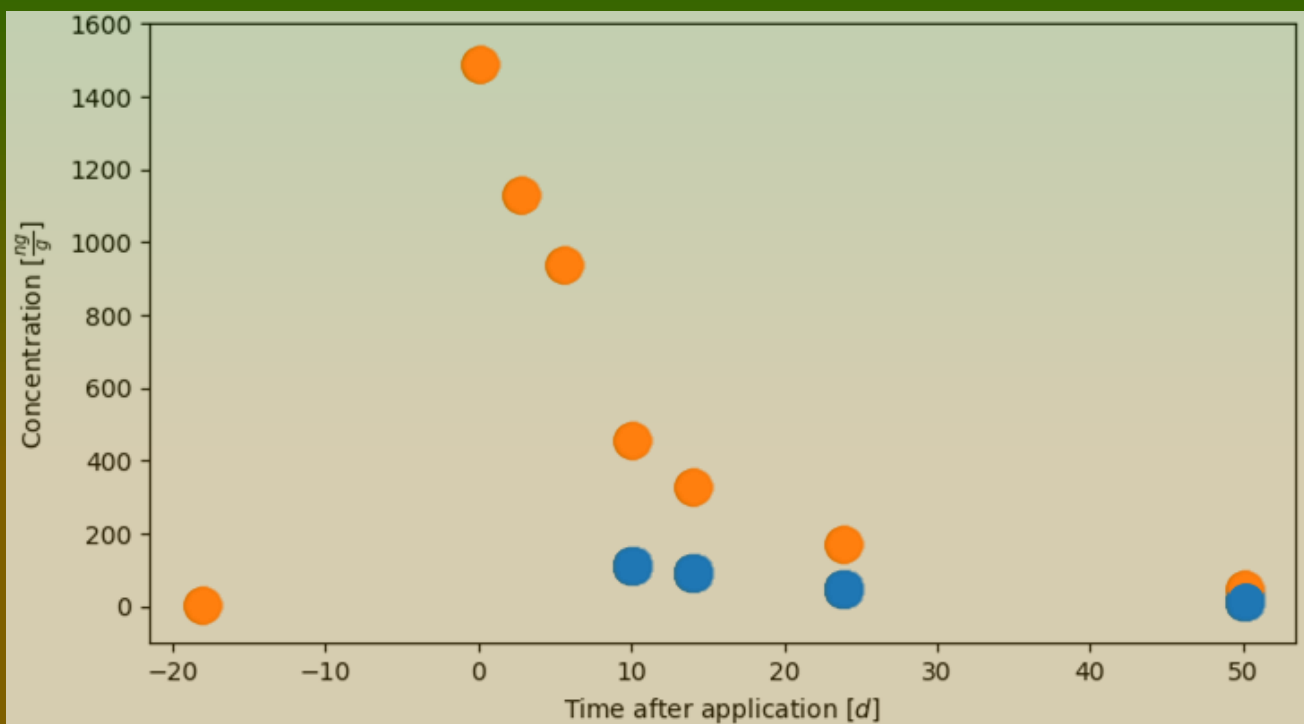


Concentration decline of S-metolachlor

The environmental fate of the active substance of a herbicide in a cornfield



author: Janine Roshardt

matura project 2020/2021

supervisor: Urs Leisinger, chemistry

Kantonsschule Zug

Table of contents

Foreword	4
1 Abstract	5
2 Introduction	6
3 S-metolachlor	7
3.1 Structure and characteristics	7
3.1.1 S-metolachlor	7
3.1.2 Metabolites	9
3.2 Phytotoxicity	10
4 Concentration decline	11
4.1 Transportation	11
4.2 Degradation	13
5 Materials and methods	15
5.1 Application of S-metolachlor	15
5.2 Method of soil sampling	15
5.2.1 Challenges	15
5.2.2 Method	16
5.2.3 Tools for soil sampling	17
5.3 Analysis method	19
5.3.1 Sample selection	19
5.3.2 Overview of the analytical procedure	21
5.3.3 Drying	26
5.3.4 Sieving and grinding	27
5.3.5 Extracting analytes	28
5.3.6 Scaling of the concentration	34
5.3.7 High-performance liquid chromatography-tandem mass spectrometry	38
5.4 Humax samples	42
5.5 Organic carbon content, soil type, grain size distribution, and pH	42
6 Model of the concentration course	44
6.1 Water movement model	44
6.1.1 First water movement model	45
6.1.2 Second water movement model	45
6.1.3 Final water movement model	46
6.2 Transport and degradation of S-metolachlor	48
6.2.1 Degradation	49
6.2.2 Transportation	49

6.2.3	Equilibrium.....	49
6.3	Metabolites	51
6.3.1	Formation	52
6.4	Comparison with the field measurements	52
6.4.1	Starting concentration of the model	53
6.4.2	Comparison with the field measurement.....	53
6.5	Variables.....	54
7	Results of the field measurements.....	56
7.1	Bulk density and soil characteristics	56
7.2	Results S-metolachlor.....	58
7.2.1	Concentrations of S-metolachlor.....	58
7.2.2	Half-life of S-metolachlor	59
7.3	Results metolachlor oxanilic acid (OA)	60
7.4	Results metolachlor ethane sulfonic acid (ESA)	61
7.5	Results of the control samples.....	62
7.5.1	Limit of quantification	62
7.5.2	Relative recovery.....	64
7.5.3	Method precision.....	64
7.5.4	Blank sample in the HPLC-MS/MS and blind sample in the HPLC-MS/MS.....	65
8	Discussion of the field measurement	66
8.1	Discussion of S-metolachlor	66
8.1.1	Precision and accuracy of the analysis	66
8.1.2	Limitations of the field measurement.....	67
8.1.3	Background concentration.....	67
8.1.4	Application rate	67
8.1.5	Kinetics	69
8.1.6	Impact of degradation and leaching	72
8.1.7	Adsorption.....	73
8.1.8	Environmental factors	75
8.1.9	Second layer	80
8.2	Discussion of the metabolites.....	82
9	Results of the model calculations.....	86
9.1	Parameters	86
9.2	Results	88
10	Discussion of the model calculations.....	93
10.1	Comparison of the model with the field measurement.....	93

10.1.1	S-metolachlor	93
10.1.2	Metabolites	94
10.2	Comparison of the water movement model with literature	95
10.3	Comparison of the concentration course model with literature.....	96
10.4	Conclusion.....	97
11	List of abbreviations and glossary.....	98
12	Table of figures	99
13	Bibliography.....	103

Foreword

I have written this paper as my matura project in the timespan between March 2020 and January 2021.

Soil is a limited resource of economic and ecological importance, which is often neglected. Alongside air and water, soil plays a fundamental role in the sustention of life on earth. Excessive use of chemicals can have a deleterious effect on soils. The idea for this research initially stemmed from my interest in residues of pollutants in the environment and their degradation processes. What is more, I have always wondered how it is possible to detect and measure low concentrations of a substance in soils.

In truth, I could not have achieved my goals without a strong support group. First of all, I would like to thank my parents, who have supported me with encouragement. Secondly, I would like to thank Paul and Susanne Marty, who generously and obligingly offered their field for my investigation. Special thanks are due to NABO and Agroscope, especially Dr. Thomas Bucheli, who made the collaboration with Agroscope possible. I want to thank Peter Schwab for the soil sampling tools he provided and for his patient explanations. Moreover, let me express a special thanks to Andrea Rösch, who explained the analysis method to me and guided me through the whole analytical procedure. I would like to thank Margrit Oetiker and Richard Schicker for their explanations and support. Finally, special thanks go to Dr. Urs Leisinger for his guidance during the whole matura project, his constructive criticism, his optimism, and his explanations.

Thank you all for your unwavering support.

1 Abstract

S-metolachlor (SMOC) is a widely used active substance of herbicides that are applied to corn-fields. This study aimed to measure the concentration decline of SMOC and two of its metabolites, metolachlor oxanilic acid (OA) and metolachlor ethane sulfonic acid (ESA), and to identify and possibly quantify the major factors determining their course of concentration. The pollutants were measured in a cornfield in Arth near the lake of Zug for two months. A model describing leaching and degradation was developed, and its results were compared with the ones of the field measurement.

The plant protection product “Calado”, which contains SMOC, was applied on 28 May 2020. Soil samples were taken from two layers of the soil (0-5 cm and 5-17 cm) prior to the application and thereafter for two months until 17 August 2020. The samples were analysed using an accelerated solvent extraction device (ASE) and a high-performance liquid chromatography-tandem mass spectrometry device (HPLC-MS/MS).

The concentration decline of SMOC in the field followed an exponential decline. Previous studies have reported that soil microorganisms are the driving force behind the concentration decline of SMOC [1].

The estimated half-life (degradation time DT50) of SMOC increased steadily over time except after the first rainfall. The increasing DT50 was probably caused by increasingly strong adsorption of SMOC molecules to the soil particles. Contrary to the expectations, there was a positive correlation between the temperature and the DT50 of SMOC. Moreover, there was a negative correlation between the rainfall volume and the DT50 of SMOC in the analysed samples, and the DT50 reached its minimum value after the first rainfall.

The accumulation of the metabolites OA and ESA in the soil was delayed, which might be because the soil microbiome had to adapt to degrade SMOC. Furthermore, the concentrations of the metabolites increased in the beginning and decreased at the end of the period under study. Their mass was higher in the second layer than in the first one while the opposite was true for the parent compound SMOC. Therefore, they were found to be more mobile than SMOC.

A finite element model was developed to identify and quantify the factors that are crucial for the fate of SMOC in the investigated soil. The key idea of the model was to divide the time into short time steps and the soil into thin slices. An exponential function approached the degradation in the model. The leaching of the pollutants was modelled based on the assumption that the compounds reached an adsorption equilibrium in every soil slice. The soil water carried the dissolved substances along. The water movement was simplified by the assumption that the outflow of a slice was proportional to the actual water content of the slice.

2 Introduction

The world population is growing and the need for food is more urgent than ever. The food industry is under tremendous pressure as its products are required in enormous quantities and they have to meet high quality standards. There is demand for food that is cheap, safe, which means free of toxic substances, and ecologically friendly. Not only humans need nutrition, but cattle and animals do so as well. In order to deliver the vast quantities required, conventional farms use fertilizer and plant protection products (PPPs). PPPs are expensive but they ensure a higher crop yield.

On the other hand, some PPPs contain active substances that can accumulate in the environment because of their high persistency and, therefore, they pollute the soil. Moreover, leaching and run-off of these active substances can lead to contamination of the ground- and surface water. From there, the active substances can easily enter the food chain and can cause harm to many species. Due to their toxicity on living beings the contamination of the environment is monitored regularly.

PPPs are generally divided into three groups based on the organism group they primarily affect:

- fungicide (against fungi)
- herbicide (against weeds)
- insecticide (against insects)

Pesticides are, for instance, applied in livestock farming and forestry. Pesticides are used to control pests and diseases in general, whereas PPPs protect the health of crops. Therefore, PPPs are a subgroup of pesticides [2].

One of the three most frequently used herbicides among the chemical group of chloroacetamides is S-metolachlor (SMOC). The chloroacetamides account for 4.2% of the pesticides that are applied globally [1]. SMOC is often considered to be an environmentally friendlier active substance in PPPs since it is classified as moderately to non-persistent and moderately mobile. However, as its metabolites are very mobile and persistent, they are often detected in ground- and surface water [3], [4].

This study aimed to measure the concentration decline of SMOC and its metabolites, metolachlor oxanilic acid (OA) and metolachlor ethane sulfonic acid (ESA), and to identify and possibly quantify the major factors determining their course of concentration. The pollutants were measured in a cornfield in Arth near the lake of Zug for two months. The obtained results were compared to literature data. Moreover, the impact of weather conditions on the course of the concentration curve was investigated. Finally, a model describing leaching and degradation of SMOC and its metabolites was developed based on the obtained results and literature. The results of the model were compared to the findings of the field measurement.

3 S-metolachlor

This chapter provides an overview of the characteristics and the environmental fate of S-metolachlor (SMOC) and two of its metabolites. Finally, the phytotoxicity of SMOC will be explained.

3.1 Structure and characteristics

This chapter focuses on the structure and properties of SMOC and its metabolites metolachlor ethane sulfonic acid (ESA) and metolachlor oxanilic acid (OA).

3.1.1 S-metolachlor

3.1.1.1 Structure

Metolachlor is a member of the chloroacetamide group of herbicides or, more precisely, of the chloroacetanilides.

Metolachlor has an asymmetric, stereogenic C-atom and, therefore, exists in two different enantiomers, S-metolachlor and R-metolachlor (1'S and 1'R). Additionally, the rotation of the aryl-C to N-bond is hindered by bulky groups, leading to an axial chirality, so that two atropisomers of every enantiomer exist (α S and α R).

Therefore, metolachlor has four stereoisomers (figure 1, figure 2, figure 3, and figure 4):

- S-metolachlor (SMOC)
 - (α S, 1'S)-metolachlor
 - (α R, 1'S)-metolachlor
- R-metolachlor
 - (α R, 1'R)-metolachlor
 - (α S, 1'R)-metolachlor

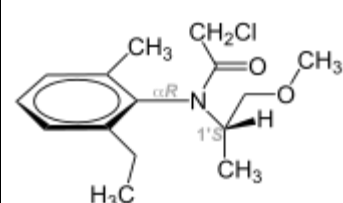
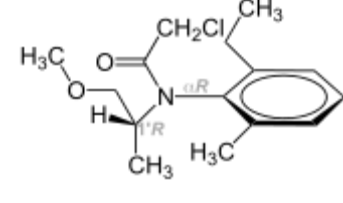
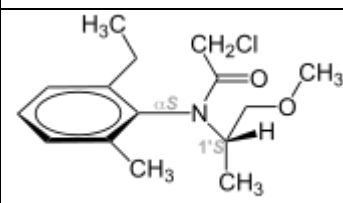
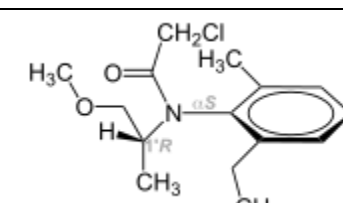
S-metolachlor	R-metolachlor
 <p>Figure 1: (αR, 1'S)-metolachlor [5]</p>	 <p>Figure 2: (αR, 1'R)-metolachlor [5]</p>
 <p>Figure 3: (αS, 1'S)-metolachlor [5]</p>	 <p>Figure 4: (αS, 1'R)-metolachlor [5]</p>

Table 1: Four stereoisomers of metolachlor

SMOC is believed to be the more active enantiomer than R-metolachlor in terms of eradicating weeds [6], [7]. Both atropisomers of SMOC show the same biological activity. Companies aim

to produce as pure SMOC as possible since this could limit the pollution of the environment because less metolachlor needs to be applied if the percentage of the enantiomer SMOC in the PPP is higher. However, the separation and the analysis pose a considerable challenge, which is why PPPs usually contain a mixture of 80% SMOC and 20% R-metolachlor [8], [6].

3.1.1.2 Environmental fate

The physical and chemical properties affect the environmental fate of SMOC. The soil adsorption coefficient (K_d) and the half-life time (degradation time DT50) are essential to assess the persistence and mobility of the substance in the soil.

K_{oc} is the soil adsorption coefficient depending on the organic carbon content (OC content) [9].

$$K_{oc} = \frac{c_{\text{absorbed to soil}} \left[\frac{\text{ng}}{\text{g}} \right]}{c_{\text{dissolved in soil water}} \left[\frac{\text{ng}}{\text{mL}} \right]} \cdot \frac{100}{OC[\%]} = K_d \cdot \frac{100}{OC[\%]}$$

DT50, usually expressed in days, is the half-life of substances in PPPs such as SMOC. This means that during each time step of DT50, 50% of the initial concentration is degraded. However, for simplicity reasons, the term DT50 used in the current study includes not only degradation but also transportation.

Literature values for K_{oc} and the DT50 for SMOC are shown below. The data were obtained from [8], [10], and [11].

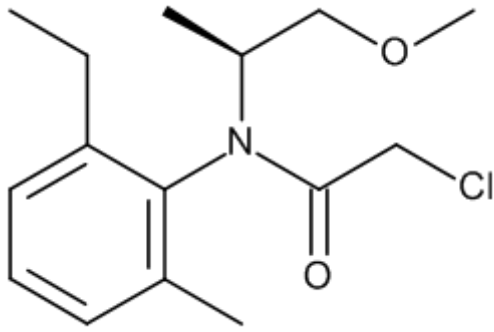
	S-metolachlor	classification
structure	 <p>Figure 5: Structure of S-metolachlor [11]</p>	Chloroacetanilide
molecular mass [g/mol]	283.79	
K_{oc} [mL/g]	288.4 (Hazardous substance data bank: 22 to 2320)	Moderately mobile
DT50 laboratory [d]	51.8 (EFSA 2018 dossier: 10.3-221 d, EU 2003 dossier lab studies DT50 range : 7.6-37.6 d)	Moderately persistent
DT50 field [d]	23.17 (EFSA 2018 dossier DT50 range: 3.55-55.7 d, EU 2003 dossier lab studies DT50 range 7.6-37.6 d)	Non-persistent

Table 2: Characteristics and environmental fate of SMOC

3.1.2 Metabolites

SMOC has more than 25 metabolites. In this field study, only metolachlor ethane sulfonic acid (ESA) and metolachlor oxanilic acid (OA) were analysed because SMOC is transformed most frequently into these two metabolites in soil [8]. The following data concerning mobility and degradation of the metabolites were taken from [8].

The estimated occurrence fraction is the fraction of SMOC that is transformed into the specific metabolite.

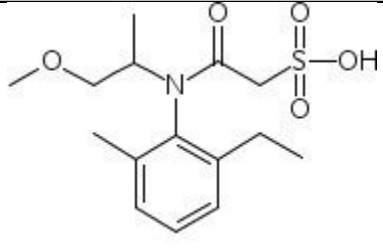
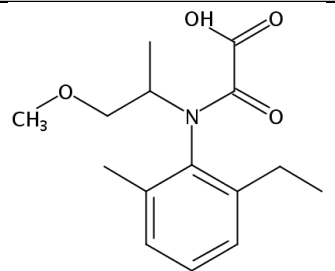
	ESA	OA	classification
structure	 <p>Figure 6: Structure of ESA [12]</p>	 <p>Figure 7: Structure of OA [13]</p>	
molecular mass [g/mol]	329.41	279.332	
K_{oc} [mL/g]	9 (EU dossier K _{oc} ranges : 3 – 22 mL/g)	17	Mobile (OA) to very mobile (ESA)
DT50 laboratory [d]	235 (EU 2018 dossier DT50 ranges : 27.2 – 1000 d)	325 (EFSA 2018 dossier: 12.2 – 1000 d)	persistent
estimated occurrence fraction	$0.213 \frac{[mol]}{[mol]} \triangleq 0.247 \frac{[g]}{[g]}$	$0.211 \frac{[mol]}{[mol]} \triangleq 0.208 \frac{[g]}{[g]}$	

Table 3: Characteristics and environmental fate of ESA and OA

These two metabolites of SMOC are more polar than SMOC. Therefore, they are more water-soluble and, thus, more mobile in the soil. In addition, both metabolites persist much longer than their parent molecule, which results in a regular detection of OA and ESA in groundwater [1], [3].

3.2 Phytotoxicity

The phytotoxicity of SMOC is not fully understood but SMOC is known to impede a lot of plant growth functions such as germination, shoot development, cell division, and biosynthesis of lipids and proteins [14]. Growing weeds absorb the herbicide mainly through the shoot system and partially through the roots [15]. S-metolachlor suppresses the growth of the weeds, especially during germination and early life stages (less than one week after germination) [16], [17]. Therefore, SMOC should be applied before weeds cover the whole field. A hypothesis on the phytotoxicity of SMOC predicts that the biosynthesis of very-long-chain fatty acids is inhibited. Other sources claim that SMOC obstructs the incorporation of uridine into the RNA [18]. The former hypothesis is presented in this chapter since it is most frequently mentioned in literature.

SMOC inhibits the production of very-long-chain fatty acids (>20 C-atoms) [19]. The synthesis of fatty acids with more than 26 C-atoms is impeded significantly. The cell membrane and the cuticular wax consist of such fatty acids. The cuticular wax is essential for protection from evaporation, for permeability, for pathogen defence, and for protection from radiation. Long-chain fatty acids play an essential role in cell division. If there are not enough fatty acids of the required length (here: very-long-chain), the cell cannot divide, or it divides but the membrane or the cuticular wax cannot function due to the wrong composition of fatty acids. Therefore, SMOC impedes the cell division.

Scientists have not indubitably identified the target molecule of SMOC. However, enzymes that metabolise acetyl-CoA are commonly believed to be the target molecule of SMOC since this cofactor is responsible for many functions in the plants such as the synthesis of fatty acids or the synthesis of the growth hormone gibberellin [15].

The molecule glutathione can react with SMOC and thereby detoxify SMOC. Only reduced glutathione can bind to SMOC. The reaction is catalysed by glutathione-S-transferase, an enzyme that generally catalyses the binding of glutathione to electrophilic hydrophobic substrates. An increased resistance towards SMOC may therefore occur due to the following reasons [15]:

- The plant has a membrane that consists of fewer very-long-chain fatty acids.
- The plant produces more glutathione.
- The plant has a greater capability to maintain the glutathione in a reduced state.
- There is a higher level of glutathione-S-transferase in the plant.
- The glutathione-S-transferase of the plant is more specific for the herbicide.

Even though corn plants produce long-chain-fatty acids of 32 C, corn has a remarkably high tolerance, which is probably due to the high level of glutathione-S-transferase in corn [19].

4 Concentration decline

SMOC does not only harm plants but also soil and water organisms. Therefore, its persistence in the soil and its leaching potential are determining factors in the environmental risk assessment of SMOC. The concentration of SMOC in a cornfield decreases mainly due to two processes.

- transportation
- degradation

These processes are described in the following chapters.

4.1 Transportation

The transportation of pesticides due to run-off, leaching, and volatilisation determines their concentration decline. SMOC is considered moderately mobile, and transportation is generally not the main factor responsible for the concentration decline of SMOC [8].

Volatilisation, i.e. transportation into the atmosphere, is negligible for SMOC because SMOC has a small Henry's law constant, the equilibrium ratio of gaseous and aqueous SMOC ($2.2 \cdot 10^{-3} \frac{\text{Pa} \cdot \text{m}^3}{\text{mol}}$) [20].

The amount of SMOC that leaches into deeper layers or runs off strongly depends on time, the parameters of the field, and environmental factors as listed below.

- **Adsorption:** If adsorption increases, leaching decreases because less SMOC is dissolved in water. The strength of the bonds between SMOC and the soil particles increases over time. This effect is called ageing and many driving forces have been proposed [21], [20]. A possible explanation is that SMOC needs time to establish an adsorption equilibrium with the soil particles [21]. Moreover, the molecules of the pollutant might diffuse into sites where they are trapped or where they are adsorbed more strongly [21]. Therefore, SMOC is less available for biodegradation and leaching [20]. This is probably one of the reasons why the amount of SMOC that is washed out decreases with an increasing time interval between application and the first rainfall [20].
- **Grain size distribution and porosity:** There is less leaching in soils consisting of small pores and small grains such as clay because the water is more strongly held back by capillary forces [20]. Consequently, leaching increases right after tillage because the soil is less dense and there are larger pores where the rain can leach through [22].
- **OC content:** With increasing OC content, leaching decreases because the adsorption coefficient K_d increases [20].
- **Method of application:** The method of application also affects SMOC surface run-off losses. The losses of SMOC due to run-off were reduced by 69% when SMOC was mixed into the surface soil before planting (preplant incorporation) instead of being applied to the surface of the soil [23].
- **Rainfall volume:** With increasing volume of rainfall, transportation increases [22]. Moreover, rain enhances degradation because it creates a humid environment (see chapter 4.2).
- **Rainfall regime:** Run-off increases if the soil is already humid before it rains. In contrast, leaching is more likely to occur after rainfall following a dry period because the dry soil has cracks and is less compact [22].

- **First rainfall:** The volume and the duration of the first rainfall after the application is crucial for the pollutant export. Subsequent rainfalls have less influence on the transportation of the pollutant because the adsorption becomes stronger over time, as explained above. Moreover, the pore spaces in the soil are reduced after the first rainfall (soil compaction), resulting in less leaching during the subsequent rainfalls [22].
- **pH:** The pH has been reported not to affect the adsorption coefficient of SMOC [8].
- **Slope of the field:** On flat fields, surface run-off is negligible [24].

Run-off and leaching losses of SMOC and especially of its metabolites OA and ESA contribute to a contamination in ground- and surface water [25]. The pollutant SMOC in surface water poses a real risk to water organisms whereas mammals are generally more tolerant. For example, half of a rat population dies if the oral intake of SMOC exceeds 2000 mg/kg of the body weight of a rat. On the other hand, half of a fish population (rainbow trout) dies if it is exposed to water containing 1.23 mg/l of SMOC for 96 hours [8]. At a concentration of 1.1 µg/l, the growth of marbled crayfish is inhibited and they lose orientation since their sensory receptors (especially olfactory) are damaged by SMOC [26]. This may decrease their ability to find mates and food, to register alarm cues, and to acquire their social status [26]. Moreover, their antioxidant defence systems are damaged at 11 µg/l [26]. The rainbow trout is reported to react less sensitively to the metabolites ESA and OA compared to SMOC [8]. However, for other fish (zebrafish) the metabolites were more toxic than the parent molecule [27]. In the lake of Zug, the concentration of SMOC was between 0.9 and 3.3 ng/l in 2016 [4].

4.2 Degradation

By 2007, 25 metabolites of SMOC had already been identified [14]. The major pathways include the nucleophilic replacement of chlorine and the major plant metabolites recovered are glutathione conjugates [4]. The simplified degradation pathways of OA and ESA are illustrated in figure 8. OA is the predominant metabolite in non-sterilised soil [14]. In this degradation pathway, the chlorine is replaced by an OH group to form an alcohol, which is further oxidised to a carboxylic acid. ESA contains a sulfur atom which traces back to glutathione.

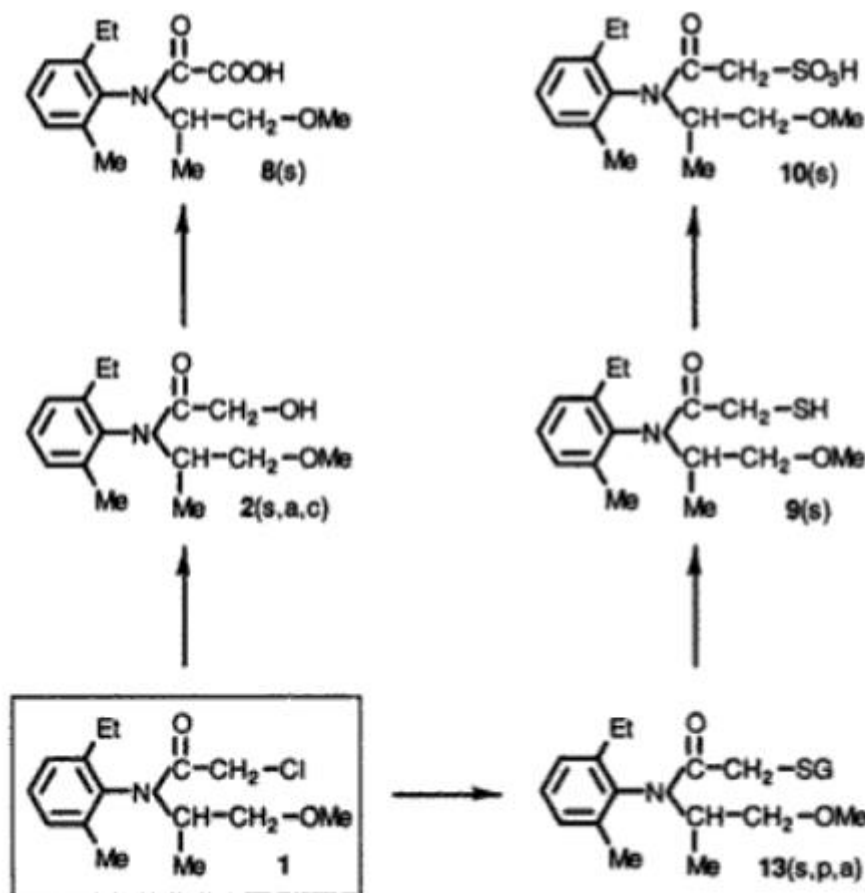


Figure 8: Degradation pathways of SMOC (1) to OA (8) and ESA (10) (G: glutathione) [14]

The factors that degrade herbicides are [23]:

- microorganisms (biodegradation)
- photolysis
- hydrolysis
- other chemical reactions with soil constituents

For SMOC, microorganisms are the main factor for degradation [28]. Photolysis, the breakdown of chemical bonds in molecules due to electromagnetic radiation, mainly light and UV, only occurs during prolonged dry periods on the surface of the soil, but SMOC is rather resistant to this kind of degradation [20]. After 146 days of photolysis in water, 50% of the initial concentration

remains [8]. SMOC is unlikely to be hydrolysed as it is stable in water at a pH that ranges between 5 and 9 at 25°C [8]. The following factors affect the degradation rate:

- **Adsorption:** As explained in chapter 4.1, the adsorption of SMOC to soil particles increases over time and, therefore, the bioavailability of the pollutant decreases. This leads to a decreasing degradation rate.
- **Number of microorganisms:** The higher the number of microorganisms that can degrade SMOC, the faster the degradation. The growth of a microbial population is affected by [23]:
 - **Temperature:** With an increasing temperature, the half-life time shortens because of increased microbial activity. Moreover, the dissolved fraction increases at high temperatures leading to greater bioavailability and possibly to more leaching [23].
 - **Moisture:** With an increasing water proportion, the degradation of SMOC increases. This may be due to increased microbial activity or increased bioavailability of SMOC as its dissolved proportion rises [23].
 - **Availability of nutrients and energy:** Some microorganisms do not use SMOC as an energy source, whereas others (*Chaetomium globosum*) can use it as a source of carbon [20], [29]. If the microorganisms do not use SMOC as an energy source and only detoxify SMOC as a by-product of their metabolism, the degradation rate increases with the amount of the energy providing compounds. If the microorganisms use SMOC as an energy source, the relationship between the degradation rate and the available energy becomes more complicated. There should be enough carbon and energy providing compounds so that the microorganisms can survive and the population can grow. On the other hand, if the easily degradable energy providing compounds are abundant, the microorganisms are not dependent on the energy source SMOC. In this case, they would not degrade SMOC and instead use another energy source. This has been confirmed by a study that showed that the CO₂ mineralisation of SMOC decreased with increasing OC content [30]. However, the degradation rate, which also includes co-metabolism of SMOC, generally increases with increasing OC content [23].
- **Application history:** Fields that were previously treated with SMOC show a shorter DT50. The reason for this is an improvement of the SMOC degradation enzymes in the microbiome [23].
- **Application rate:** In another study, a correlation between the application rate and the DT50 of SMOC was shown [23]. The higher the application rate, the longer the DT50. This is a common phenomenon observed with PPPs. The activity of the microorganisms degrading SMOC is suppressed when the concentration of SMOC is too high [31].
- Soil texture and pH have an insignificant impact on the degradation rate [23].

5 Materials and methods

This chapter illustrates the methods used to collect and analyse the soil samples.

5.1 Application of S-metolachlor

The applied PPP Calado contained the active substance SMOC. The concentration of SMOC in Calado, an emulsifiable concentrate, was 960 g/l [17].

The active compounds of Calado consist of 86.5% SMOC while the rest is R-metolachlor [32]. However, in this field study, SMOC and R-metolachlor were not distinguished during the analysis [33].

The PPP Calado was applied to a cornfield at Rindelstrasse 26 in Arth, at 10 a.m. on 28 May 2020 using a spraying technique (figure 9). According to the farmer, the application rate was 0.5 l/ha.



Figure 9: Application method (spraying) of Calado in Arth

5.2 Method of soil sampling

5.2.1 Challenges

It was challenging to take a series of representative soil samples for the whole field over time due to the following reasons:

Challenge: The PPP was not homogeneously applied on the whole field. The PPP was sprayed on the field with a tractor, which had to turn at the border of the field. Therefore, the contamination at the border of the field was probably different from the one at the centre and would not have represented the contamination of the field.

Solution: Not just one individual sample but several individual ones were taken. These made up a composite sample. The samples were taken 13 m from the border (figure 11).

Challenge: To compare the concentrations of the soil samples, the location of the sampling had to stay the same throughout the period under study (from May until July).

However, the corn plants grew and impeded the localisation of the previous sampling.

Solution: Poles were put in the soil where the sampling had taken place. In the early stages of the sampling, the farmer drove over the field to spread fertilizer, which is why the poles were removed. Therefore, two waypoints served to reconstruct the position of the poles. In the later stages of the sampling, the poles were left in the soil.

5.2.2 Method

The samples were taken for two months (from 10 May until 17 July 2020). In the early stages after the application, the samples were taken more frequently (every three days) since the degradation was expected to be exponential. Moreover, sampling took place before and after rainfall. The samples were taken in an area of 10 m x 10 m, which represented the whole field. Four poles marked the corners of the square. The distances of the poles to two waypoints were measured. The waypoints (F1 is a pole in front of a tree and F2 is a stone border) and their distance to two poles of the 10 m x 10 m plot (A and B) are illustrated in figure 11.

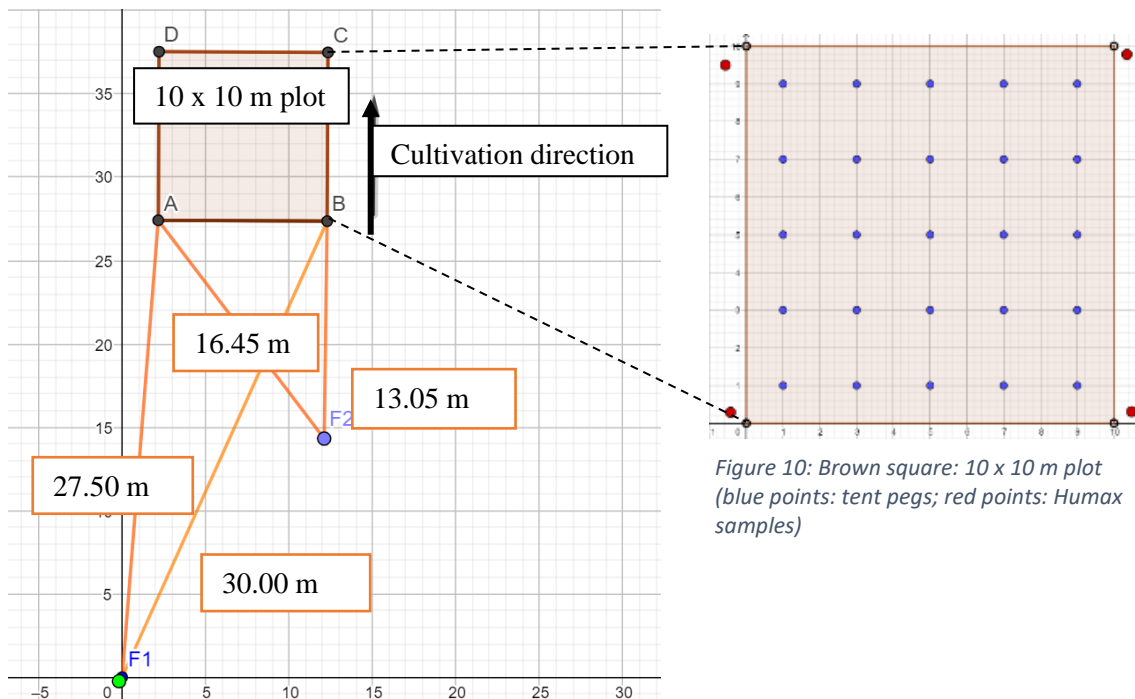


Figure 10: Brown square: 10 x 10 m plot (blue points: tent pegs; red points: Humax samples)

Figure 11: Distances of the two poles (A, B) of the 10 x 10 m plot to the waypoints (F1, F2)

This 10 m x 10 m square was evenly split into a grid of 25 smaller squares each with an area of 4 m². The centres of these smaller squares were marked with tent pegs (blue points in figure 10). During each sampling, the individual samples were taken from a randomly chosen location around each tent peg. The more individual samples are taken, the more representative the composite sample is. Each individual sample was divided into two layers, a top layer consisting of the uppermost 5 cm of soil and a bottom sample containing the soil below the top layer to a depth of 17 cm. For each of the two layers, the 25 individual samples were mixed together and made up a composite sample, which was later analysed.

Four Humax samples were taken on the first and the last sampling after the application (red points in figure 10). Humax samples served to determine the composition of the soil in terms of air, water, fine soil, and soil solids (chapter 5.4).

Immediately after having taken the samples, they were stored in a freezer at -20°C to prevent any losses of SMOC due to further degradation.

5.2.3 Tools for soil sampling

The following tools were used to collect the individual samples (figure 12):

- (1) half-pipe drill (diameter: 2 cm)
- (2) plastic bag
- (3) spatula
- (4) wooden template

The wooden template was 5 cm in length and was used, together with the spatula, to divide the two layers of the soil.

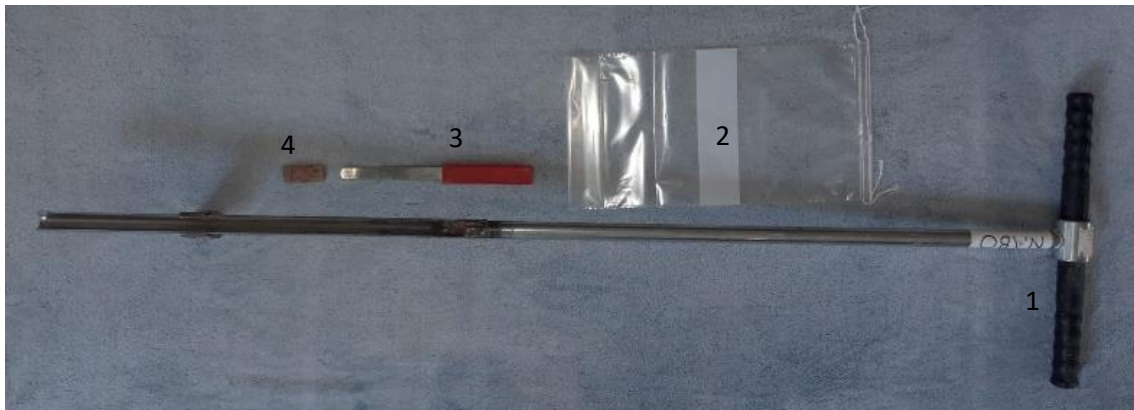


Figure 12: Tools: half-pipe drill (1), plastic bag (2), spatula (3), wooden template (4)

Figure 13 and figure 14 illustrate the usage of the half-pipe drill.



Figure 13: The half-pipe drill is pushed into the soil.



Figure 14: Half-pipe drill with soil

The following tools were used to take the Humax samples (figure 15):

- (5) Humax drill (with a diameter of 48 mm)
- (6) hammer
- (7) plastic tube

Figure 16 illustrates the usage of the Humax drill.



Figure 15: Humax drill (5), hammer (6), plastic tube (7)



Figure 16: Pulling out the Humax drill containing soil

5.3 Analysis method

In this chapter, the method to analyse the soil samples is presented.

5.3.1 Sample selection

The samples were taken on 21 days (figure 17). Every sampling yielded two composite samples, one of the first layer and one of the second layer, which is why there were 42 samples in total. From here on, a sample always refers to the composite sample of a sampling.

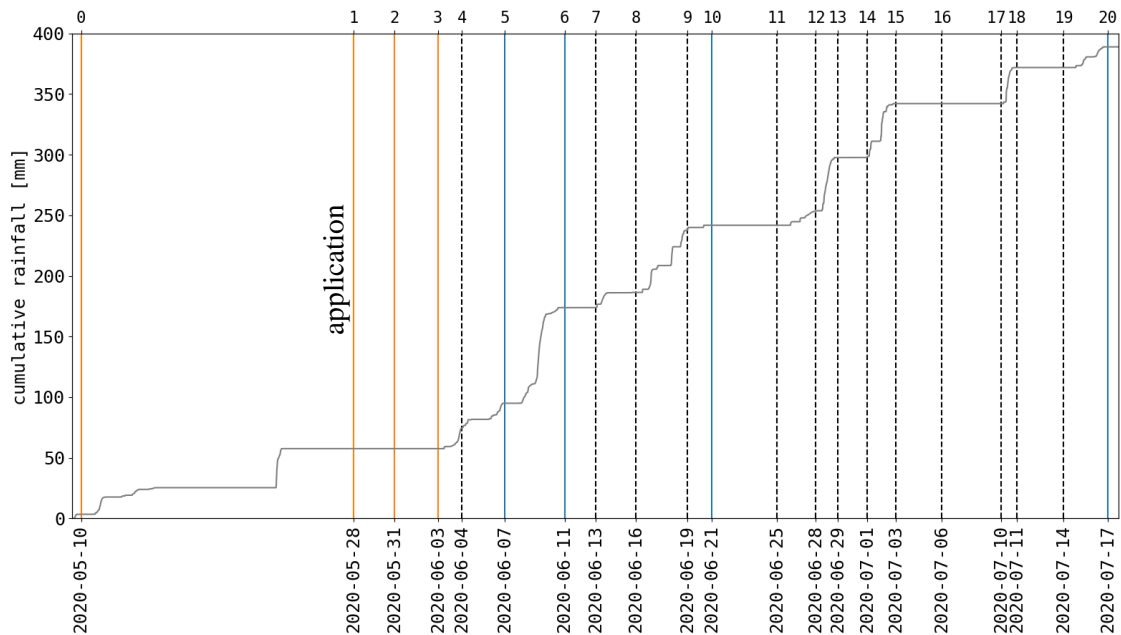


Figure 17: Overview of the rainfall and the samples (grey: cumulative rainfall; orange: only the sample of the first layer was analysed; blue: the samples of both layers were analysed; black: the samples were not analysed.)

The capacity of the analytical equipment was limited and not all the 42 samples could be analysed. Therefore, twelve samples were selected based on the rainfall during the examination (figure 17) and the following hypotheses:

1. Ploughing equalises the concentrations in both layers.
2. Immediately after the application, only the concentration in the first layer changes since the product is applied to the surface of the soil.
3. The degradation is exponential, which is why more samples were analysed in the early stages after the application.
4. Only rain transports SMOC into deeper layers. Leaching stops as soon as the rainfall ends. Therefore, the analysis of both layers was only carried out if it had rained since the last sampling.

The following table explains why the respective samples were chosen. The numbers of the samples in the left column refer to the numbering in figure 17. The numbers in the right column refer to the hypotheses listed above.

sample	layer	reason	hypothesis
background sample / sample 0	layer 0-5 cm	This sample gave information about the background presence of SMOC since it was taken before the application of the PPP. Only the layer from 0-5 cm was analysed because the soil was ploughed.	3
sample 1	layer 0-5 cm	This sample provided information about the amount of the PPP that was applied because it was taken 6 h after the application.	4
sample 2	layer 0-5 cm	This sample served to investigate the degradation rate during a dry period.	1, 2
sample 3	layer 0-5 cm	The reason is the same as for sample 2. Additionally, this sample served as a reference for sample 5.	1, 2
sample 5 sample 6 sample 10	layer 0-5 cm layer 5-17 cm	These samples served to determine the amount of SMOC that was transported into deeper layers due to rainfall. Samples 5 and 6 were chosen because there was heavy rainfall in between.	2
sample 20	layer 0-5 cm layer 5-17 cm	Sample 20 was the last one and was the end of the sample series.	2

Table 4: Sample selection with reasons

5.3.2 Overview of the analytical procedure

5.3.2.1 Overview of the analytical steps

The samples were processed in five steps (figure 18):

- drying the soil (chapter 5.3.3)
- sieving and grinding the soil (chapter 5.3.4)
- extracting the analytes (chapter 5.3.5)
- scaling the concentration (chapter 5.3.6)
- HPLC-MS/MS analysis (chapter 5.3.7)

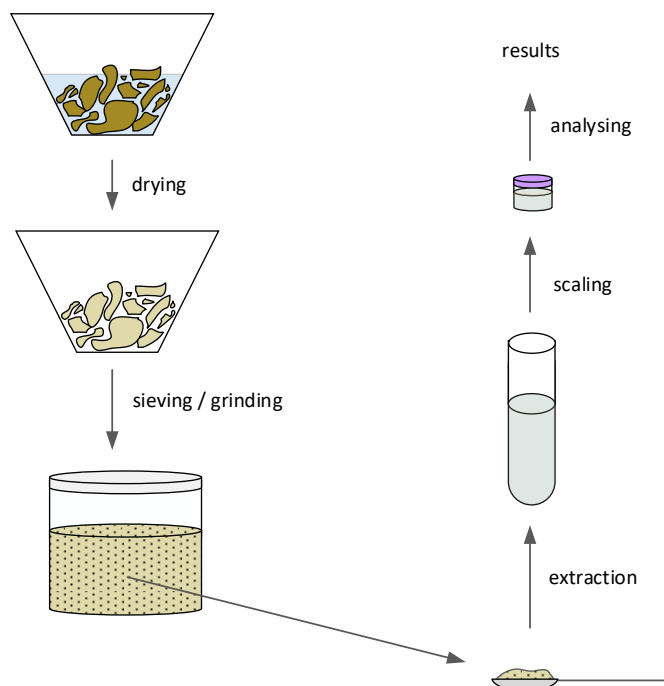


Figure 18: Overview of the analytical procedure

5.3.2.2 Important terms

Important terms which are used frequently in the following chapters are listed below.

analyte

The analyte is the substance that is the target of the analysis or the measurements [33]. In this case, the analytes were SMOC, OA, and ESA.

matrix

The matrix includes other components of the sample apart from the analyte [33]. These components might influence the analysis because they interact with the analyte (e.g. adsorption).

spike

To spike means to add a known amount of a substance (e.g. SMOC) to a sample [33].

aliquot

An aliquot is an exact portion of a sample (e.g. 5 mL subsamples taken from the same 50 mL solution).

ASE

The accelerated solvent extraction (ASE) is the extraction method used. The extraction is carried out at high temperature and pressure, which speeds up the process compared to traditional methods.

HPLC-MS/MS

A high-performance liquid chromatography coupled to triple quadrupole tandem mass spectrometry (HPLC-MS/MS) device was used to separate and identify individual analytes and to measure their concentrations.

IS

IS is the abbreviation for internal standard. Isotope-labelled internal standards are molecules that have the same (or very similar) physicochemical characteristics as the target analytes and only differ from the target analytes by their mass [34]. Therefore, the HPLC-MS/MS device, which measures the mass-to-charge ratio, can distinguish the analyte from the IS. In this study, SMOC d11 and ESA d6 were used, which means that 11 and 6 hydrogen atoms were replaced with 11 and 6 deuterium atoms respectively.

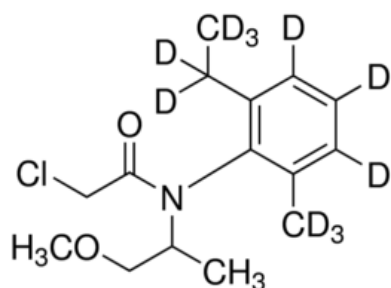


Figure 19: Structure of SMOC d11 [35]

What was the purpose of the IS?

The analytical results were expressed as the ratio of the concentrations of the analyte and the IS. By spiking the IS into the samples any losses of the target analyte could be compensated since the IS and the analyte have the same physicochemical characteristics. Their relative losses are equal, and their ratio stays constant during the analytical procedure (figure 20).

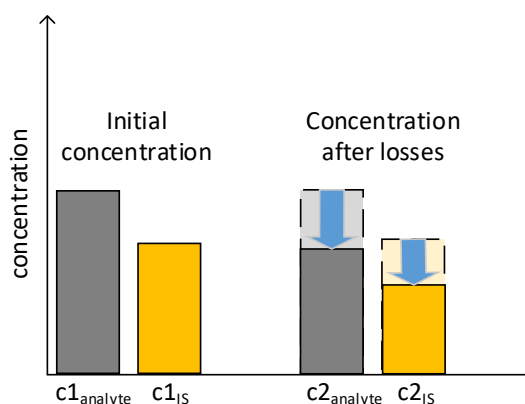


Figure 20: The concentration of the analyte (grey) and the IS (yellow) before the analytical procedure ($c_{1analyte}$ and c_{1IS}) and after possible losses ($c_{2analyte}$ and c_{2IS}). $\frac{c_{1analyte}}{c_{1IS}} = \frac{c_{2analyte}}{c_{2IS}}$

5.3.2.3 Calculation of the concentration

The HPLC-MS/MS produced a signal. The intensity of the signal climbed with increasing concentrations of the analyte in the sample. For example, SMOC in the field samples produced a peak in the HPLC-MS/MS signal at the retention time of SMOC. In addition, the added IS of SMOC in the sample created another peak in the HPLC-MS/MS signal. The two peaks have the same HPLC retention time and, thus, arrive at the same time at the MS, but are separated in the MS due to the deuteration of the IS.

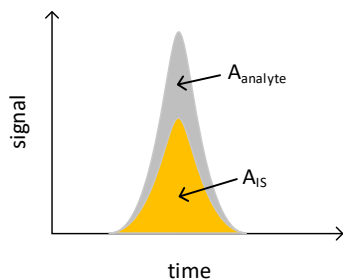


Figure 21: The signal produced by the HPLC-MS/MS over time (grey: area of the peak of the analyte ($A_{analyte}$); yellow: area of the peak of the IS (A_{IS}))

The area refers to the integrated area under the peak of the analyte. For OA there was no IS available, which is why the IS of ESA was used. The area ratio was defined as:

$$A_{ratio} = \frac{A_{analyte}}{A_{IS}}$$

In order to calculate the concentration ratio based on the area ratio, the calibration curve was used. The calibration curve is a function that describes the linear relationship between the area ratio and the concentration ratio.

$$\frac{A_{analyte}}{A_{IS}} = m \cdot \frac{c_{analyte}}{c_{IS}} + q$$

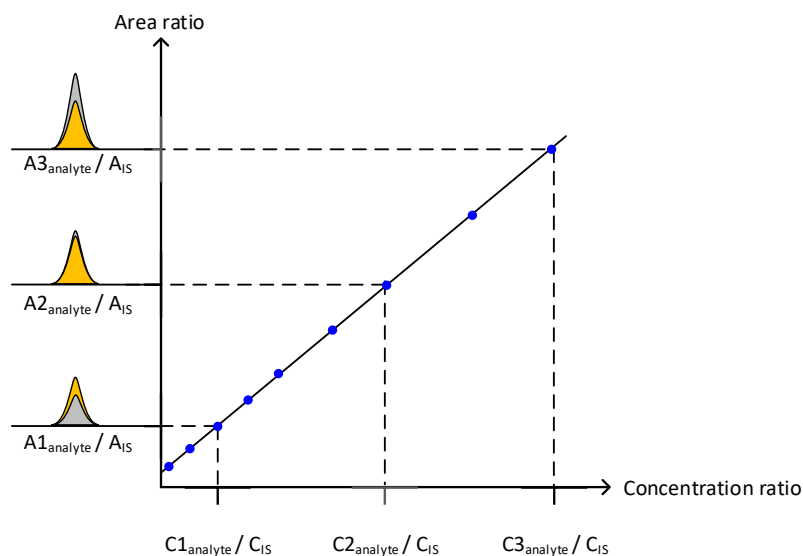


Figure 22: Example of a calibration curve (blue points: example of concentration ratios and area ratios in calibration samples; $C1_{analyte} / C_{IS}$: concentration ratio in the first calibration sample; $A1_{analyte} / A_{IS}$: area ratio in the first calibration sample)

The calibration curve was obtained from the data of calibration samples with a known concentration ratio. More information on the calibration samples can be found in chapter 5.3.6.4. The concentration of the analyte was defined as:

$$c_{analyte} = \left(\frac{\frac{A_{analyte}}{A_{IS}} - q}{m} \right) \cdot c_{IS}$$

The $c_{analyte}$ was measured in ng/mL and c_{IS} was 1 ng/mL (chapter 5.3.6.3). Table 5 shows how to convert ng/mL into ng/g and lists the analytical procedure in reversed order. The following paragraph gives a short explanation of the analytical procedure:

5 g (m_{FS} in table 5) of each soil sample were extracted so that the extract volume of each sample was 50 mL of solvent (V_3). Depending on the aliquot type (a), a portion of 5 mL or 0.5 mL (V_2) was taken from the extract volume, which corresponded to 0.5 g or 0.05 g soil respectively. The 0.5 mL aliquot was taken for the samples 1, 2, 3, 5, and 6, and the 5 mL aliquot was taken for the samples 0, 10, and 20. Different types of aliquots were necessary to move the concentration of a sample into the range of detection. The aliquot was then evaporated, and the remainder was re-dissolved in 1 mL of HPLC solvent (V_1). 2 mL of this solution therefore contained the analytes extracted from 1 g or 0.1 g of soil respectively.

point in the analytical procedure	volume of solvent [mL] or mass of fine soil [g]	mass of the analyte	concentration of the analyte
before the analysis in the HPLC-MS/MS (chapter 5.3.6.6)	V_1	m_1	$c_1 = \frac{m_1}{V_1} \left[\frac{ng}{mL} \right]$
after having taken the aliquot (chapter 5.3.6.3)	$V_2 = V_1 \cdot a$	$m_2 = m_1$	$c_2 = \frac{c_1}{a} \left[\frac{ng}{mL} \right]$
after extraction (chapter 5.3.6.2)	$V_3 = V_2 \cdot \frac{50}{a}$	$m_3 = m_2 \cdot \frac{50}{a}$	$c_3 = c_2 \left[\frac{ng}{mL} \right]$
after having filled the extraction cells (chapter 5.3.5.2)	$m_{FS} \triangleq \frac{V_3}{10}$	$m_4 = m_3$	$c_4 \triangleq c_3 \cdot 10 \left[\frac{ng}{g} \right]$

Table 5: How to convert ng/mL to ng/g (blue: known or measured; orange: calculations; $m_{FS} = 5$ g of fine soil; $V_1 = 1$ mL of solvent; $V_2 = 5$ mL of solvent or 0.5 mL of solvent; $a =$ aliquot type = 0.5 or 5; $V_3 = 50$ mL of solvent)

It can therefore be concluded that:

$$c_4 \left[\frac{ng}{g} \right] \triangleq \frac{10}{a} \cdot c_1 \left[\frac{ng}{mL} \right]$$

The specific formula for the 5 mL aliquot was: $c_4 \left[\frac{ng}{g} \right] \triangleq 2 \cdot c_1 \left[\frac{ng}{mL} \right]$ and the one for the 0.5 mL aliquot was: $c_4 \left[\frac{ng}{g} \right] \triangleq 20 \cdot c_1 \left[\frac{ng}{mL} \right]$

The concentration of the samples 1, 2, 3, and 10 (both layers) lay outside of the range of detection. Therefore, these samples were diluted 1:10 and their measured concentration had to be multiplied by 10.

5.3.2.4 Control samples

Besides the twelve selected samples from the field, four different types of control samples were analysed.

type	content	point in the analytical procedure	purpose
extraction blank	sea sand	prepared before ASE (chapter 5.3.5.3)	to measure the contamination during the whole analytical procedure and to determine the limit of quantification (LOQ).
spike	soil of the background sample of the field	prepared before ASE (chapter 5.3.5.3)	to measure the relative recovery and the method precision.
blank in HPLC-MS/MS	methanol and water	prepared before the HPLC-MS/MS (chapter 5.3.6)	to measure the contamination of the HPLC-MS/MS.
blind in HPLC-MS/MS	methanol, water, and IS	prepared before the HPLC-MS/MS (chapter 5.3.7.1)	to measure the contamination of the IS.

Table 6: Overview of the type and the characteristics of the control samples

5.3.3 Drying

The water in the soil samples could have prevented nonpolar organic solvents from reaching the adsorbed analyte during the ASE, which is why the soil samples had to be dried before extraction [36].

5.3.3.1 Challenges

Challenges: The analyte might have degraded at high temperatures leading to a concentration decline in the samples [23].

Solution: The soil was dried at a maximum temperature of 40°C to prevent any analyte losses. At 40°C, the concentration decline of SMOC, OA, and ESA due to degradation was expected to be negligible [33].

5.3.3.2 Method

The soil samples were put into open aluminium containers and were dried in a drying chamber for 72 h at 40°C. The weight of the soil samples was recorded before they were put into the drying chamber, after 24 h, after 48 h, and after 72 h. Weight stabilisation was a sign that all the water had evaporated. The average percentual mass decline of the samples of the first and second layer is illustrated in figure 23.

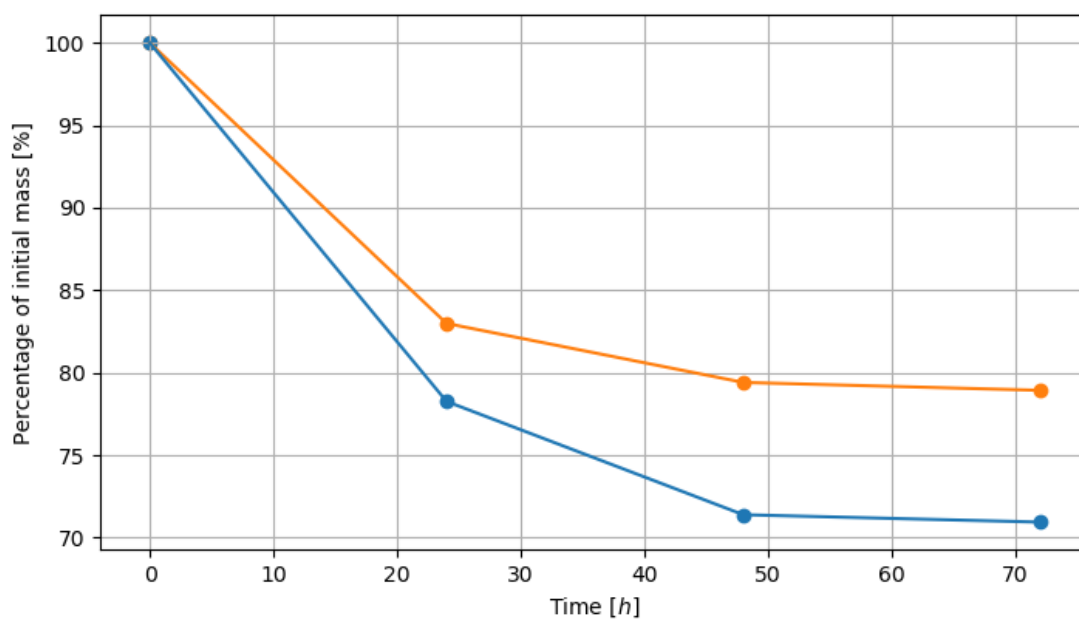


Figure 23: Average percentual mass decline of the soil samples of the first (orange) and the second layer (blue) during the drying

5.3.4 Sieving and grinding

The dried soil was sieved to separate the soil from stones, roots, and plants. Sieving also impacted the homogeneity of the sample and, therefore, the final analytical result. If the soil is ground, the extraction is faster because there is more surface area, where the solvent can reach the analyte more efficiently [36].

5.3.4.1 Challenges

Challenge: The soil contained a lot of clay. Therefore, the soil aggregates became very hard after drying and it was challenging to sieve them by hand.

Solution: A mortar was used to grind the soil before it was sieved.

Challenge: All samples were sieved using the same equipment. This could have led to contamination of the equipment and could have falsified the results.

Solution: After every sample, the sieve, the mortar, and the machine were cleaned with water and an air pistol.

5.3.4.2 Method

The dried soil was sieved through a 2 mm sieve. After this, it was transferred into a machine that sieved the soil even finer so that the sample became more homogenous.

The ground soil was then transferred into labelled jars that had been cleaned with water and ethanol. The soil was stored in these jars so that the analysis results could be verified by analysing the soil a second time. Furthermore, a part of the soil was used for the Humax samples (chapter 5.4).

5.3.5 Extracting analytes

The analytes were extracted using an accelerated solvent extraction device (ASE). The ASE was used to dissolve the analytes, which were adsorbed to the soil particles, in a solvent since the HPLC-MS/MS could only analyse liquids and not solids. Before the extraction started, the extraction cells (figure 24) were filled with the soil of the samples (described in more detail in chapter 5.3.5.2). In the course of the extraction, the analytes dissolved in the solvent, which was then stored in glass bottles (figure 24).

5.3.5.1.1 Challenges

Challenge: The bigger the difference between the concentration of the analyte in the soil and in the solvent, the more of the analyte is desorbed [37]. Since an adsorption equilibrium is established during the extraction, no more analyte molecules can be desorbed from the soil.

Solution: The extraction cell was refilled multiple times with fresh solvent. However, if the extraction cell had been flushed with too much solvent, the analyte would have become too diluted in the extract and it would have taken longer to evaporate the solvent after the extraction. Experience showed that the extraction works best if the cell is rinsed three times with an organic solvent and then twice with an acidic solvent [33].

Challenge: The polarity of the solvent should have been equal to the one of the analyte in order to improve efficiency. The challenge was that different analytes with different polarities were analysed.

Solution: Two solvents of different polarities were used.

Challenge: The ASE device might have been contaminated.

Solution: The ASE device was cleaned before the analytes in the next cell were extracted. Two blank samples and two spiked samples were prepared to measure the contamination (chapter 5.3.5.3).

5.3.5.1.2 ASE method

The ASE is an efficient technique to extract analytes as it works under high temperature and high pressure. A higher temperature increases the ability of the solvent to desorb the analyte because the thermal energy can overcome the activation energy to desorb the analytes. In addition, the solvents are more fluid and their surface tension decreases at a higher temperature, which enhances the ability to reach the analytes on the soil particles. High pressure makes it possible that the solvents are still liquid even though the temperature is above the boiling point. Additionally, the high pressure enables the solvent to reach the analytes that are caught in pores [37].

Figure 24 shows the schematic instrumentation of an ASE device.

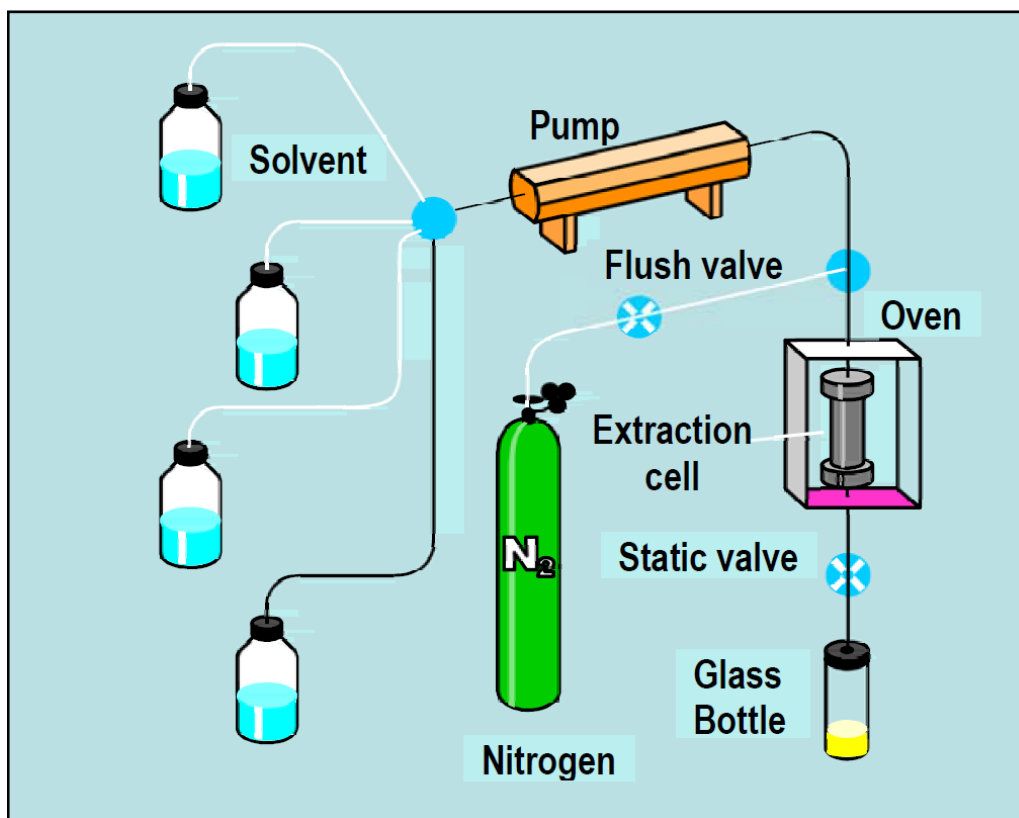


Figure 24: Schematic instrumentation of an ASE device [34]

There were two extractions using two solvents. First, all extraction cells were flushed with the first solvent and then all extraction cells were rinsed with the second solvent.

The mixture of the first, organic solvent was the following:

substance	ratio [%]
acetone	65
acetonitrile	25
methanol	10

Table 7: Mixture of the first solvent

The mixture of the second, acidic solvent was the following:

substance	ratio [%]
acetone	70
phosphoric acid (1%)	30

Table 8: Mixture of the second solvent

The conditions during the first and the second extraction are presented in table 9. As an example, the procedure for one extraction cell during the first extraction is described in the following paragraph:

The cell was transported on a disk into a small oven, where it was filled with the first solvent (figure 24). The static time is the time during which the solvent was kept under high pressure in the cell and during which the analytes were desorbed from the soil particles. After a static cycle,

60% of the solvent left the cell (flush volume). The time required for purging is called purge time. Afterwards, the cell was refilled with a fresh solvent. This was repeated three times (static cycles). After the last static cycle, N₂ was blown through the cell to remove all of the solvent from the cell. The solvent was stored in glass bottles and the ASE system was cleaned before the next cell underwent the same procedure.

	first, organic extraction	second, acidic extraction
volume of the cell [mL]	10	10
static cycles	3	2
static time [min]	7	5
flush volume [%]	60	60
purge time [s]	60	100
pressure [psi]	1600	1900
temperature [°C]	65	120

Table 9: Conditions in the ASE during the first and the second extraction

Figure 25 shows the ASE device used at Agroscope.

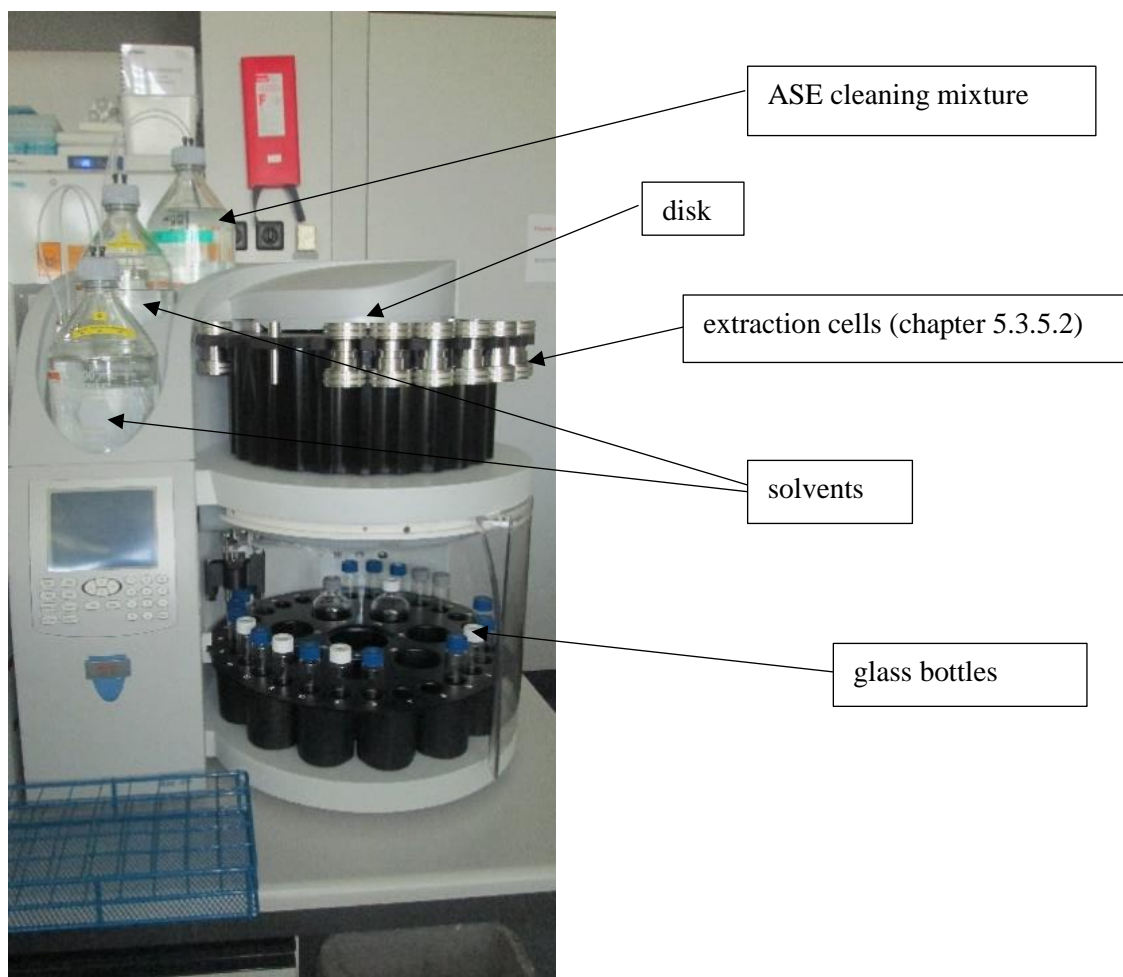


Figure 25: ASE device at Agroscope

5.3.5.2 Filling the extraction cells

The following chapters detail the preparation of the extraction cells. Before the ASE started, the extraction cells were prepared and filled with the soil of the samples.

5.3.5.2.1 Challenges

Challenge: The dry soil was put into glass jars three days before the extraction. The analytes might have settled to the bottom or to the side of the jars and the sample might have no longer been homogenous.

Solution: The soil in the jars was mixed with a machine called “Turbula” before part of the soil was transferred into an extraction cell.

Challenge: The ground soil was very fine and could have blocked the filters in the extraction cell, which would have impeded the extraction.

Solution: Sea sand was put into the cell before and after the field soil was added. This sea sand should not have been contaminated with SMOC and had a large grain size, which would keep the filters clear. Additionally, a second glass fibre filter was put onto the steel filter to prevent any blockage of the steel filter by the soil particles.

Challenge: If too much soil had been put into the cells, the concentration of the analyte in the solvent after the ASE would have been higher. This would have been beneficial if the concentrations had been too low to be detected. However, this would have entailed the risk that the concentrations of the analyte exceeded the upper detection limit of the HPLC-MS/MS. Furthermore, not only the analytes were extracted but also other components of the matrix (e.g. humic substances). The more soil is put into the cell, the more matrix is co-extracted, which can impede the analysis and can therefore lead to wrong results.

Solution: Experience showed that 5 g of soil work best [33].

Challenge: The tools for the weighing of the soil might have been contaminated.

Solution: The tools (spoon and funnel) were cleaned with water.

5.3.5.2.2 Method

The ASE cells consisted of a body and two covers. The covers contained a glass fibre filter and a steel filter through which the soil particle could not pass. The solvent passed through a tiny hole in the covers.

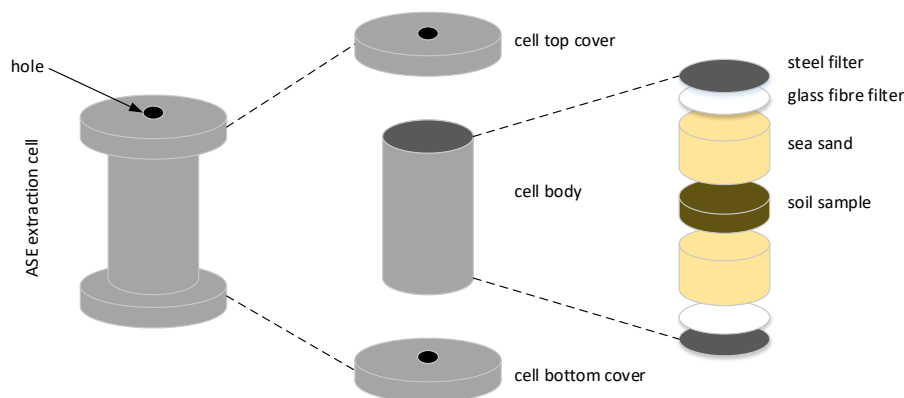


Figure 26: Basic parts of the ASE extraction cell

A spoonful (about 3 g) of sea sand was put into the cell body, onto the cell bottom cover. Afterwards, 5 g of the soil sample were added onto the sea sand. Finally, another spoonful of sea sand was placed onto the field soil and the cover was put onto the cell body. The tools were cleaned after every filling.

5.3.5.3 Spiked samples and blank samples

Two extraction blank cells were only filled with sea sand. These blank samples had a predicted concentration of the analyte of 0 ng/g. However, due to contamination during the analytical procedure, the concentration in the blank samples is usually higher than 0 ng/g. The extraction blank samples were used to determine the limit of quantification (LOQ) (chapter 7.5.1). The LOQ is the lowest concentration of SMOC that can be reliably quantitatively measured [38].

However, effects like adsorption during the extraction, which are influenced by the soil type, were not considered with the blank samples. The soil type of the sea sand differed considerably from the field soil of Arth and, therefore, the analyte in the blank samples behaved in a different way than the one in the field samples.

This is the reason why two spiked samples were prepared before the extraction. Spiked means a known amount of SMOC, OA, and ESA (50 ng) was put onto the soil of the background presence in the extraction cell (5 g) using a pipette. The predicted concentration of the spiked sample was:

$$c_{\text{spiked_sample}} = c_{\text{background}} + c_{\text{spiked}} = c_{\text{background}} + \frac{50 \text{ ng}}{5 \text{ g}}$$

The measured concentration of the spiked samples was compared to the predicted concentration. This principle is illustrated in figure 27. The relative recovery was used to estimate the loss or

gain of SMOC from extraction to analysis (chapter 7.5.2). What is more, the spiked samples were used to determine the method precision.

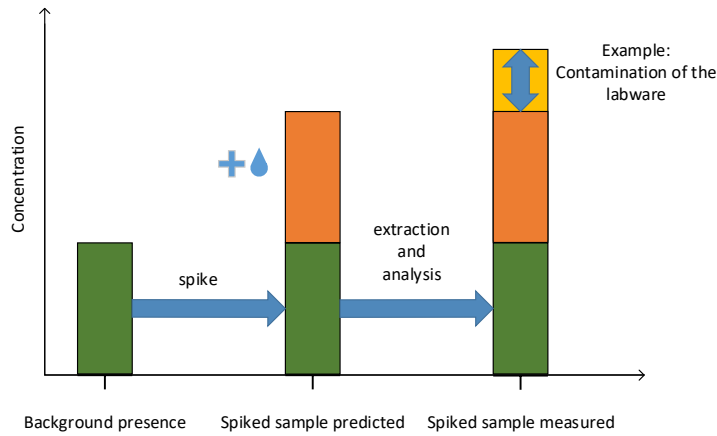


Figure 27: Principle of spiked samples (green: the concentration of the background presence; orange: the spiked concentration; yellow: an example of the concentration after the analytical procedure)

In order to make a reliable statement about the relative recovery, it would be ideal if the spiked concentration (orange in figure 27) corresponded to the concentration in the background sample (green in figure 27). The concentration in the background sample was unknown before the analysis. Therefore, the concentration was estimated by Andrea Rösch [33]. The two spiked samples were rested overnight because it took time for the spiked analytes to interact with the soil particles and to adsorb to it.

5.3.6 Scaling of the concentration

After the extraction, the analytes were dissolved in a solvent. The next step was to scale the concentration in the solvent. The goal was to obtain a vial containing the dissolved analytes in a concentration fulfilling the following conditions:

- The absolute concentration of the analyte in the vial had to lie within the range of detection of the HPLC-MS/MS.
- The concentration ratio of the analyte to the IS had to lie within the range of the calibration samples (0.1 to 25, see chapter 5.3.2.3). The reason for this is that the calibration curve may not have been linear outside the measured calibration samples.

Figure 28 shows the procedure of scaling the concentration in the extracted samples.

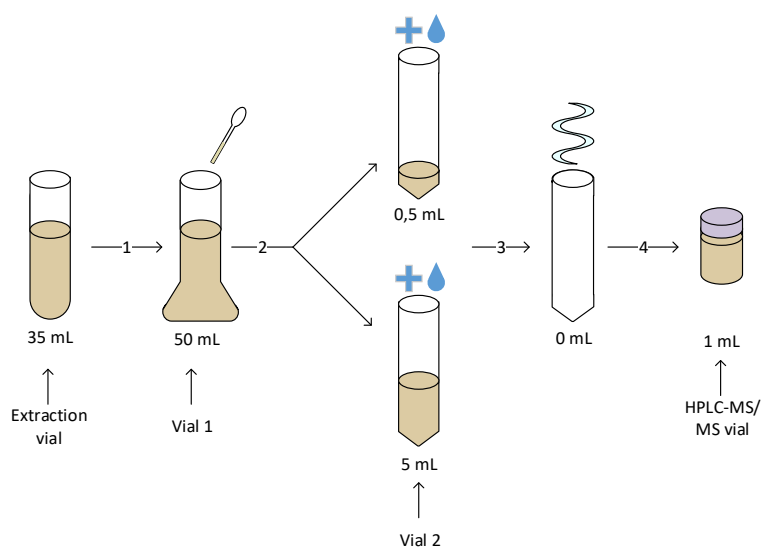


Figure 28: Procedure of scaling the concentration in the extracted samples (1: levelling out volumes; 2: taking an aliquot and adding the IS (blue drop); 3: evaporation; 4: filling of the vials for the HPLC-MS/MS)

5.3.6.1 Challenges

Challenge: The analytes might not have been homogeneously spread in the extracts. If this had been the case, the aliquot in vial 2 would not have represented the concentration in vial 1 (see figure 28)

Solution: The extract in vial 1 was vortexed before an aliquot was taken.

Challenge: The extracts after the ASE contained acidic and organic solvents. However, the HPLC only used methanol and water to separate the analytes. Moreover, the ratio of water to methanol needed to be precisely 9:1 because the HPLC started to separate the analyte at that ratio.

Solution: The solvents were evaporated and then filled with water and methanol at a ratio of 9:1.

Challenge: If the samples had been exposed to high temperatures during the evaporation in step 3, the analytes might have been degraded.

- Solution:** The solvent was evaporated by heating the liquid up to 40°C and by blowing N₂ onto the liquid. By doing this, the exposure of the analyte to high temperatures was avoided.
- Challenge:** The procedure of scaling is imprecise. Especially during evaporation, some molecules of the analyte might have got lost and might not have reached the final HPLC-MS/MS vial.
- Solution:** An isotope labelled internal standard (IS) was added into the extract (chapter 5.3.2).
- Challenge:** The IS might have been contaminated with SMOC.
- Solution:** A blind sample was prepared. The blind sample contained only the IS, water, and methanol.

5.3.6.2 Step 1: Levelling out volumes

In order to take an aliquot in step 2, the volumes of the extracts had to be the same. However, the volumes of the samples in the extraction vials were only approximately 35 mL. Therefore, the extracts were transferred into a 50 mL flask (vial 1) after having vortexed them. Then, all the extracts were filled up to precisely 50 mL with acetone.

5.3.6.3 Step 2: Taking an aliquot

In the second step, an aliquot of 5 mL or 0.5 mL was taken from the vial 1 and 1 ng of the IS was added. If the IS had been added earlier, the results would have been more reliable. However, if the IS had been added before taking an aliquot, much more IS would have been necessary, and the IS mixes were very expensive.

All molecules in the 5 mL and 0.5 mL flask ideally reached the HPLC-MS/MS vial since no more aliquots were taken after this step (figure 28). Therefore, the amount of the analyte in the aliquot had to be within the detectable range. 5 mL were taken because the amount of the analyte in 5 mL is usually within the range of detection and there was not too much co-extracted matrix in 5 mL [33]. Nevertheless, another aliquot of 0.5 mL was prepared in addition to the 5 mL aliquot for the samples with the highest concentration expected (sample 2, 3, 4, 5 (both layers), 6 (both layers)). It turned out that the concentrations of several samples were higher than expected and were not within the range of detection, which is why they were measured a second time but diluted 1:10 (see chapter 5.3.6.7).

5.3.6.4 Spiking of the calibration samples

Between steps 2 and 3, the calibration samples, which were used to establish the calibration curve, were prepared. The calibration curve was used to convert the measured area ratio of the field samples into a concentration ratio (see chapter 5.3.2.3). In order to do so, the concentration ratio in the calibration samples had to be known and, consequently, the spiking method, which served to determine the relative recovery, was used a second time. Different amounts of the analytes (0.1 to 25 ng) and a constant amount of their IS (1 ng) were spiked into nine prepared vials, which contained 5 mL acetone (figure 29). There was no IS available for OA, which is why the IS of ESA was taken. Afterwards, the calibration samples were treated the same way as the field samples (evaporation and filling the HPLC-MS/MS vial).

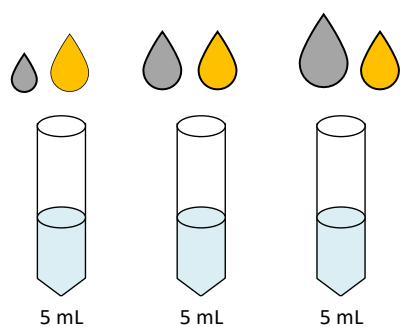


Figure 29: Spiking three calibration samples with different amounts of SMOC and a constant amount of IS (yellow drop: solvent containing the IS; grey drop: solvent containing the analytes (SMOC, ESA, and OA))

5.3.6.5 Step 3: Evaporation

In step 3, the solvent (a mixture of acetone, acetonitrile, methanol, and phosphoric acid (1%)) in the vials was evaporated by heating the liquid up to 40°C and by blowing N₂ onto the liquid (figure 30). Halfway through the evaporation, the walls were rinsed with acetone so that any remaining substances on the walls were transported to the bottom of the vials.

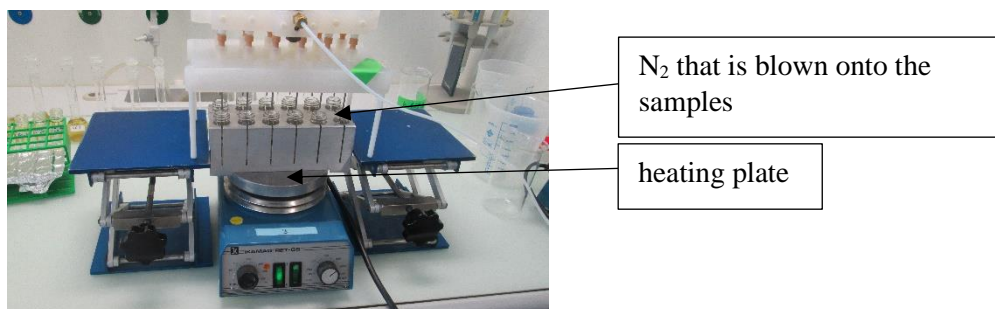


Figure 30: N₂ evaporator

5.3.6.6 Step 4: Filling of the HPLC-MS/MS vials

In step 4, 100 µL of methanol was put into the vials of step 3 with a pipette. The vials were vortexed so that the substances on the bottom of the vial mixed with methanol. Afterwards, 900 µL of water was added. The 1 mL liquid was then transferred into the HPLC-MS/MS vial using a pipette. Since 1 ng of the IS was added in step 2, the concentration of the IS in the HPLC-MS/MS vials was 1 ng/mL.

5.3.6.7 Dilution of the field samples

After the analysis in the HPLC-MS/MS, it transpired that the concentration in the samples 1, 2, 3, and 10 (both layers) was higher than expected. Therefore, they did not fulfil the conditions mentioned in the beginning of chapter 5.3.6. Therefore, the samples were measured again, but in a dilution 1:10. The area ratio between SMOC and the IS stayed the same, but the absolute area of SMOC became smaller (figure 31). Therefore, the average area of the IS in the undiluted samples and the area of SMOC in the diluted sample was used to calculate the area ratio (figure 31). The concentration ratio was then calculated using the calibration curve and was multiplied by 10.

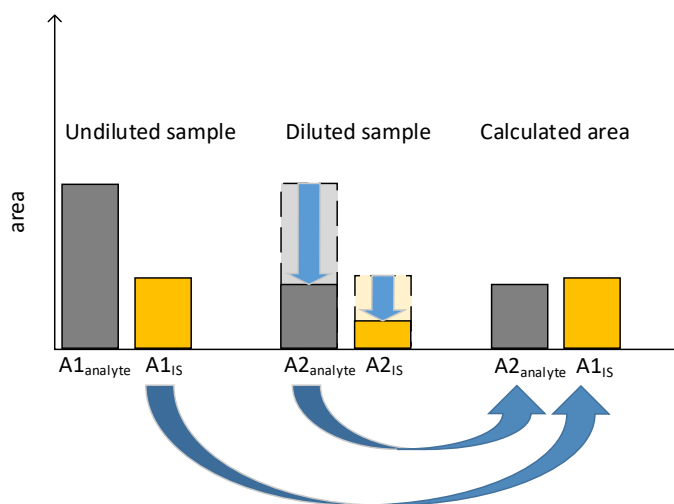


Figure 31: Method to calculate the area ratio in the samples 1, 2, 3, and 10 ($A1_{analyte}$: area of the analyte in the undiluted samples; $A1_{IS}$: area of the IS in the undiluted sample; $A2_{analyte}$: area of the analyte in the diluted sample; $A2_{IS}$: area of the IS in the diluted sample)

5.3.7 High-performance liquid chromatography-tandem mass spectrometry

A portion of the solvent in the HPLC-MS/MS vial was injected into the HPLC-MS/MS device. The HPLC-MS/MS device measured the area ratio under the peaks of the analytes and the IS.

In order to calculate the concentration ratio in the samples, the calibration curve was used.

$$\frac{A_{analyte}}{A_{IS}} = m \cdot \frac{c_{analyte}}{c_{IS}} + q$$

$c_{analyte}$ was measured in ng/mL and c_{IS} was 1 ng/mL. In order to convert the concentration into ng/g, the measured concentration of the HPLC-MS/MS was multiplied by 2 for the 5 mL aliquots and multiplied by 20 for the 0.5 mL aliquots (for more information consult table 5 in chapter 5.3.2).

The HPLC-MS/MS consisted of an HPLC and two mass spectrometers. An electrospray ionisation interface (ESI) connected the HPLC to the MS/MS.

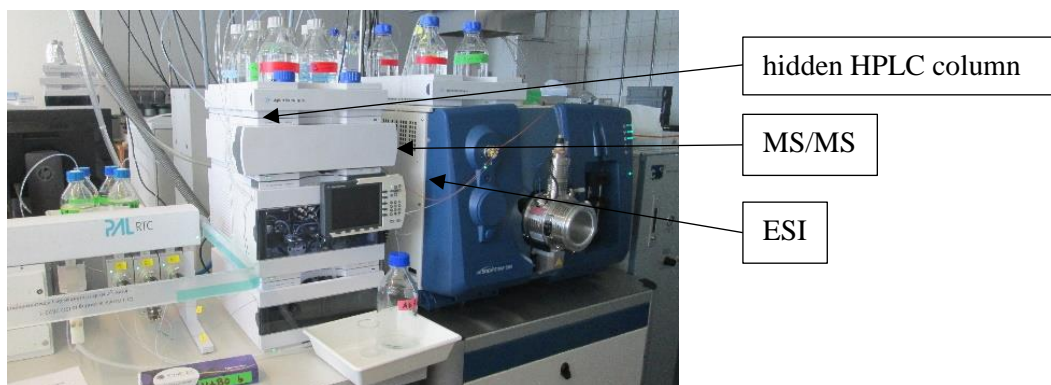


Figure 32: HPLC-MS/MS

5.3.7.1 Challenges

Challenge: The HPLC-MS/MS might have been contaminated.

Solution: A blank sample was analysed, which contained only water and methanol. This blank sample was called blank sample HPLC-MS/MS.

5.3.7.2 Method of the high-performance liquid chromatography

The HPLC device with reversed-phase chromatography separated the compounds in the sample from each other based on their different physicochemical characteristics.

The general instrumentation of an HPLC is illustrated in figure 33.

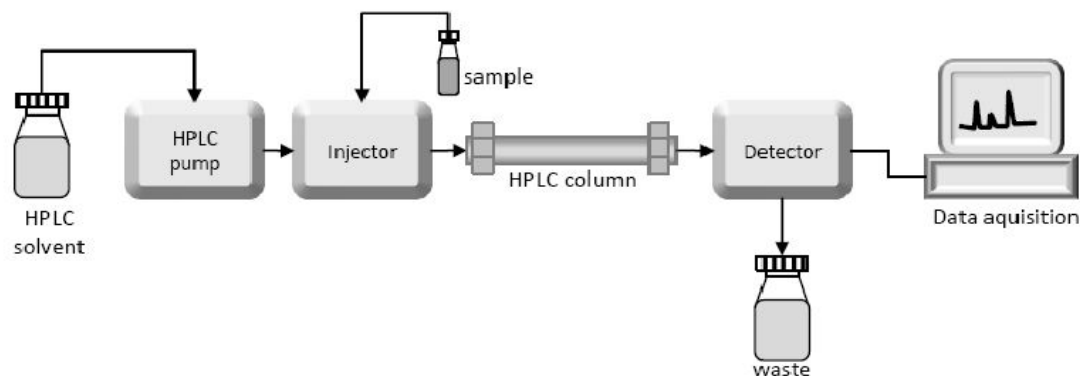


Figure 33: Schematic instrumentation of an HPLC device [39]

An HPLC pump took up the HPLC mobile phase, a solvent, and forced it through the HPLC column using high pressure. The HPLC column (Kinetex Biphenyl 100 Å column of Phenomenex) had a diameter of 4.6 mm and a length of 100 mm. The flow rate in the HPLC was 750 $\mu\text{L}/\text{min}$. The sample was automatically injected into the HPLC column as shown in figure 33. The stationary phase of the column consisted of silica gel with a particle size of 5 μm . Since a reversed-phase chromatography was used, C18 (a molecule containing 18 carbon atoms) was covalently bound to the silica gel. Therefore, the surface of the stationary phase was nonpolar.

In order to separate the substances, a polar mobile phase was needed. The lower the polarity of a component is, the stronger it adsorbs to the stationary phase and the more it is held back by the stationary phase and the longer its retention time is. In this study, the solvent gradually became more nonpolar. In the beginning, the solvent consisted of 90% water and 10% methanol. After 2 min the concentration of methanol rose to 50% and after 12 min the solvent consisted of 100% methanol. An altering composition of the solvent had two advantages [39]:

- It allowed better resolution of the peaks in the signal of the MS/MS. If the composition of the solvent had stayed the same, some compounds might have eluted at similar retention times and their peaks might have been too crowded to distinguish them. The peaks could be separated by changing the conditions during the analysis.
- It sped up the separation in the HPLC because the polarities of the analytes varied significantly. Nonpolar analytes, which adsorbed more strongly to the stationary phase, were desorbed more quickly when the mobile phase became more nonpolar.

5.3.7.3 Method of the mass spectrometer

The MS/MS consisted of an ion source, three quadrupoles, and a detector.

An ESI interface was used as an ion source and connected the HPLC to the MS/MS. The analytes had to be separated from the solvent and ionised to continue the procedure in the MS, where the ions were separated based on their mass-to-charge ratio. A capillary ionised the analytes under high voltage. When the droplets of ions left the capillary, they were still in solution. Before they reached the MS, the solvent had evaporated. The evaporation of the solvent was assisted using high temperatures and N_2 . The evaporation consequently increased the charge density in the droplets, which is why the droplets repulsed. The individual ions were then detected in the MS [40].

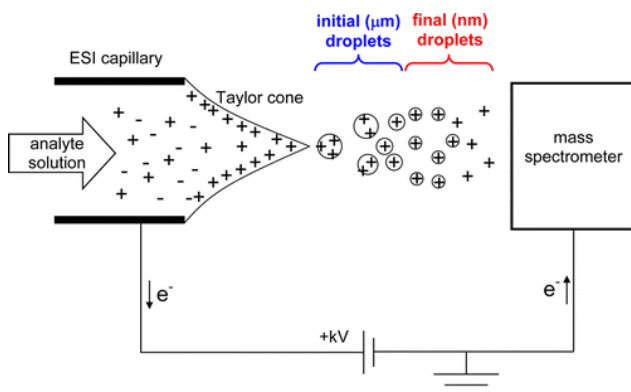


Figure 34: Schematic instrumentation of an ESI [40]

The ions from the ESI entered the first quadrupole (Q1 in figure 35), which consisted of four rods. An oscillating voltage was applied to the rods, creating an electric field. Only the ions with the right m/q reached the second quadrupole. The other ones collided with the rods, where they were neutralised (figure 36). In the second quadrupole (Q2), a collision gas split the ions into fragments. In the third quadrupole (Q3), the fragments of the ions were again separated according to their m/q , which allowed a selective identification [41]. The first and the third quadrupole were both mass filters and, therefore, the MS is called MS/MS [42].

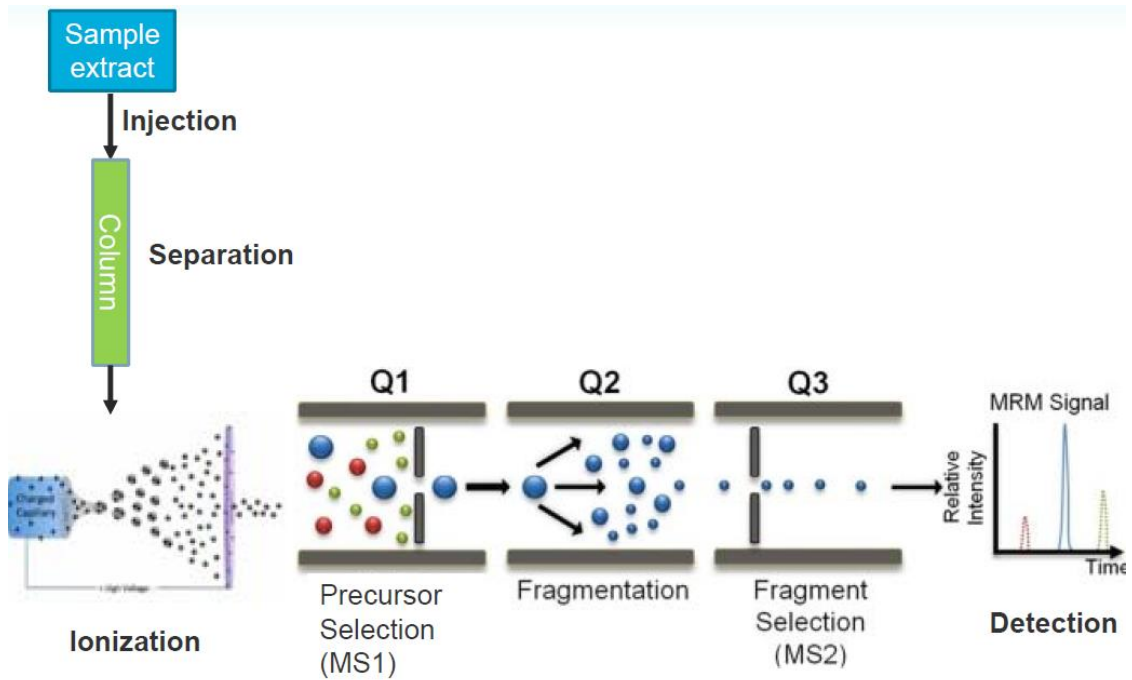


Figure 35: Schematic instrumentation of an MS/MS with three quadrupoles [34]

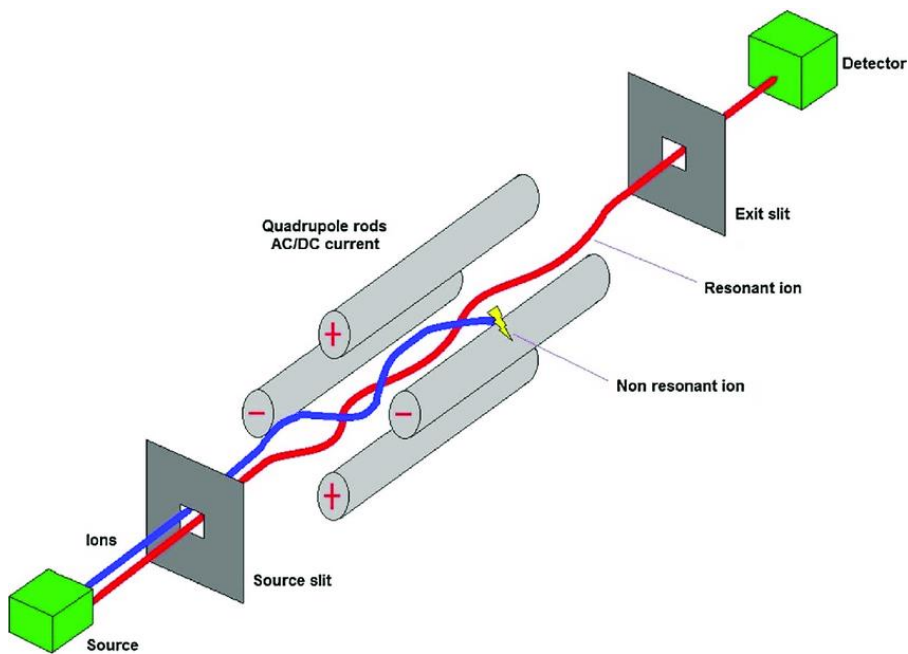


Figure 36: Schematic instrumentation of a quadrupole and the illustration of its separation method [43] (DC: direct current; AC: alternating current)

5.4 Humax samples

Besides the concentration of the substances SMOC, OA, and ESA, the composition of four Humax samples was determined. Humax samples served to determine the bulk density (BD) of the soil, which is the mass of fine soil (m_{FS}) per volume: $BD = \frac{m_{FS}}{V}$. The goal was to relate the measured concentration (analyte mass per soil mass) to the soil volume and to convert $\frac{m_{analyte}}{m_{FS}}$ into $\frac{m_{analyte}}{V}$ using the BD.

The Humax samples had the form of a cylinder with a diameter of 48 mm and a height ranging between 19 and 20 cm. The mass of fine soil in the volume of a Humax sample was measured after eliminating the other soil components.

The ground consists of three constituent parts: water, air, and solid substances. The solid phase can be subdivided into two other components: Roots, stones, and fine soil. The fine soil consists of sand, silt, and clay [44].

water			
air			
solid substances			
roots and stones (> 2 mm)	Fine soil (< 2 mm)		
	Sand (0.05 - 2 mm in diameter)	Silt (0.002 - 0.05 mm in diameter)	Clay (< 0.002 mm in diameter)

Table 10: Composition of the soil

The water content was measured by weighing the samples before and after their drying at 105 °C for 48 h.

After having eliminated weight of the water, the weight of the solid substance was left. The fine soil was washed out through a 2 mm sieve and the remaining stones and roots were weighed. The difference between the weight of the dried Humax sample (m_{dried}) and the weight of the stones and roots (m_{stones}) was the mass of the fine soil:

$$m_{FS} = m_{dried} - m_{stones}$$

5.5 Organic carbon content, soil type, grain size distribution, and pH

The OC content, the grain size distribution, and the pH are important characteristics of the soil. The OC in the soil is the energy supply for many of the organisms that inhabit it. It stores water and some minerals, manages the heat in the soil, and gives the soil structure. Moreover, it adsorbs pollutants such as SMOC [45]. The grain size distribution affects the water and air transport and storage, the availability of nutrients, and, therefore, the fertility of the soil [46]. The pH affects the availability of nutrients and the biological activity in the soil [47].

The OC content was estimated with Peter Schwab, an expert at NABO, by looking at the colour of the soil [48], [49], [44].

The soil type was determined using the Munsell soil colour charts [49].



Figure 37: Munsell colour charts with the soil

The grain size distribution was estimated by feeling and rolling the soil into a sausage shape. The characteristics of soil with a lot of sand, silt, or clay are presented in the following table [50].

	sand	silt	clay
rolling test	cannot be rolled out	can be rolled out with cracks in the surface	can be rolled out like plasticine
feel test	grainy	silky, floury	sticky and plastic (like plasticine)

Table 11: Characteristics of soil with a lot of sand, silt, or clay

The pH was estimated with a “hellige Pehameter” [51]. An indicator fluid was mixed with the soil. The resulting colour was compared with a colour pH scale.

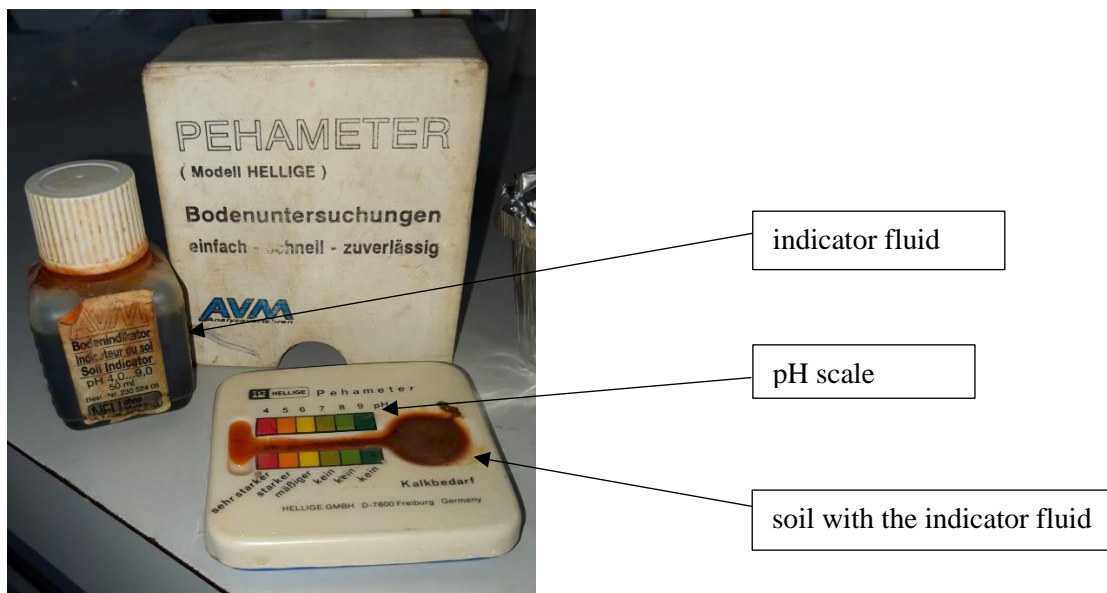


Figure 38: Hellige Pehameter

6 Model of the concentration course

A mathematical model was developed for a more detailed understanding of the S-metolachlor (SMOC) degradation and leaching processes.

The goal was to predict the concentration of SMOC, OA, and ESA depending on depth, time, and metrological data. The concentration was calculated numerically with a time-stepping finite elements approach using python. In this model, the soil is divided into thin slices and the time into short time intervals. During each time step, the mass transfer and the concentrations in every slice were calculated, beginning at the surface of the soil and progressing towards the bottom. A description of the variables can be found in chapter 6.5.

The following natural processes were simulated in the model:

Parent molecule (SMOC):

- degradation
- leaching

Metabolites (OA and ESA):

- formation (by degradation of SMOC)
- degradation
- leaching

Run-off was excluded since it was negligible for the field under study (for more reasons see chapter 8.1.6).

6.1 Water movement model

First, a water movement model was developed to describe the leaching of the pollutants. Water in this context always refers to the water stored in the pores of the soil. The water flow in unsaturated and in saturated soil is complicated [52], [53]. The water movement in the model was therefore highly simplified.

There are two types of water storages in the soil. The first type is immobile because it is stored in extremely small pores, where capillary forces are strong. The second type of water storage is transported [54]. It is called mobile water and its movement was modelled in three ways. The first two models are not explained in detail because the final model was considered to be the most realistic one. Moreover, the key ideas of the first and the second model were combined in the final model.

6.1.1 First water movement model

The first model had the following characteristics:

- The capacity of a slice was unlimited.
- The outflow of the water volume of a slice was proportional to the current water volume in the slice (red valve in figure 39). Consequently, if the inflow into a slice stopped, the water volume in the slice decreased exponentially.

Figure 39 illustrates the first water movement model.

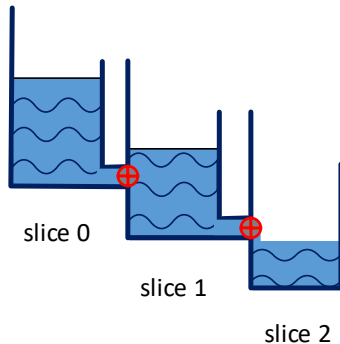


Figure 39: Water movement according to the first model (blue: water; red: proportional valve)

6.1.2 Second water movement model

The second model had the following characteristics:

- The capacity of a slice was limited and was the same for all slices.
- There were two scenarios:
 - If it was raining, a slice was filled up until it reached its capacity. During the filling, the outflow was set to zero. If the slice had reached the capacity, the outflow was equal to the inflow. During a rainy period, the slices can be visualised as jars (figure 40).
 - If it stopped raining, the water still flowed into deeper slices. The first slice was emptied first and then the second and third one followed (figure 40). In this case, the water volume flowing out of a slice during a time step was a constant and did not depend on the current water volume in the slice. If a slice was empty, its outflow stopped.

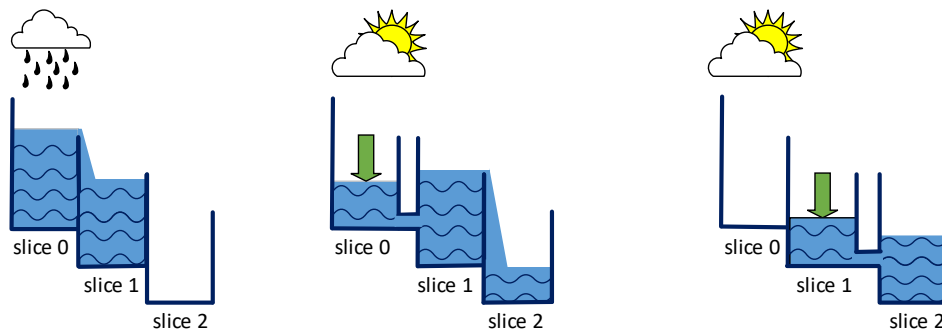


Figure 40: Water movement according to the second model during the rainy period and the dry period (The picture on the right shows the water movement during the dry period as soon as slice 0 was empty.)

6.1.3 Final water movement model

The final water movement model combined the exponential water outflow in the first model and the limited capacity of the slices in the second model. The model had the following characteristics:

- The outflow of the water volume of a slice was proportional to the current water volume in the slice.
- The capacity of a slice was limited and equal for all slices.
- There was a water reservoir of unlimited capacity. If the water in slice 0 exceeded the capacity, the water was transferred into the water reservoir. As soon as the water volume in slice 0 fell below the capacity, the water in the water reservoir was used to fill the slice up. The reservoir thus simulated ponding of the water on the soil.

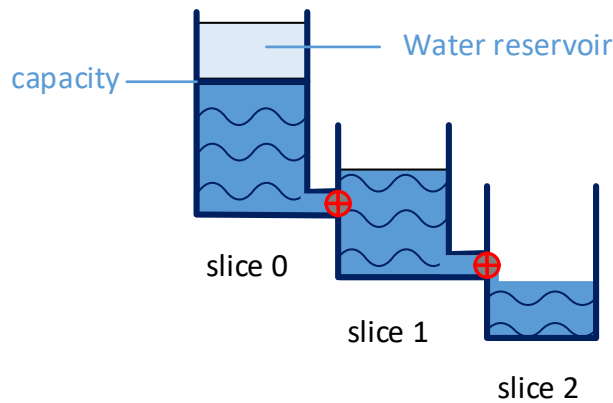


Figure 41: Water movement according to the final model (blue: water; red: proportional valve)

The mobile water volume in a slice z at time t was defined as:

$$V_w(t + \Delta t, z) = V_w(t, z) + V_{w_{in}}(t + \Delta t, z) - V_{w_{out}}(t + \Delta t, z)$$

$$V_w(t + \Delta t, z) = V_w(t, z) + \Delta t \cdot \frac{p}{d} \cdot V_w(t, z - 1) - \Delta t \cdot \frac{p}{d} \cdot V_w(t, z)$$

The water movement was assumed to be inversely proportional to the thickness of a slice (d). The thicker the slice was, the less water flowed out of a slice during Δt .

The water movement constant “ p ” was the same for all slices and was determined using the following model:

As soon as the inflow into a slice had stopped, a fully filled slice of the standard thickness $d_{standard}$ was emptied to 1% of the capacity after t_{empty} .

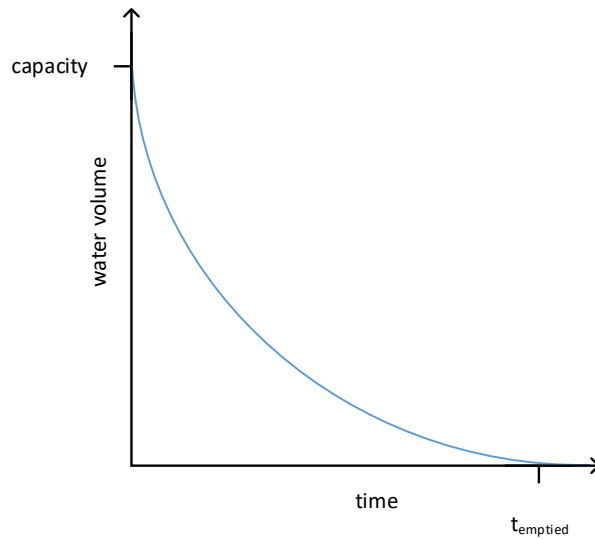


Figure 42: The water volume decline in a slice with a standard thickness $d_{standard}$ as soon as the inflow had stopped (1% of the capacity remains after $t_{emptied}$.)

$$0.01 \cdot capacity = capacity * e^{-p \cdot \frac{t_{emptied}}{d_{standard}}}$$

$$p = -\ln(0.01) \cdot \frac{d_{standard}}{t_{emptied}}$$

V_{win} of slice 0 was determined by the rainfall and the water in the reservoir. First, the rainfall was always stored in the water reservoir. Then, the water reservoir released just the right amount of water into slice 0 so that the water volume in slice 0 did not exceed a defined capacity.

Since the water volume in slice 0 was limited, the maximum outflow of slice 0 into slice 1 during Δt was limited as well ($V_{w_{out_{max}}} = \frac{\Delta t}{d} \cdot p \cdot capacity$). The reason why the water volume in the subsequent slices could not exceed the capacity either is explained below:

If the water volume in slice 0 reached the capacity, the maximum water volume flowed into slice 1. The same water volume flowed out of slice 1 and into slice 1 as soon as slice 1 had reached the capacity:

$$V_{win}(t, 1) = V_{w_{out_{max}}}$$

$$V_w(t, 1) = capacity$$

$$V_{w_{out}}(t, 1) = \frac{\Delta t}{d} \cdot p \cdot V_w(t, 1) = \frac{\Delta t}{d} \cdot p \cdot capacity = V_{w_{out_{max}}}$$

Therefore, the water volume in slice 1 stayed constant as soon as the inflow reached its maximum value and the slice was filled up to capacity:

$$V_{win}(t, 1) = V_{w_{out}}(t, 1)$$

However, integration steps that are too large can lead to a water volume exceeding the capacity, a simulation inaccuracy that is caused by the finite size of the simulation elements.

6.2 Transport and degradation of S-metolachlor

Several processes change the concentration of SMOC. Obviously, these processes take place simultaneously. Since the model was based on short time steps, it was assumed that all these processes affect the concentration instantly (figure 43 and figure 44). The sequence of the calculations of the concentration of SMOC in the soil during two time steps is shown in figure 43. The starting concentration of a time step was always the concentration of the last time step.

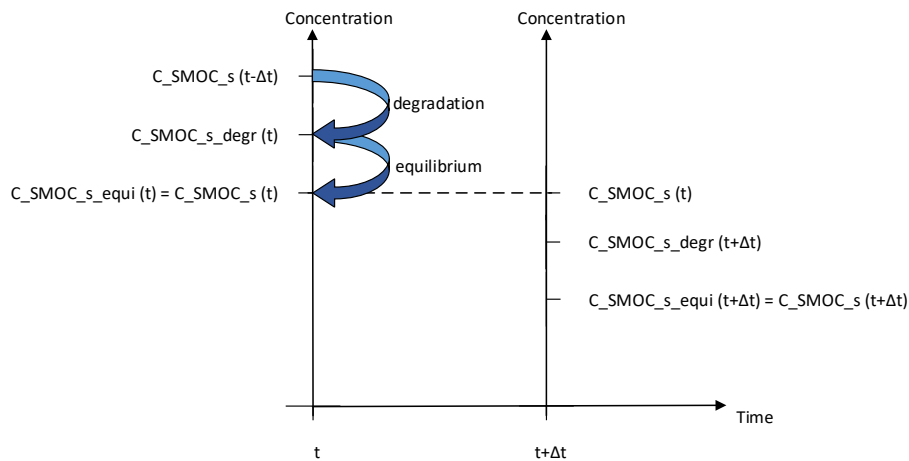


Figure 43: Sequence of the calculations of the concentrations of SMOC in a single slice in the soil from t to $t+\Delta t$ (for a description of the variables see chapter 6.5)

The sequence of the calculations of the concentration of SMOC in the water during two time steps is shown in figure 44.

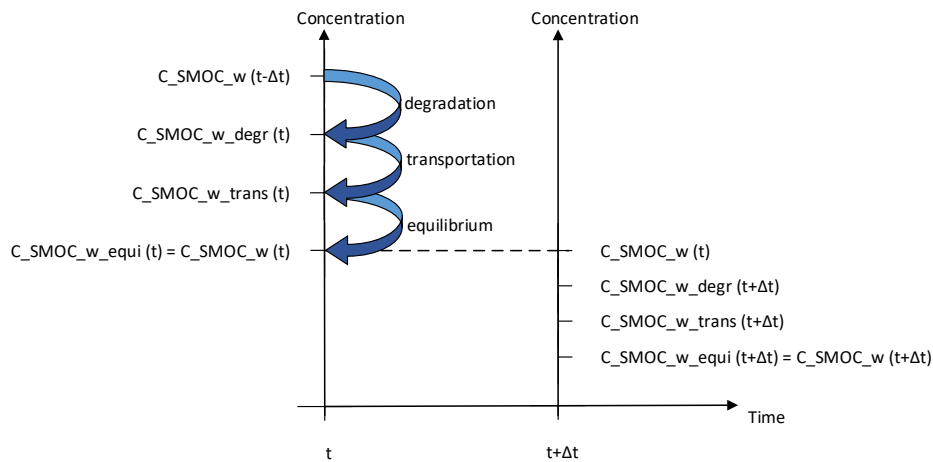


Figure 44: Sequence of the calculations of the concentrations of SMOC in a single slice in the soil water from t to $t+\Delta t$ (for a description of the variables see chapter 6.5)

6.2.1 Degradation

The degradation was modelled by an exponential concentration decline. SMOC can be dissolved in the water or adsorbed to the soil. Therefore, the degradation in the soil and in the water were considered separately. $c_{SMOC_s}(t, z)$ and $c_{SMOC_w}(t, z)$ were set equal to the concentration of SMOC in the soil and in the water respectively after the establishment of the adsorption equilibrium at the end of the previous time step (see figure 43 and figure 44).

In the soil:

$$c_{SMOC_{s_{degr}}}(t + \Delta t, z) = c_{SMOC_s}(t, z) \cdot \left(\frac{1}{2}\right)^{\frac{\Delta t}{DT50_{SMOC}}}$$

In the water:

$$c_{SMOC_{w_{degr}}}(t + \Delta t, z) = c_{SMOC_w}(t, z) \cdot \left(\frac{1}{2}\right)^{\frac{\Delta t}{DT50_{SMOC}}}$$

6.2.2 Transportation

The water transported SMOC into deeper slices. It was assumed that SMOC was evenly spread in the mobile and in the immobile water so that the concentration was the same in the mobile and immobile water. c_{SMOC_w} denotes the concentration in the soil water in ng/mL:

$$\begin{aligned} & c_{SMOC_{w_{trans}}}(t + \Delta t, z) \\ &= \frac{c_{SMOC_{w_{degr}}}(t + \Delta t, z) \cdot (V_w(t, z) + V_{w_{immobile}}) + c_{SMOC_{w_{degr}}}(t + \Delta t, z - 1) \cdot V_{w_{in}}(t + \Delta t, z)}{(V_w(t + \Delta t, z) + V_{w_{immobile}})} \\ & - \frac{c_{SMOC_{w_{degr}}}(t + \Delta t, z) \cdot V_{w_{out}}(t + \Delta t, z)}{(V_w(t + \Delta t, z) + V_{w_{immobile}})} \end{aligned}$$

For the first slice, as there was no leaching from the slice above, the term responsible for the inflow is omitted:

$$\begin{aligned} & c_{SMOC_{w_{trans}}}(t + \Delta t, 0) \\ &= \frac{c_{SMOC_{w_{degr}}}(t + \Delta t, 0) \cdot (V_w(t, 0) + V_{w_{immobile}}) - c_{SMOC_{w_{degr}}}(t + \Delta t, 0) \cdot V_{w_{out}}(t + \Delta t, 0)}{(V_w(t + \Delta t, 0) + V_{w_{immobile}})} \end{aligned}$$

6.2.3 Equilibrium

The concentrations in the water and in the soil changed after the degradation and the transportation during a time step and, therefore, the concentrations were no longer in adsorption equilibrium. In the model, it was assumed that the equilibrium is established immediately. The formula was derived from the fact that the total mass of SMOC in a slice (in the water and in the soil) before the establishment of the equilibrium equals the mass at equilibrium. The variable $c_{SMOC_{s_{equi}}}$ stands for the concentration of the adsorbed SMOC per m_{FS} , the mass of the fine soil.

$$\begin{aligned} & m_{SMOC_{w_{trans}}}(t + \Delta t, z) + m_{SMOC_{s_{degr}}}(t + \Delta t, z) \\ &= m_{SMOC_{w_{equi}}}(t + \Delta t, z) + m_{SMOC_{s_{equi}}}(t + \Delta t, z) \end{aligned}$$

$$\begin{aligned}
& c_{SMOC_{wtrans}}(t + \Delta t, z) \cdot (V_w(t + \Delta t, z) + V_{wimmob}) + c_{SMOC_{sdegr}}(t + \Delta t, z) \cdot m_{FS} \\
& = c_{SMOC_{wequi}}(t + \Delta t, z) \cdot (V_w(t + \Delta t, z) + V_{wimmob}) + c_{SMOC_{sequi}}(t + \Delta t, z) \\
& \quad \cdot m_{FS}
\end{aligned}$$

K_d denotes which portion of a substance (e.g. SMOC) is adsorbed to the soil in equilibrium:

$$K_{dSMOC} = \frac{c_{SMOC_{sequi}}}{c_{SMOC_{wequi}}}$$

And therefore:

$$\begin{aligned}
& c_{SMOC_{wtrans}}(t + \Delta t, z) \cdot (V_w(t + \Delta t, z) + V_{wimmob}) + c_{SMOC_{sdegr}}(t + \Delta t, z) \cdot m_{FS} \\
& = \frac{c_{SMOC_{sequi}}(t + \Delta t, z)}{K_{dSMOC}} \cdot (V_w(t + \Delta t, z) + V_{wimmob}) + c_{SMOC_{sequi}}(t + \Delta t, z) \\
& \quad \cdot m_{FS}
\end{aligned}$$

Solved for $c_{SMOC_{sequi}}$, the general formula was:

$$\begin{aligned}
& c_{SMOC_{sequi}}(t + \Delta t, z) \\
& = \frac{(c_{SMOC_{wtrans}}(t + \Delta t, z) \cdot (V_w(t + \Delta t, z) + V_{wimmob}) + c_{SMOC_{sdegr}}(t + \Delta t, z) \cdot m_{FS}) \cdot K_{dSMOC}}{K_{dSMOC} \cdot m_{FS} + V_w(t + \Delta t, z) + V_{wimmob}}
\end{aligned}$$

$c_{SMOC_{wequi}}(t + \Delta t, z)$ can be calculated in the following way:

$$c_{SMOC_{wequi}} = \frac{c_{SMOC_{sequi}}}{K_{dSMOC}}$$

At the end of a time step, $c_{SMOC_{sequi}}(t + \Delta t, z)$ and $c_{SMOC_{wequi}}(t + \Delta t, z)$ were equalised to $c_{SMOC_s}(t + \Delta t, z)$ and $c_{SMOC_w}(t + \Delta t, z)$. $c_{SMOC_s}(t + \Delta t, z)$ and $c_{SMOC_w}(t + \Delta t, z)$ were the starting concentrations of the next time step.

6.3 Metabolites

The formulas for the metabolites were basically the same ones as the ones for SMOC. The difference lay in the formation of the metabolites. The procedure is exemplified here with the metabolite OA.

The sequence of the calculations of the concentration of OA in the soil during two time steps is shown in figure 45.

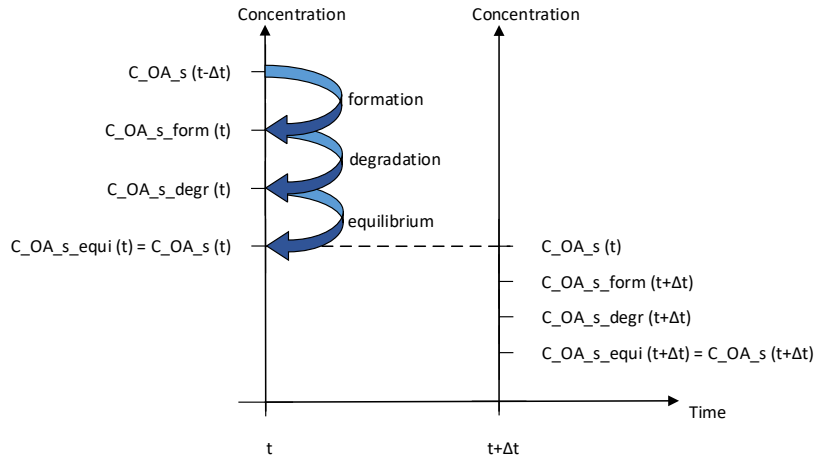


Figure 45: Sequence of the calculations of the concentrations of OA in a single slice in the soil from t to $t+\Delta t$ (for a description of the variables see chapter 6.5)

The sequence of the calculations of the concentration of OA in the water during two time steps is shown in figure 46.

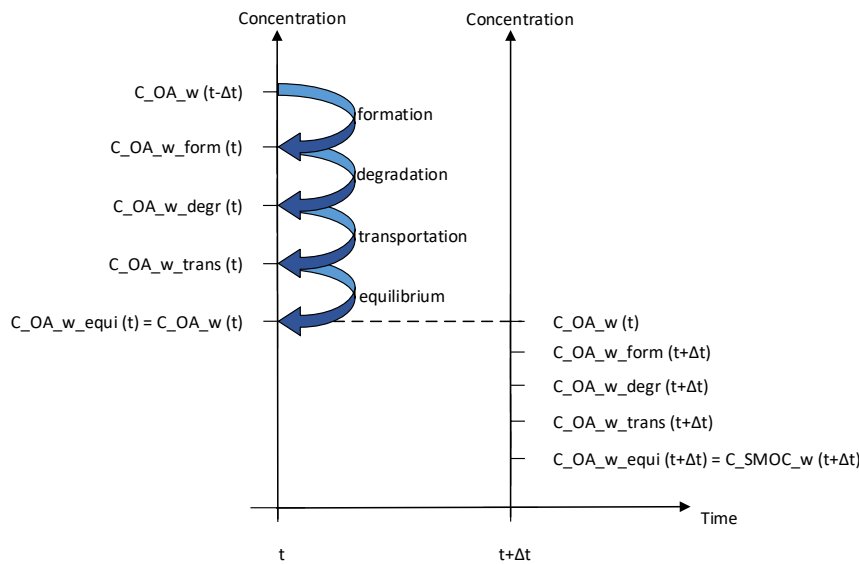


Figure 46: Sequence of the calculations of the concentrations of OA in a single slice in the water in the soil from t to $t+\Delta t$ (for a description of the variables see chapter 6.5)

6.3.1 Formation

The formation of the OA in the soil and the water was defined as $\left(c_{SMOC_s}(t, z) - c_{SMOC_s_{degr}}(t + \Delta t, z) \right) \cdot OF_{OA}$, resulting in the following concentration after their formation:

$$c_{OA_s_{form}}(t + \Delta t, z) = c_{OA_s}(t, z) + \left(c_{SMOC_s}(t, z) - c_{SMOC_s_{degr}}(t + \Delta t, z) \right) \cdot OF_{OA}$$

$$c_{OA_w_{form}}(t + \Delta t, z) = c_{OA_w}(t, z) + \left(c_{SMOC_w}(t, z) - c_{SMOC_w_{degr}}(t + \Delta t, z) \right) \cdot OF_{OA}$$

The equations for the transportation and equilibrium of the metabolites were based on the same principle as those of SMOC.

6.4 Comparison with the field measurements

This chapter describes how to compare the results of the model with the measured concentrations in the field. It had to be considered that $c_{SMOC_s}(t, 0)$ of the model did not necessarily correspond to the measured concentration in the first layer of the field, which is due to the following reasons:

- The concentration of the field samples also included the mass of SMOC in the soil water because they were dried.
- Slice 0 might be thinner than the measured layer depending on the chosen thickness of the slices (figure 47).

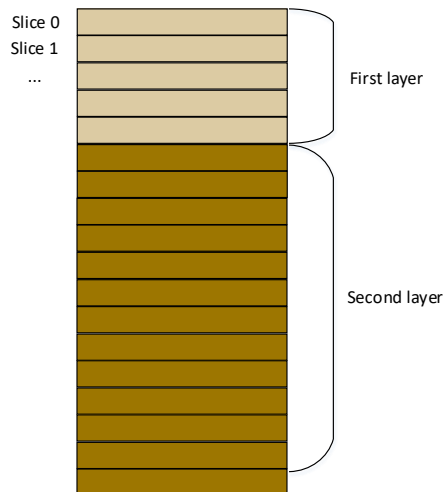


Figure 47: The difference between the measured layers and the first slices with a thickness of 1 cm

These two aspects were considered when the measured concentrations after the application were used as the starting concentrations of the model (chapter 6.4.1) and when the concentrations of the model were compared with the measurements (chapter 6.4.2).

6.4.1 Starting concentration of the model

The measured mass of SMOC in the first dried field sample after the application ($m_{SMOC_{field}}(0, z)$) had to be the same as the added mass of SMOC in the soil ($m_{SMOC_s}(0, z)$) and in the water ($m_{SMOC_w}(0, z)$) of the model. It was assumed that the starting concentrations were in equilibrium.

$$m_{SMOC_s}(0, z) + m_{SMOC_w}(0, z) = m_{SMOC_{field}}(0, z)$$

$$c_{SMOC_s}(0, z) \cdot m_{FS} + c_{SMOC_w} \cdot (V_w(0, z) + V_{w_{immobile}}) = c_{SMOC_{field}}(0, z) \cdot m_{FS}$$

$$c_{SMOC_w} = \frac{c_{SMOC_s}}{K_{d_{SMOC}}}$$

The starting concentration in the soil and in the water of the model was therefore defined as:

$$c_{SMOC_s}(0, z) = \frac{c_{SMOC_{field}}(0, z) \cdot m_{FS} \cdot K_{d_{SMOC}}}{K_{d_{SMOC}} \cdot m_{FS} + V_w(0, z) + V_{w_{immobile}}}$$

$$c_{SMOC_w}(0, z) = \frac{c_{SMOC_{field}}(0, z) \cdot m_{FS}}{K_{d_{SMOC}} \cdot m_{FS} + V_w(0, z) + V_{w_{immobile}}}$$

The concentrations of all slices of the model included in the first layer of the field were calculated based on the $c_{SMOC_{field}}$ of the first layer. The ones included in the second layer were calculated based on the $c_{SMOC_{field}}$ of the second layer (figure 47).

6.4.2 Comparison with the field measurement

After having calculated all concentrations, the results of the model were compared with the measured field concentrations. In order to do so, the results of the model ($c_{SMOC_{result}}(t, z)$) were also expressed as the sum of the mass of SMOC in the soil and in the water:

$$m_{SMOC_{result}}(t, z) = m_{SMOC_s}(t, z) + m_{SMOC_w}(t, z)$$

$$c_{SMOC_{result}}(t, z) = \frac{c_{SMOC_s}(t, z) \cdot m_{FS} + c_{SMOC_w}(t, z) \cdot (V_w(t, z) + V_{w_{immobile}})}{m_{FS}}$$

The results of the concentrations in the first and second layer were averaged over all the slices of the first and the second layer respectively (figure 47).

6.5 Variables

variable	meaning
t	the time after application measured in 10 min
Δt	the time interval between two time steps in 10 min
z	the slice number in the soil ($z = 0 =$ first slice)
d	the thickness of a slice in m
$V_w(t, z)$	the volume of the mobile water in slice z at the time t in mL
$V_{w_{in}}(t + \Delta t, z)$	the water volume that was transported into the slice z from t to $t + \Delta t$ in mL
$V_{w_{out}}(t + \Delta t, z)$	the water volume that was transported out of the slice z from t to $t + \Delta t$ in mL
p	the constant that determined the speed of the water movement.
$t_{emptied}$	the time required to empty a slice with thickness $d_{standard}$ to 1% of the capacity as soon as the inflow had stopped (measured in 10 min)
$d_{standard}$	the standard thickness of a slice of the defined emptying process (see $t_{emptied}$) in m
<i>capacity</i>	the water holding capacity of a slice in mL
$V_{w_{out_{max}}}$	the maximum possible water outflow of a slice during Δt
$c_{SMOC_s}(t, z)$	the concentration of SMOC in the soil in the slice z at the end of a time step t and at the start of the next time step $t + \Delta t$ in ng/g
$c_{SMOC_w}(t, z)$	the concentration of SMOC in the water in the slice z at the end of a time step t and at the start of the next time step $t + \Delta t$ in ng/mL
$c_{SMOC_{s_{degr}}}(t, z)$	the concentration of SMOC in the soil in the slice z at time t after degradation in ng/g
$c_{SMOC_{w_{degr}}}(t, z)$	the concentration of SMOC in the water in the slice z at time t after degradation in ng/mL
$DT50_{SMOC}$	the half-life time of SMOC (measured in 10 min)
$c_{SMOC_{w_{trans}}}(t, z)$	the concentration of SMOC in the water in the slice z at time t after transportation in ng/mL
$V_{w_{immobile}}$	the immobile water volume in a slice in mL
$m_{SMOC_{s_{degr}}}(t, z)$	the mass of SMOC in the soil in the slice z at time t after degradation in ng
$m_{SMOC_{w_{trans}}}(t, z)$	the mass of SMOC in the water in the slice z at time t after transportation in ng
$m_{SMOC_{s_{equi}}}(t, z)$	the mass of SMOC in the soil in the slice z at time t after the establishment of the adsorption equilibrium in ng
$m_{SMOC_{w_{equi}}}(t, z)$	the mass of SMOC in the water in the slice z at time t after the establishment of the adsorption equilibrium in ng

variable	meaning
$c_{SMOC_{s_{equi}}}(t, z)$	the concentration of SMOC in the soil in the slice z at time t after the establishment of the adsorption equilibrium in ng/g
$c_{SMOC_{w_{equi}}}(t, z)$	the concentration of SMOC in the water in the slice z at time t after the establishment of the adsorption equilibrium in ng/mL
$K_{d_{SMOC}}$	the soil adsorption coefficient for SMOC in mL/g
OC	the organic carbon content in the soil in %
m_{FS}	the mass of fine soil in a slice in g
$c_{OA_s}(t, z)$	the concentration of OA in the soil in the slice z at the end of a time step t and at the start of the next time step $t + \Delta t$ in ng/g
$c_{OA_w}(t, z)$	the concentration of OA in the water in the slice z at the end of a time step t and at the start of the next time step $t + \Delta t$ in ng/g
$c_{OA_s_{form}}(t, z)$	the concentration of OA in the soil in the slice z at time t after formation in ng/g
$c_{OA_w_{form}}(t, z)$	the concentration of OA in the water in the slice z at time t after formation in ng/mL
OF_{OA}	the occurrence fraction of OA
$c_{OA_s_{degr}}(t, z)$	the concentration of OA in the soil in the slice z at time t after degradation in ng/g
$c_{OA_w_{degr}}(t, z)$	the concentration of OA in the water in the slice z at time t after degradation in ng/mL
$c_{OA_w_{trans}}(t, z)$	the concentration of OA in the water in the slice z at time t after transportation in ng/mL
$c_{OA_s_{equi}}(t, z)$	the concentration of OA in the soil in the slice z at time t after the establishment of the adsorption equilibrium in ng/g
$c_{OA_w_{equi}}(t, z)$	the concentration of OA in the water in the slice z at time t after the establishment of the adsorption equilibrium in ng/mL
$m_{SMOC_{field}}(t, z)$	the measured mass of SMOC in the field in the slice z at time t after the application in ng
$m_{SMOC_s}(t, z)$	the calculated mass of SMOC in the soil in the slice z at time t in ng
$m_{SMOC_w}(t, z)$	the calculated mass of SMOC in the water in the slice z at time t in ng
$c_{SMOC_{field}}(t, z)$	the measured concentration of SMOC in the field in the slice z at time t after the application in ng/g
$m_{SMOC_{result}}(t, z)$	the model result of the mass of SMOC in the slice z at time t after the application in ng
$c_{SMOC_{result}}(t, z)$	the model result of the concentration of SMOC in the slice z at time t after the application in ng/g

Table 12: Meaning of the variables and the parameters

7 Results of the field measurements

7.1 Bulk density and soil characteristics

Humax samples serve to determine the bulk density (BD) of the soil, which is the mass of fine soil (m_{FS}) per volume: $BD = \frac{m_{FS}}{V}$. The goal was to convert the measured concentration of the analyte from $\frac{m_{analyte}}{m_{FS}}$ into $\frac{m_{analyte}}{V}$ using the BD. The mass of SMOC per volume of the soil was necessary to calculate the mass of SMOC in the field and to calculate the application rate of the PPP (chapter 8.1.3).

Eight Humax samples were taken on two days: on the first sampling day after the application and on the last sampling day.

date	sample name	h (cm)	d (mm)	V (cm ³)	initial mass (g)	mass of water (g)	mass of SS without FS (g)	mass of FS (g)	BD FS (g/cm ³)
28.05.20	A1	20.5	48	370.96	414.41	101.01	64.1	249.35	0.67
28.05.20	B1	19	48	343.82	391.28	113.89	14.1	263.31	0.77
28.05.20	C1	20.3	48	367.34	392.30	122.63	8.3	261.34	0.71
28.05.20	D1	19.3	48	349.24	460.66	130.20	10.8	319.64	0.92
17.07.20	A2	20	48	361.91	442.95	135.96	12.9	294.06	0.81
17.07.20	B2	20	48	361.91	482.75	135.38	10.2	337.13	0.93
17.07.20	C2	20	48	361.91	443.52	133.48	15.6	294.43	0.81
17.07.20	D2	19	48	343.82	393.69	108.39	6.7	278.62	0.81

Table 13: Composition of the Humax samples (h: the height of the cylinder of the Humax samples; d: the diameter of the cylinder of the Humax samples; V: the volume of the cylinder of the Humax sample; SS: solid substance; FS: fine soil, BD: bulk density)

The confidence interval (CI) was calculated based on the standard deviation (σ), the number of samples (n), and a constant (z) for the t-distribution interval with a confidence level of 95% (two-sided), which is 3.182 for three degrees of freedom (= number of samples - 1). The mean, the standard deviation (SD), and the CI of the BD are shown in table 14.

$$CI = z \cdot \frac{\sigma}{\sqrt{n}} = 3.182 \cdot \frac{\sigma}{2}$$

date	mean (g/cm ³)	SD (g/cm ³)	CI (g/cm ³)
28.05.20	0.77	0.11	0.17
17.07.20	0.84	0.06	0.09

Table 14: The mean, the standard deviation (SD), and the confidence intervals (CI) of the BD (t-distribution, confidence level 95%, two-sided)

The Humax samples were only taken on two dates. In order to calculate the BD for all dates during the sampling, it was assumed that the soil steadily densified over time (t=the time after the application):

$$BD(t) = \frac{BD_2 - BD_1}{\Delta t} \cdot t + BD_1 = \frac{0.07 \frac{g}{cm^3}}{50 d} \cdot t + 0.77 \frac{g}{cm^3}$$

The soil characteristics, shown in table 15, were estimated and they turned out to be identical for both layers. The pH was visually estimated by using a hellige Pehameter [51] and the humus content was visually estimated using a colour table [48], [49]. The OC content was calculated based on the humus content: $\%OC = \frac{\% Humus}{1.72}$. The clay, silt, and sand content were estimated by feeling the texture [50]. The soil type was determined by comparing its colour to the Munsell-colour chart [49].

measure	results
pH	< 5 (approximately 4.9)
humus ($\frac{m_{humus} [\frac{g}{g}]}{m_{FS}}$) %	2.2 (slightly over 2)
OC ($\frac{m_{oc} [\frac{g}{g}]}{m_{FS}}$) %	1.28
clay ($\frac{m_{clay} [\frac{g}{g}]}{m_{FS}}$) %	18 (clearly more than 15 but less than 21)
silt ($\frac{m_{silt} [\frac{g}{g}]}{m_{FS}}$) %	30 (clearly less than 40)
sand ($\frac{m_{sand} [\frac{g}{g}]}{m_{FS}}$) %	52
Munsell-colour	10 YR 4.5/2
soil type	Profound, acidic brown soil
topsoil	Acidic, low humus content, slightly skeletal sandy clay

Table 15: Soil characteristics of the soil in Arth (OC: organic carbon; m_{oc} : mass of organic carbon; m_{FS} : mass of fine soil). Both layers showed identical characteristics.

7.2 Results S-metolachlor

7.2.1 Concentrations of S-metolachlor

The concentration of S-metolachlor (SMOC) was determined for 68 days in a cornfield in Arth in two layers 0-5 cm and 5-17 cm, which are referred to as first and second layer. From here on, a sample always refers to the composite sample of a layer which is the entirety of the 25 individual samples of a single sampling. The eight samples of the first layer and the four samples of the second layer were analysed after extraction with an HPLC-MS/MS device. The concentrations were expressed in ng of SMOC per g of fine soil.

The concentration of ng SMOC per cm³ of soil was calculated in the following way:

$$c_{SMOC} \left[\frac{ng}{cm^3} \right] (t) = \frac{m_{SMOC}}{m_{FS}} \cdot \frac{m_{FS}}{V_{soil}} = c_{SMOC} \left[\frac{ng}{g} \right] (t) \cdot BD (t)$$

V_{soil} = the volume of the Humax sample in cm³

m_{FS} = the mass of fine soil in the Humax sample in g

$BD(t)$ = the bulk density of the Humax sample in g/cm³, t days after the application of SMOC (calculations in chapter 7.1)

Table 16 shows the concentrations of SMOC in the first and second layer.

sample	date	concentration [ng/g]	concentration [ng/cm ³]
background presence (0-5 cm)	10.05.2020	3.56	2.63
sample 1 (0-5 cm)	28.05.2020	1489.63	1141.31
sample 2 (0-5 cm)	31.05.2020	1131.78	871.80
sample 3 (0-5 cm)	03.06.2020	936.12	725.16
sample 5 (0-5 cm)	07.06.2020	458.65	358.38
sample 5 (5-17 cm)	07.06.2020	112.52	87.92
sample 6 (0-5 cm)	11.06.2020	328.28	258.48
sample 6 (5-17 cm)	11.06.2020	92.23	72.62
sample 10 (0-5 cm)	21.06.2020	171.85	137.85
sample 10 (5-17 cm)	21.06.2020	50.18	40.25
sample 20 (0-5 cm)	17.07.2020	47.35	39.87
sample 20 (5-17 cm)	17.07.2020	13.97	11.77

Table 16: Results of SMOC

The measured concentrations in ng/g for both layers are plotted in figure 48.

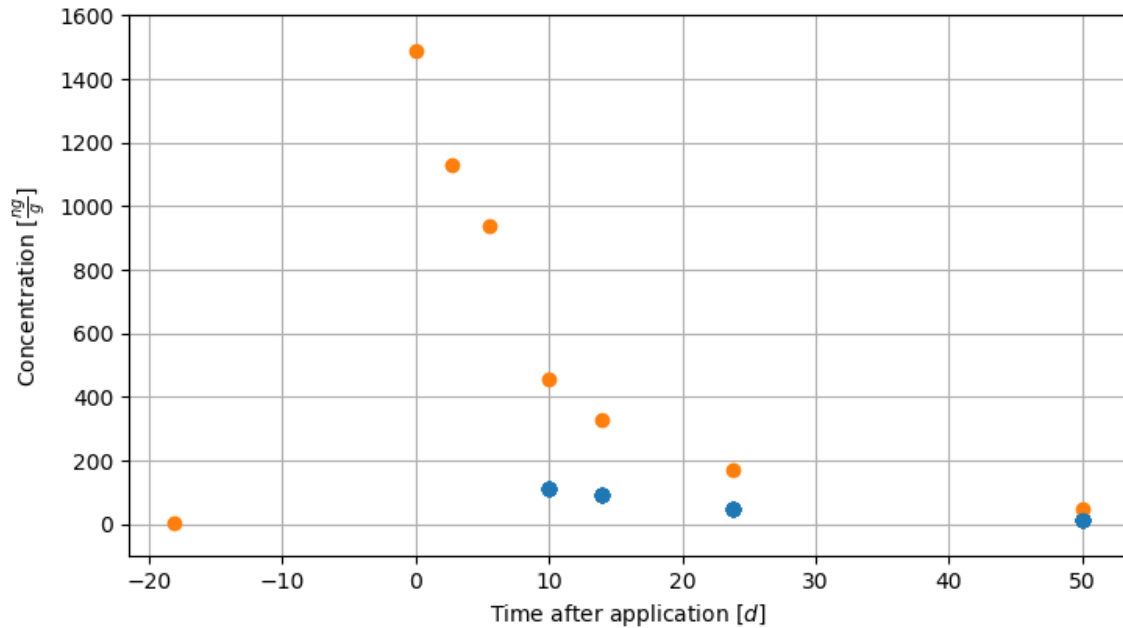


Figure 48: Time course of the concentration of SMOC in two soil layers (orange dots: first layer (0-5 cm), blue dots: second layer (5-17 cm))

7.2.2 Half-life of S-metolachlor

In order to compare the rate of the concentration decline between sample n and sample n+1 to the rate of the concentration decline between sample n+1 and n+2, the half-life (degradation time DT50) between the concentration in sample n and sample n+1 was calculated:

$$c_{n+1} = c_n \cdot \left(\frac{1}{2}\right)^{\frac{\Delta t}{DT50}}$$

$$DT50 = -\ln(2) \cdot \frac{\Delta t}{\ln\left(\frac{c_{n+1}}{c_n}\right)}$$

The determined DT50 of SMOC are shown in figure 49. Sample 1-2 means that the DT50 was calculated between samples 1 and 2.

sample interval	DT50 [d]
sample 1-2 (0-5 cm)	6.85
sample 2-3 (0-5 cm)	10.47
sample 3-5 (0-5 cm)	4.32
sample 5-6 (0-5 cm)	8.20
sample 5-6 (5-17 cm)	13.80
sample 6-10 (0-5 cm)	10.47
sample 6-10 (5-17 cm)	11.13
sample 10-20 (0-5 cm)	14.11
sample 10-20 (5-17 cm)	14.23

Table 17: DT50 between two samples

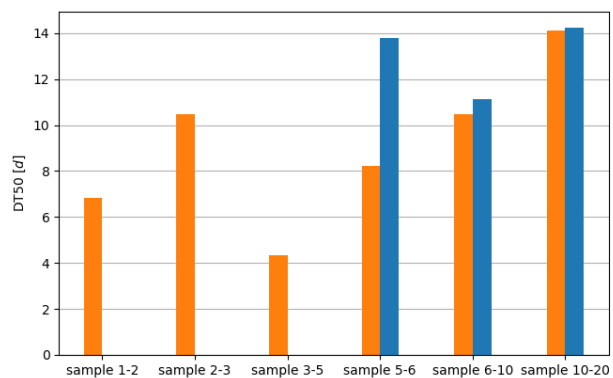


Figure 49: DT50 between two samples of the first (orange) and the second layer (blue)

7.3 Results metolachlor oxanilic acid (OA)

Metolachlor oxanilic acid (OA) is a metabolite of SMOC. The method to measure the concentration of OA in two layers (0-5 cm and 5-17 cm) was the same as the one for SMOC. The concentration of OA was too low in the first four samples to be detected.

sample	date	concentration [ng/g]	concentration [ng/cm ³]
background presence (0-5 cm)	10.05.2020	0	0
sample 1 (0-5 cm)	28.05.2020	0	0
sample 2 (0-5 cm)	31.05.2020	0	0
sample 3 (0-5 cm)	03.06.2020	0	0
sample 5 (0-5 cm)	07.06.2020	4.33	3.39
sample 5 (5-17 cm)	07.06.2020	4.98	3.89
sample 6 (0-5 cm)	11.06.2020	8.19	6.45
sample 6 (5-17 cm)	11.06.2020	7.89	6.21
sample 10 (0-5 cm)	21.06.2020	12.55	10.07
sample 10 (5-17 cm)	21.06.2020	11.89	9.54
sample 20 (0-5 cm)	17.07.2020	6.89	5.80
sample 20 (5-17 cm)	17.07.2020	4.89	4.12

Table 18: Results of OA

Figure 50 presents the results.

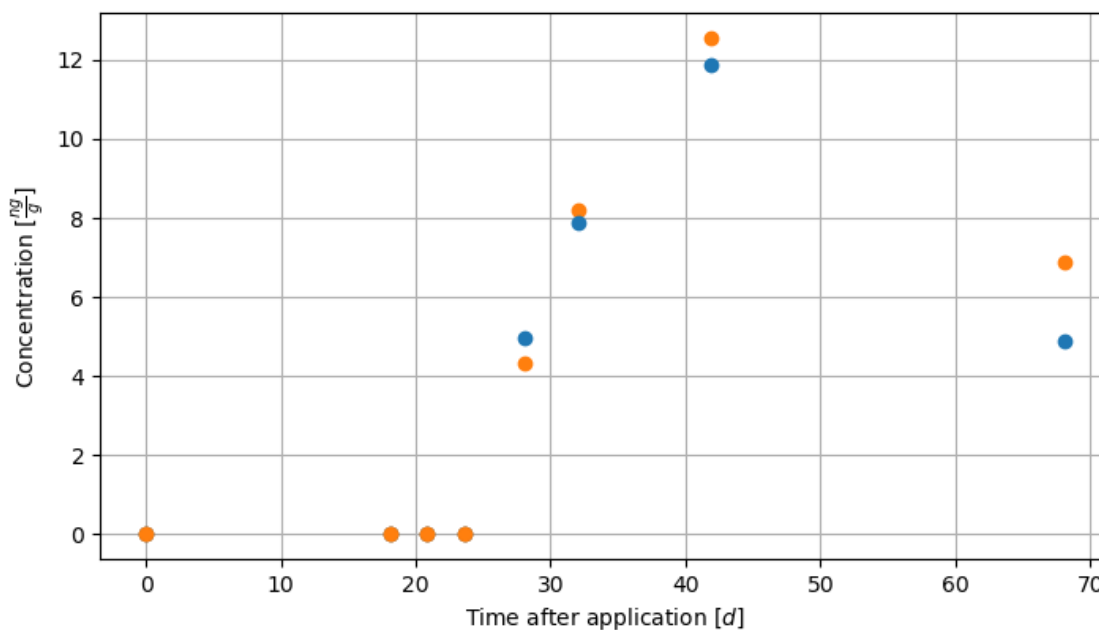


Figure 50: Concentration of OA in the two layers (orange: first layer (0-5 cm); blue: second layer (5-17 cm))

7.4 Results metolachlor ethane sulfonic acid (ESA)

Metolachlor ethane sulfonic acid (ESA) is another metabolite of SMOC. The method to measure the concentration of ESA in two layers (0-5 cm and 5-17 cm) was the same as the one for SMOC. The concentration of ESA was too low in the first four samples to be detected.

sample	date	concentration [ng/g]	concentration [ng/cm ³]
background presence (0-5 cm)	10.05.2020	0	0
sample 1 (0-5 cm)	28.05.2020	0	0
sample 2 (0-5 cm)	31.05.2020	0	0
sample 3 (0-5 cm)	03.06.2020	0	0
sample 5 (0-5 cm)	07.06.2020	4.14	3.23
sample 5 (5-17 cm)	07.06.2020	5.15	4.02
sample 6 (0-5 cm)	11.06.2020	6.35	5.00
sample 6 (5-17 cm)	11.06.2020	7.52	5.92
sample 10 (0-5 cm)	21.06.2020	7.82	6.28
sample 10 (5-17 cm)	21.06.2020	12.88	10.33
sample 20 (0-5 cm)	17.07.2020	3.70	3.12
sample 20 (5-17 cm)	17.07.2020	7.69	6.47

Table 19: Results of ESA

Figure 51 visualises the results.

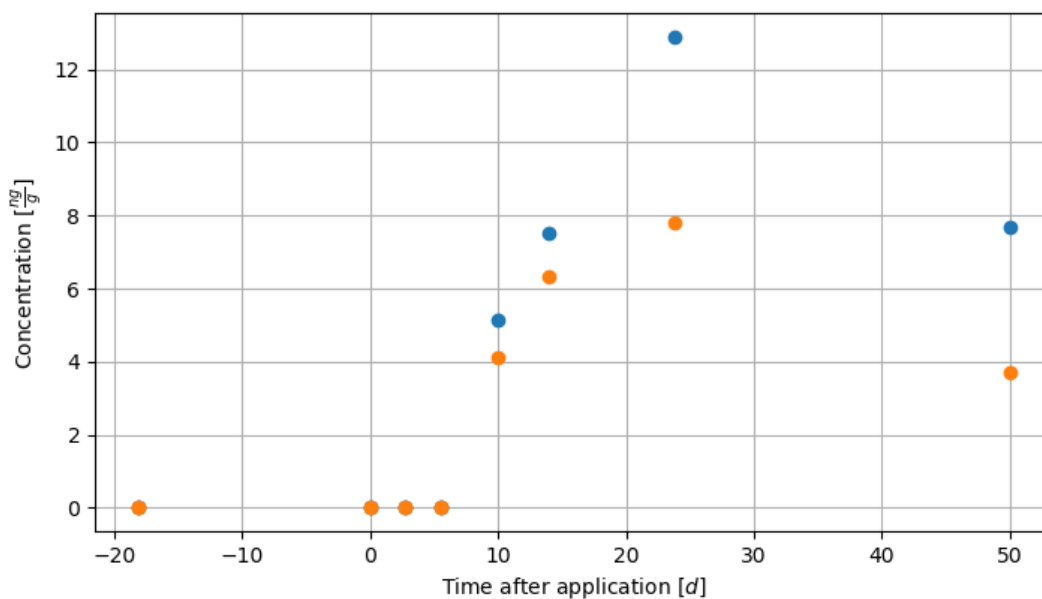


Figure 51: Concentration of ESA in the two layers (orange: first layer (0-5 cm); blue: second layer (5-17 cm))

7.5 Results of the control samples

An overview of the types and the characteristics of the control samples can be found in chapter 5.3.2.4.

7.5.1 Limit of quantification

The LOQ is the lowest concentration of the analyte that can be reliably quantitated as an exact value [38].

The formulas for the LOQ are only applicable if the HPLC-MS/MS could detect an amount of the analyte in the two prepared blank samples (chapter 5.3.5.3). The predicted concentration of the analytes in the blank samples is 0 ng/g. However, due to contamination during the analytical procedure, the concentration in the blank samples is usually higher than 0 ng/g.

7.5.1.1 S-metolachlor

HPLC-MS/MS could detect a quantity of SMOC in the two prepared blank samples. Therefore, the following formula for the LOQ was used [55]:

$$LOQ = \bar{c}_{blank} + 10 \cdot sd_{blank}$$

\bar{c}_{blank} = the mean of the concentration in the two blank samples

sd_{blank} = the sample standard deviation of the measured concentration in the two blank samples

The measured concentrations in the two blank samples and the LOQ are shown in table 20. The result of the LOQ need to be put into perspective because two blank samples are statistically not relevant – usually, 20 blank samples are measured [56]. However, it was out of the scope of a matura project to measure 20 blank samples.

concentration blank 1 [ng/g]	0.16
concentration blank 2 [ng/g]	0.15
\bar{c}_{blank} [ng/g]	0.16
sd_{blank} [ng/g]	0.01
LOQ [ng/g]	0.26

Table 20: LOQ of SMOC (blue: measurements; orange: calculations)

7.5.1.2 Metabolites

The HPLC-MS/MS could not detect any of the metabolites OA and ESA in the two prepared blank samples. Therefore, the LOQ was determined visually with the signal-to-noise ratio in the HPLC-MS/MS. In this case, the LOQ is the lowest concentration in the calibration samples where the signal is ten times higher than the noise.

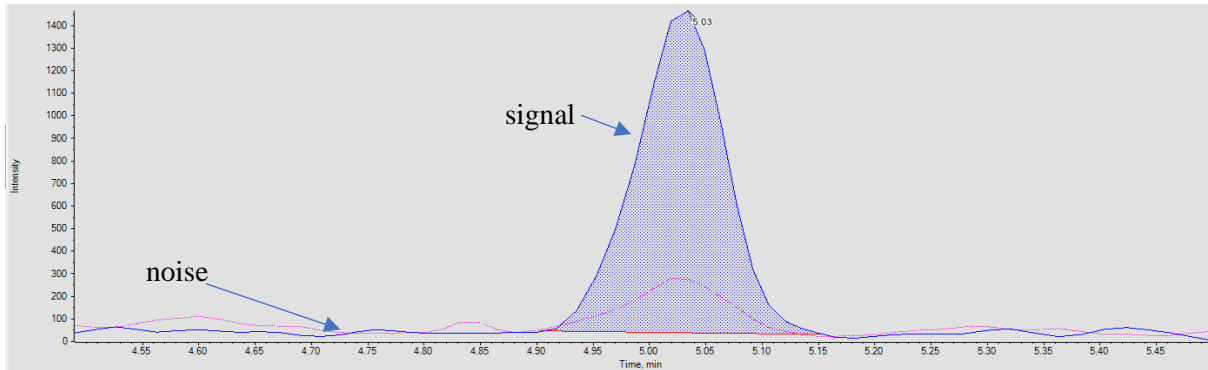


Figure 52: Signal and noise in the LOQ of OA (concentration = 2 ng/g)

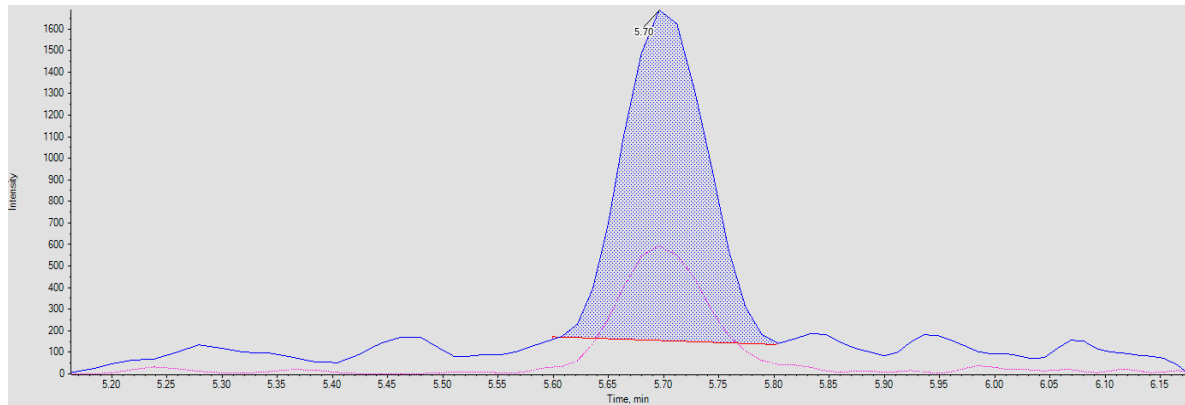


Figure 53: Signal and noise in the LOQ of ESA (concentration = 1 ng/g)

	OA	ESA
LOQ [ng/g]	2.00	1.00

Table 21: LOQ of ESA and OA

7.5.2 Relative recovery

The relative recovery measures the accuracy of the method. It was calculated using the concentration of the two spiked samples.

The relative recovery was defined as:

$$\text{relative recovery [\%]} = \frac{\bar{c}_{\text{spiked_sample}} - c_{\text{background}}}{c_{\text{spiked}}} \cdot 100$$

The average concentration of the two spiked samples was used for $\bar{c}_{\text{spiked_sample}}$ and c_{spiked} was 10 ng/g (chapter 5.3.5.3).

The relative recoveries of SMOC, OA, and ESA are shown in table 22. There were only two spiked samples, which is why the results need to be put into perspective.

	SMOC	OA	ESA
concentration in spike 1 [ng/g]	15.63	11.32	10.38
concentration in spike 2 [ng/g]	14.23	9.43	9.67
$\bar{c}_{\text{spiked_sample}}$ [ng/g]	14.93	10.37	10.03
c_{spiked} [ng/g]	10	10	10
$c_{\text{background}}$ [ng/g]	3.56	0	0
relative recovery [%]	113.65	103.73	100.28

Table 22: Relative recovery of SMOC, OA, and ESA (blue: measurements; orange: calculations)

7.5.3 Method precision

The method precision reflects the precision of the method by comparing the concentration in the spiked samples [57]. It measures the random errors of a method whereas the relative recovery measures a systematic error. The difference between accuracy (relative recovery) and precision (method precision) is shown in figure 54.

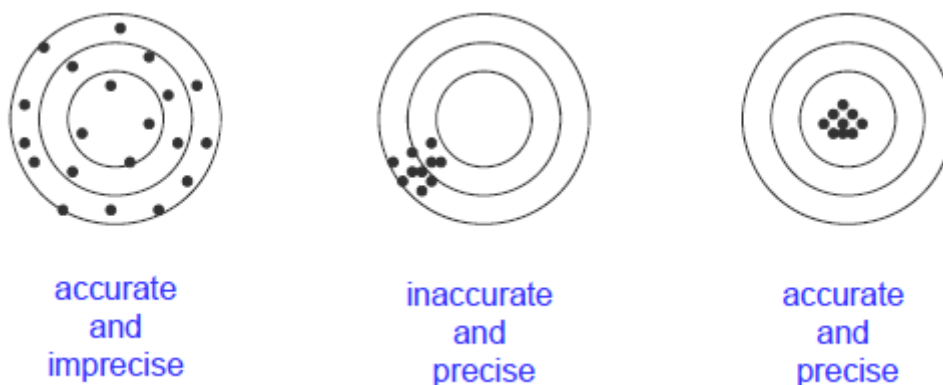


Figure 54: The difference between accuracy and precision [34]

$$\text{precision} = \frac{sd_{\text{spiked_sample}}}{\bar{c}_{\text{spiked_sample}}} \cdot 100$$

$\bar{c}_{\text{spiked_sample}}$ = the mean of the concentrations in the two spiked samples

$sd_{\text{spiked_sample}}$ = the sample standard deviation of the measured concentrations in the spiked samples

The method precisions for SMOC, OA, and ESA are shown in table 23. Again, there were only two spiked samples, which is not relevant in statistical terms.

	SMOC	OA	ESA
concentration in spike 1 [ng/g]	15.63	11.32	10.38
concentration in spike 2 [ng/g]	14.23	9.43	9.67
\bar{c}_{spiked_sample} [ng/g]	14.93	10.37	10.03
sd_{spiked_sample} [ng/g]	0.99	1.34	0.50
method precision [%]	6.63	12.87	5.03

Table 23: Method precision of the analysis for SMOC, OA, and ESA (blue: measurements, orange: calculations)

7.5.4 Blank sample in the HPLC-MS/MS and blind sample in the HPLC-MS/MS

In addition to the extraction blank and the spiked samples, there were two more control samples (chapter 5.3.2.4):

1. The blank sample of the HPLC-MS/MS
2. The blind sample of the HPLC-MS/MS

The concentrations of SMOC, OA, and ESA in the blank and the blind sample of the HPLC-MS/MS were under the detection limit. Therefore, no contamination in the HPLC-MS/MS nor in the IS was detected.

8 Discussion of the field measurement

8.1 Discussion of S-metolachlor

The numbers of the samples in the following chapter refer to the numbering in figure 55.

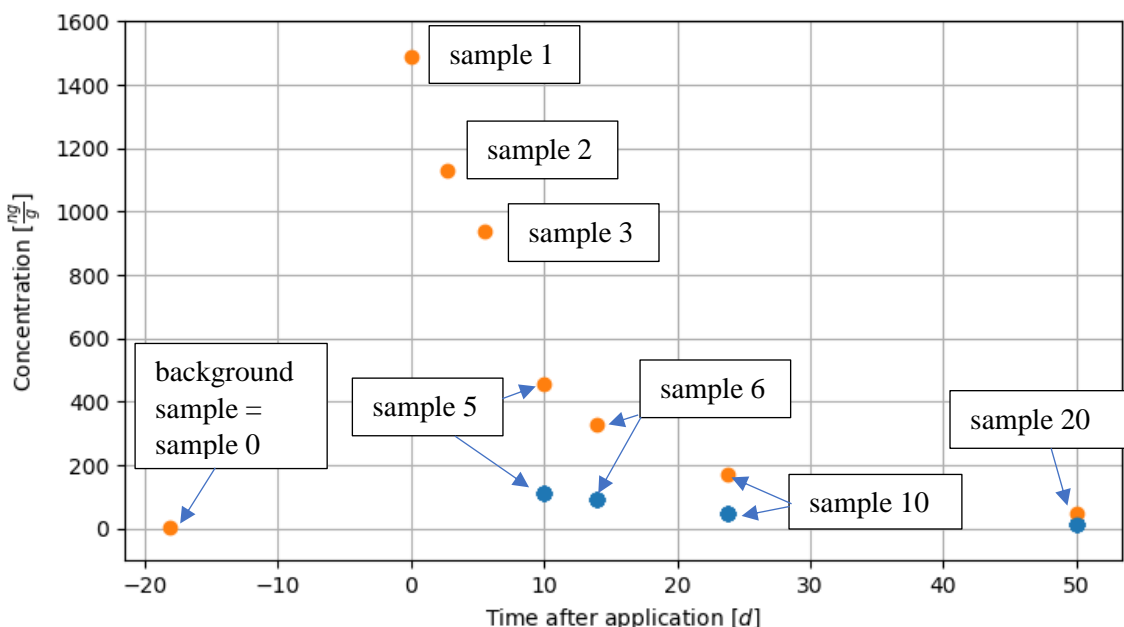


Figure 55: Concentration of SMOC in the first (orange) and the second (blue) layer with numbering

The weather measurements were taken from Agrometeo [58]. Sample 1-2 refers to the sample interval between samples 1 and 2.

sample interval	average temperature 2 m above the ground [°C]	average volume of rainfall per day [mm/d]
sample 1-2	15.58	0.00
sample 2-3	18.52	0.00
sample 3-5	15.43	8.42
sample 5-6	12.97	19.97
sample 6-10	16.46	6.95
sample 10-20	20.03	5.61

Table 24: Weather data during the period under study

8.1.1 Precision and accuracy of the analysis

The relative recovery of the analytes was within the acceptable range of 70-120% and the method precision was below the upper limit of acceptable values of 15% [59].

Only if the changes of the concentrations of an analyte over time and depth are above the LOQ, the changes can be reliably quantified. The LOQ of SMOC was 0.26 ng/g, which means that remarkably small concentration changes of only 0.26 ng/g could be quantified. The concentration changes of SMOC over time were 80 to 5720 times higher than the LOQ of SMOC. The concentration changes of the metabolites over time were 1.5 to 5.5 times higher than their LOQ. The differences between the concentrations of SMOC in the two layers of a sample were 130 to 1330 times higher than the LOQ, and the ones of ESA were 1 to 5 times higher than the LOQ, whereas

the ones of OA were not always higher than the LOQ. Therefore, the statements about the time course of the concentrations of the pollutants and their qualitative depth comparison are well-founded.

8.1.2 Limitations of the field measurement

There are five general limitations to the interpretation of the field measurement:

1. There are too few samples to make a reliable statement about the reasons for the concentration decline, especially for the second layer, where only four samples have been analysed. Hence, more field samples should be analysed.
2. Having measured the concentration in the field, it is difficult to identify with certainty the environmental factors that caused the concentration decline. Several different processes take place simultaneously in nature and neither the final products of degradation nor the efflux of the second layer could be directly quantified. Therefore, it is not possible to determine with certainty which proportions of SMOC were transported or degraded. In order to isolate and observe the impact of a single process, an experimental setup or much more frequent measurements that would allow for precise mass balances would be necessary.
3. The Humax samples were only taken for the layer 0-20 cm of the field and not for the layer 0-5 cm and the layer 5-12 cm separately. The first layer contains usually less fine soil [60]. Therefore, the mass of SMOC per cm^3 in the first layer is probably smaller than assumed.
4. There were only two Humax samples, which is why it was assumed that the bulk density of the soil increased linearly (chapter 7.1). For more precision, Humax samples should have always been taken together with every composite sample. However, the soil densified only about 10% over 50 days, which is why it will not be considered in the discussion.
5. The soil in the sample for the background concentration was ploughed, which means that there was probably less fine soil per cm^3 and, therefore, less mass of the pollutant per cm^3 in the background sample than assumed.

8.1.3 Background concentration

SMOC has only been widely used since 1998 and the farmer reported that he had never applied a PPP containing SMOC in the last 20 years [8]. Nevertheless, the background presence of SMOC was about ten times higher than the LOQ.

To find the reason for this contradiction, a sample of a location that has never been cultivated (e.g. a forest) should be analysed together with the field samples of this study.

8.1.4 Application rate

Hypothesis:

The concentration of SMOC increases after application. The application rate was 0.5 l/ha according to the farmer.

Testing of the hypothesis:

The mass of SMOC within the first layer per hectare was calculated in the following way:

$$m_{SMOC} = c_{SMOC} \left[\frac{ng}{cm^3} \right] \cdot V_{layer} [cm^3] = c_{SMOC} \left[\frac{ng}{cm^3} \right] \cdot 5 [cm] \cdot 10^8 [cm^2]$$

The calculated mass of SMOC in the background sample within the first layer per hectare was:

$$m_{SMOC_{background_sample}} = 1.31 \text{ g}$$

The calculated mass of SMOC in the first sample after the application within the first layer per hectare was:

$$m_{SMOC_{sample1}} = 570.66 \text{ g}$$

The amount of the applied PPP Calado per hectare was calculated based on the measurements:

$$m_{SMOC_{applied}} = m_{SMOC_{sample1}} - m_{SMOC_{background_sample}} = 569.35 \text{ g}$$

$$V_{calado} = \frac{m_{SMOC_{applied}}}{c_{calado}}$$

$m_{SMOC_{applied}}$ = the calculated mass of SMOC that has been applied to a hectare

c_{calado} = the concentration of SMOC in the PPP Calado in g/l

V_{calado} = the calculated volume of Calado that has been applied to a hectare

According to the farmer's information, he applied 0.5 l of Calado per hectare, and the concentration of SMOC in the PPP Calado was 960 g/l (see chapter 5.1). The application rate measured is shown in table 25.

actual application rate [l/ha]	application rate measured [l/ha]	absolute error [l/ha]	relative error [%]
0.50	0.59	0.09	18.61

Table 25: Application rate measured and application rate according to the farmer with absolute and relative error

Explanation:

Possible reasons for the deviation between the measured and the reported values are listed below:

- The application of Calado was inhomogeneous. The farmer might have sprayed more than 0.5 l/ha onto the soil of the investigated part of the field.
- In order to calculate the mass of SMOC within the first layer per hectare, the measured bulk density of the soil was used. The bulk density was measured as an average of the first and the second layer. However, there is often less fine soil in the first than in the second layer. Taking the average of the first and the second layer wrongly increased the mass of SMOC in the first layer.
- The relative recovery was higher than 100%, which indicates that the analytical procedure increased the concentration in a sample, for example due to contamination in the labware.

8.1.5 Kinetics

Hypothesis:

The concentration of SMOC was expected to decrease because various processes, such as biodegradation and transportation, took place while no new SMOC entered the system. Moreover, the concentration decline was expected to be exponential since degradation processes follow first-order kinetics [23].

Testing of the hypothesis:

The exponential trendline yielded a high correlation coefficient for the data (the first layer: $r^2 = 0.9896$, the second layer: $r^2 = 0.9980$). It was assumed that SMOC is completely degraded after an infinitely long period of time. Therefore, the general function looked like this:

$$c_{SMOC} = a \cdot e^{-k \cdot t}$$

In order to find the parameters of the trendline, the absolute square deviations were minimised using the solver in Excel. The last sample had a stronger impact on the relative trendline than on the absolute one (figure 56). This was avoided by using absolute minimisation.

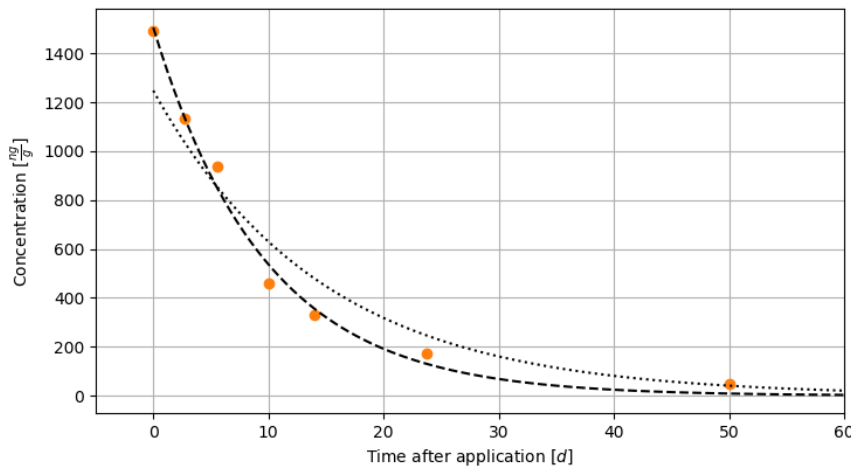


Figure 56: Trendlines using different minimisation techniques (dotted: relative minimisation; dashed: absolute minimisation; orange points: measured concentration of the samples in the first layer)

The trendlines for the first and the second layer with absolute minimisation were the following:

$$c_{layer1}(t) = 1505.35 \left[\frac{ng}{g} \right] \cdot e^{-0.1031 [d^{-1}] \cdot t}$$

$$c_{layer2}(t) = 113.07 \left[\frac{ng}{g} \right] \cdot e^{-0.05610 [d^{-1}] \cdot t}$$

The trendline function can be written in the following way, where c_0 is the starting concentration:

$$c(t) = c_0 \cdot e^{-k \cdot t}$$

The term $e^{-k \cdot t}$ determines the DT50 (in days):

$$DT50 = \frac{\ln(2)}{k}$$

$$c(t) = c_0 \cdot \left(\frac{1}{2}\right)^{\frac{t}{DT50}}$$

$$c_{layer1}(t) = 1505.35 \left[\frac{ng}{g}\right] \cdot e^{-0.1031 [d^{-1}] \cdot t} = 1505.35 \left[\frac{ng}{g}\right] \cdot \left(\frac{1}{2}\right)^{\frac{t}{6.72 [d]}}$$

$$c_{layer2}(t) = 113.07 \left[\frac{ng}{g}\right] \cdot e^{-0.05610 [d^{-1}] \cdot t} = 113.07 \left[\frac{ng}{g}\right] \cdot \left(\frac{1}{2}\right)^{\frac{t-10.3 [d]}{12.36 [d]}}$$

The trendlines are shown in figure 57 and figure 58.

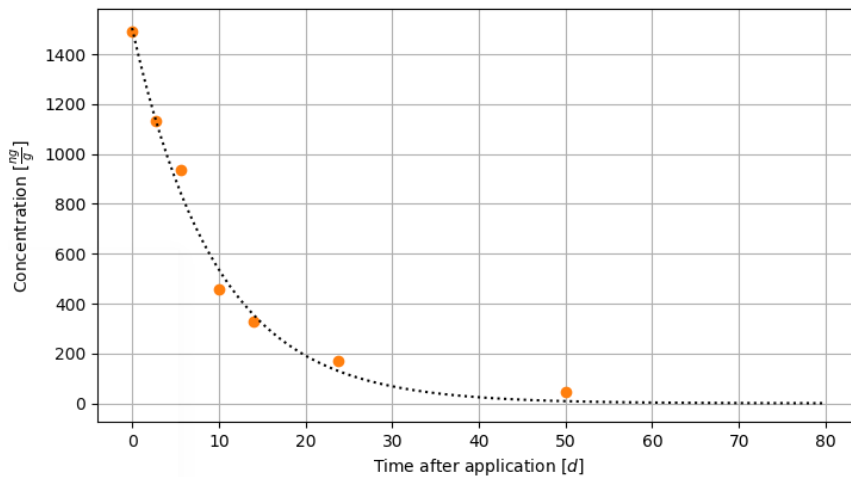


Figure 57: Trendline of the concentration decline in the first layer using absolute minimisation

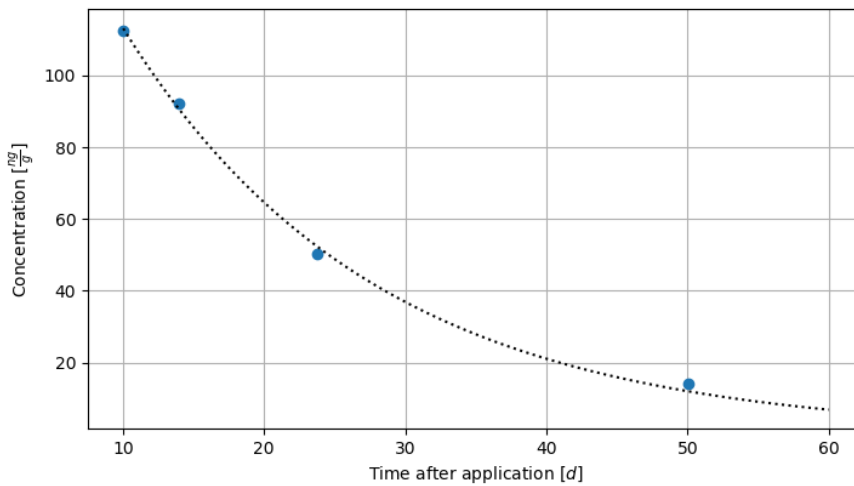


Figure 58: Trendline of the concentration decline in the second layer using absolute minimisation

The correlation coefficients of the trendlines in the first and second layer were the following:

$$r1^2 = 0.9896$$

$$r2^2 = 0.9980$$

The main reason why the correlation coefficient of the second layer was higher is probably that there were less samples in the second layer. Additionally, the samples in the first layer included

the shift from the dry to the rainy period, and the first layer was more exposed to environmental factors. Furthermore, the samples of the second layer were taken in the later stages of the sampling, when the degradation might have already stabilised.

8.1.6 Impact of degradation and leaching

Hypothesis:

The primary reason for the concentration decline of SMOC was expected to be biodegradation [28]. SMOC is a rather nonpolar molecule that is not very soluble in water, resulting in a small convective transport [8]. Leaching was expected to be the major factor for transportation since volatilisation of SMOC is negligible, and the effect of run-off can be expected to be minimal for this field because the slope of the field was only between 0.7% (length) and 2.3% (width) [20], [61], [24].

The concentration decline of the metabolites was expected to be mainly attributed to leaching as they are more polar. Moreover, their concentration increase had to be due to the degradation of SMOC.

Testing of the hypothesis:

Both leaching and degradation had taken place during the period under study. Firstly, there was a considerable amount of SMOC in the second layer, which means that the SMOC, which was applied to the surface, leached into the second layer. Moreover, two of the degradation products of SMOC could be detected after the first rainfall. Therefore, a part of SMOC must have been degraded.

A strong indication of leaching or biodegradation as major factors would be if the sum of the masses of SMOC in the top and bottom layers were constant over time (leaching) or the sums of the molar amounts of SMOC and its degradation products in a layer were constant (biodegradation).

The masses of SMOC in both the first and second layer decreased over time. This indicates that SMOC was degraded or leached out of the second layer. If leaching had been the major factor for the concentration decline, the concentration decline during the rainy period would have been much higher than during the dry period. While the DT50 during the first rainfall was much shorter than the DT50 during the dry period, the DT50 increased during the subsequent rainfalls, and the DT50 of SMOC in the first and second layers converged (chapter 8.1.9). This indicates that leaching stopped during the later stages of the period under study and biodegradation became the major factor. During the dry period, it is most likely that SMOC was degraded. However, leaching cannot be excluded since no samples of the second layer were analysed. The concentration decline of SMOC during the dry period is most likely attributed to a plant uptake since none of the two metabolites OA and ESA were detected. This follows from the following considerations:

If the biodegradation to these two metabolites had been a major factor determining the concentration decline, their concentrations would have had to increase significantly. However, the measured occurrence fraction was too low to explain the concentration decline of SMOC thoroughly (chapter 8.2.1.3). Possible explanations are presented below:

- The most likely explanation seems to be plant uptake of SMOC since plants were excluded from the analysis (chapter 8.2.1.4).
- There was a considerable washout of the metabolites from the second layer. This finding was supported by the fact that the more polar and thus more mobile degradation products reached higher proportions in the deeper layers, which indicates that the main route for the accumulation of degradation products is not leaching of SMOC and biotransformation, but rather biodegradation and then leaching of the more water-soluble degradation products (chapter 8.2.1.2).

- Other metabolites were formed. However, there was no indication in literature for different degradation pathways with such a significant turnover.

In conclusion, the measurements do not provide enough evidence to accept or reject the hypothesis that biodegradation is the major factor for the concentration decline. Therefore, the samples should be taken in shorter time intervals to measure a more continuous concentration course. Moreover, samples of thinner and deeper layers would help to examine the movement in the soil in more detail. If the plants are analysed as well, the uptake of SMOC by the plant can be measured.

8.1.7 Adsorption

Hypothesis:

The DT50 of SMOC is a constant because degradation usually follows first-order kinetics [23].

Testing of the hypothesis:

Figure 59 shows that the DT50 varied considerably. In fact, it increased steadily in the course of both the dry and the rainy periods; only during the first rainfall, it decreased by more than 1/2 (sample 3-5), which is explained in chapter 8.1.8.2.2. An intervening rainfall cannot be the only reason for the increasing DT50 because the DT50 also increased during the precipitation free period. The only environmental factor known to have changed during the dry period was temperature. It is unlikely that the temperature is responsible for the increasing DT50 as the temperature increased during the dry period (chapter 8.1.8.1), which would result in faster degradation. Therefore, a different factor must have slowed down the degradation and leaching kinetics, the most probable candidate being an increased adsorption strength over time.

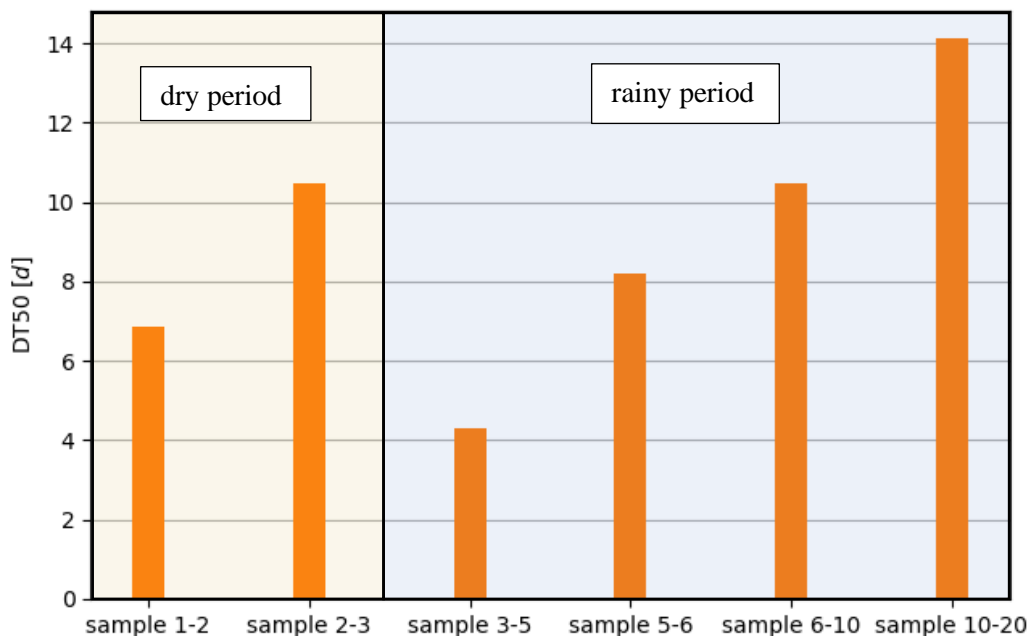


Figure 59: DT50 between two samples in the first layer

Explanation:

If the adsorption of SMOC to soil particles increases, the pollutant is less available for biodegradation and leaching. It has been reported that the adsorption of SMOC increases over time (ageing) because SMOC needs time to establish an adsorption equilibrium with the soil particles [21]. Moreover, the molecules of the pollutant might diffuse into sites where they are trapped or where they are adsorbed more strongly. Therefore, SMOC becomes less available for biodegradation and leaching over time [21], [20].

Additionally, the average adsorption of the SMOC molecules increased over time due to the concentration decline [20]. Since the soil of the field was inhomogeneous and the magnitude of the adsorption strength of SMOC varied, the more bioavailable and less adsorbed molecules were degraded first [62], [21]. This means only the strongly adsorbed molecules remained after some time and the average adsorption coefficient increased.

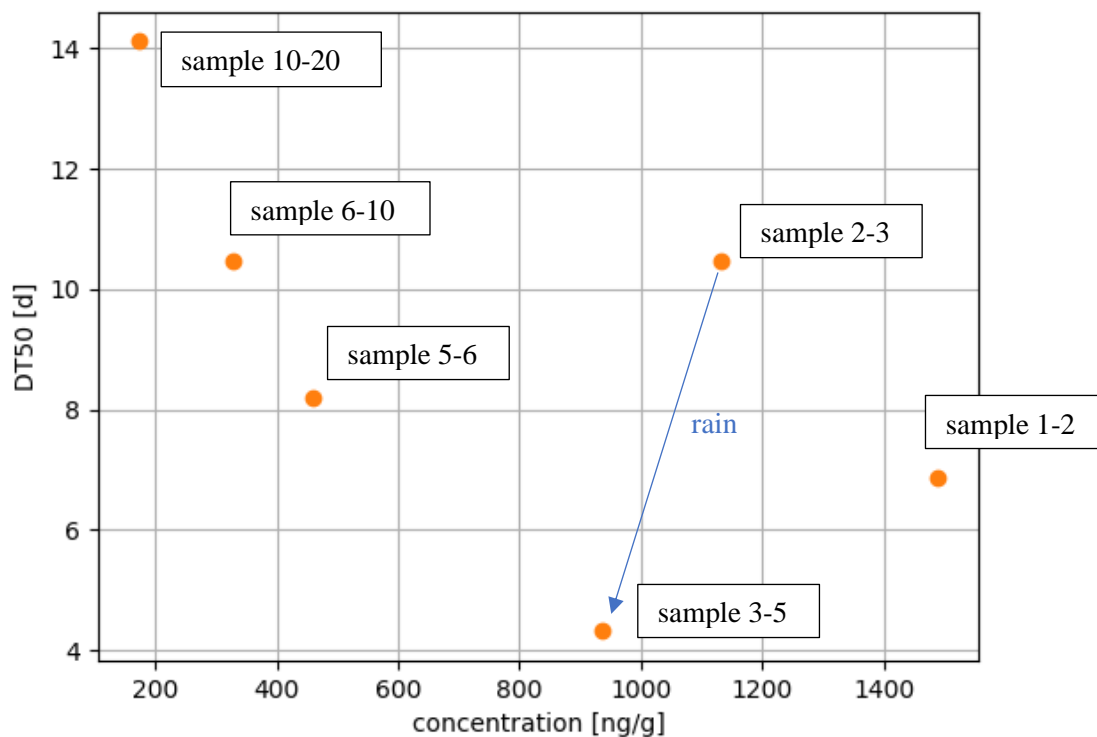


Figure 60: Correlation between the concentration and the DT50

8.1.8 Environmental factors

The impact of temperature and rainfall on the concentration decline will be discussed in the following chapters.

8.1.8.1 Impact of temperature

Hypothesis:

According to literature, higher temperature increases the degradation rate and shortens the DT50 of SMOC [23].

Testing of the hypothesis:

There was no proof of a negative correlation between the DT50 of SMOC in the first layer and the average temperature 2 m above the ground during the time between sample n and sample n+1. In figure 61, the correlation between the temperature, which was averaged over time between two measurements, and the DT50 of the samples in the first layer is shown. There is no strong correlation but the DT50 tend to increase with increasing temperature.

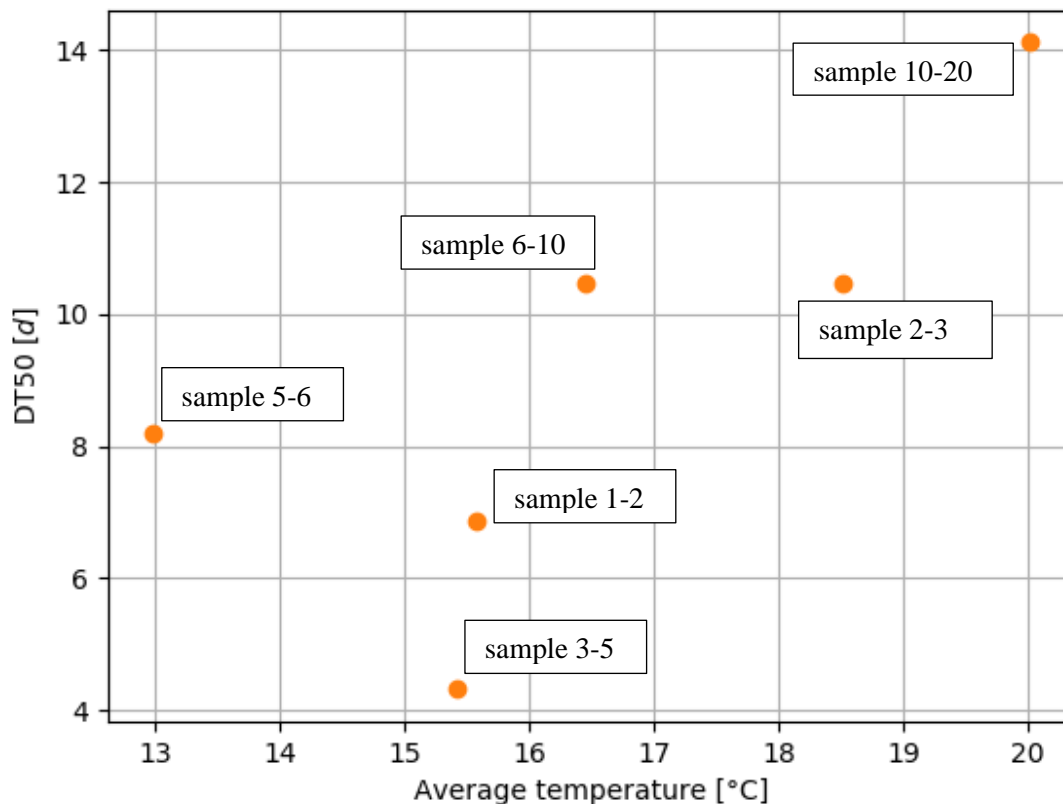


Figure 61: Correlation between the average temperature 2 m above the ground and DT50 in the first layer

Explanation:

The effect of temperature was limited, presumably because other factors had a more decisive influence on the leaching and degradation velocities. The sampling took place during the spring and the temperature increased towards summer. Meanwhile, the adsorption increased and the rainfall volume decreased, leading to a higher DT50 (chapter 8.1.7 and 8.2.1.2).

8.1.8.2 Impact of rainfall

Hypothesis:

The DT50 shortens with rain because rain increases leaching and provides the moisture necessary for biodegradation [22].

Testing of the hypothesis:

The DT50 of the first layer during the dry period was compared to the one during the rainy period. The DT50 in the first layer increased over time (see chapter 8.1.7). If there had been no rain, the DT50 would have continued to increase (dashed black line in figure 62). The DT50 was diminished as a result of rain (blue arrow in figure 62).

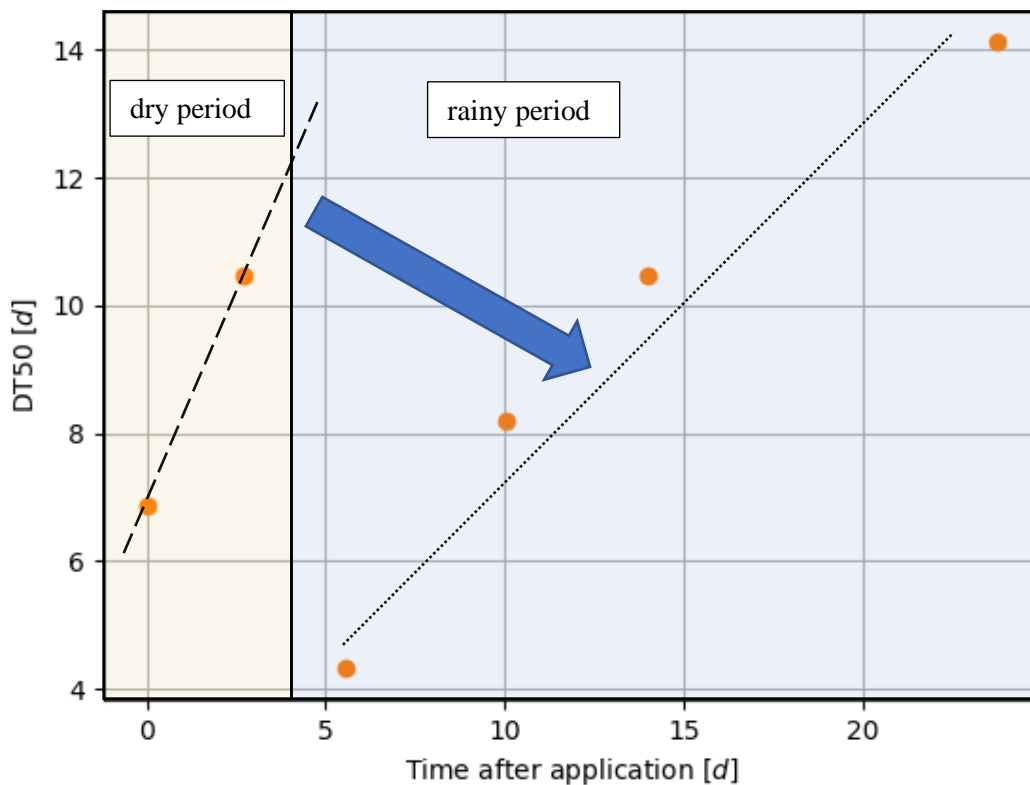


Figure 62: Correlation between time and the DT50. (time after application: the time when sample n was taken; DT50: DT50 between sample n and $n+1$; blue arrow: impact of the rain; dashed black line: increasing DT50 during the dry period; dotted black line: increasing DT50 during the rainy period)

Explanation:

Rainfall increases leaching and biodegradation [22]. The degradation is thought to increase with moisture since the molecule is more bioavailable for the microorganisms if it is dissolved in water [23]. Furthermore, some microorganisms are more active with a higher moisture level [23].

8.1.8.2.1 Rainfall volume

Hypothesis:

The higher the rainfall volume, the shorter the DT50 because rainfall increases leaching and degradation [22].

Testing of the hypothesis:

The DT50 between the sample n and n+1 in the first layer during the rainy period was compared to the average volume of the rainfall per day between the sample n and n+1 (figure 63 and figure 64). In order to make a reliable statement, more samples should be analysed. The DT50 generally increased with decreasing precipitation volume. The DT50 after the first rainfall (sample 3-5) was an exception (see chapter 8.1.8.2.2).

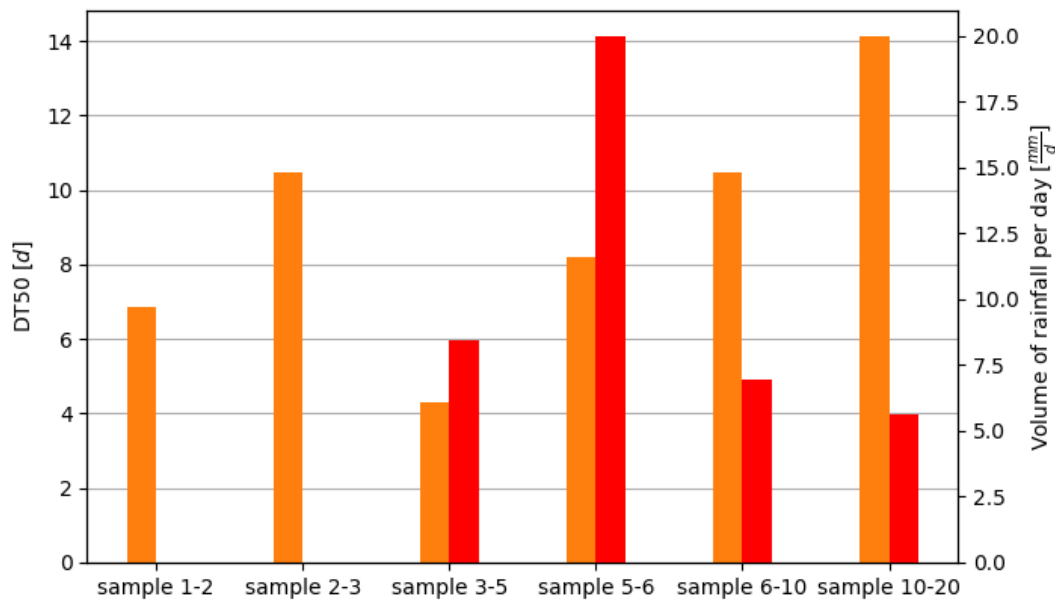


Figure 63: DT50 between two samples of the first layer (orange) and the average volume of the rainfall per day between two samples (red)

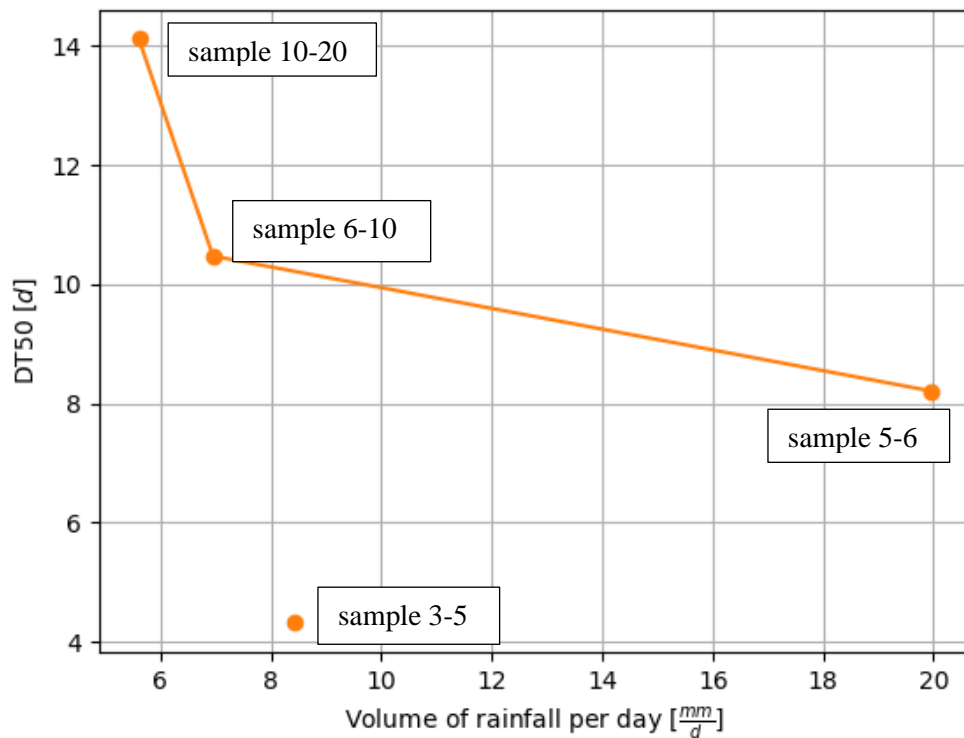


Figure 64: Correlation between DT50 and the average volume of the rainfall per day

Explanation:

If the rainfall volume decreases, there is less transportation and the soil is drier, resulting in a slower degradation rate [22], [23]. However, the increase of the DT50 might be wrongly attributed to the decreasing rainfall volume since the adsorption increased at the same time (see chapter 8.1.7).

8.1.8.2.2 First rainfall

The DT50 was found to be the shortest between the samples 3 and 5, when it also rained for the first time (figure 65).

If the rainfall volume had been the major factor determining the short DT50 of the first rainfall, similar rainfall volumes should have had the same effect on the concentration decline during the subsequent period, which was not the case (chapter 8.1.8.2.1).

Literature states that the effect of leaching during rainfalls after long dry periods is increased because there are more cracks in the soil, where the water can leach through more easily [22]. However, the long dry period before the first rainfall cannot be the only reason for the short DT50 since there were also a lot of dry periods between samples 10 and 20, which is when the DT50 reached its maximum value (figure 66).

Therefore, the DT50 increased in the subsequent period probably because the adsorption coefficient increased due to ageing and decreasing concentrations, as explained in chapters 4.1 and

8.1.7. This resulted in slower degradation and less leaching. Moreover, the compaction of the soil during the first rainfall reduced the leaching during the subsequent rainfalls [22].

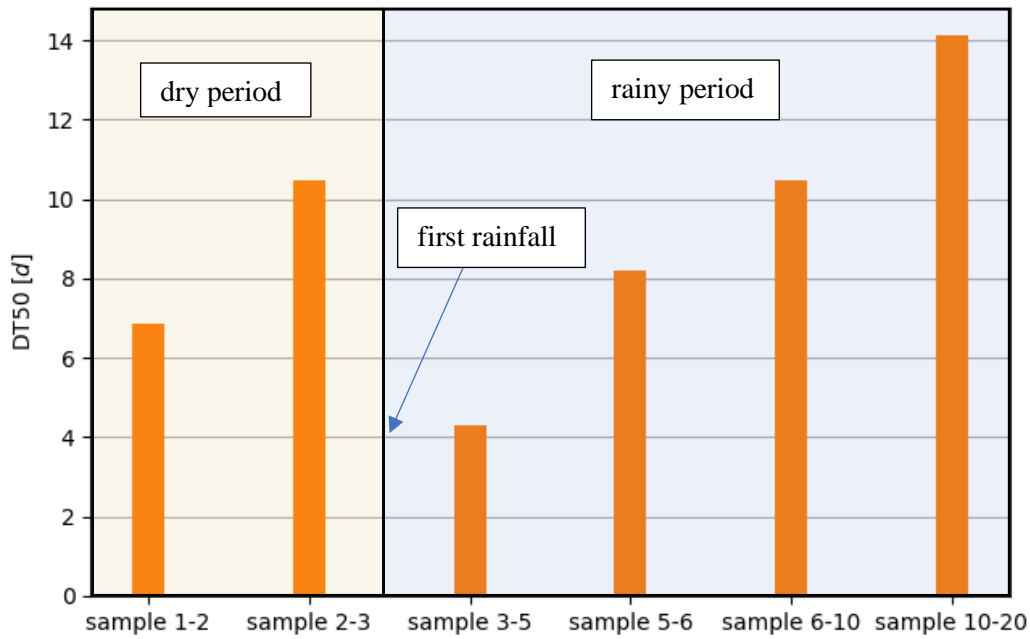


Figure 65: DT50 between two samples of the first layer

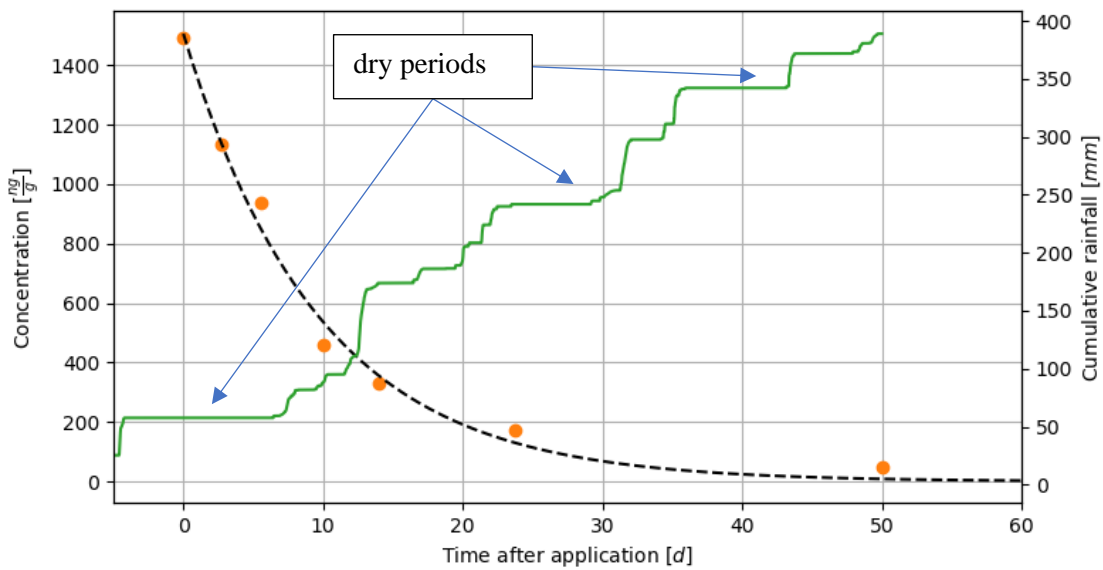


Figure 66: Concentration decline in the first layer with the trendline and the cumulative rainfall (dashed: trendline using absolute minimisation; orange: measured samples in the first layer; green: cumulative rainfall since the background sample)

8.1.9 Second layer

Hypothesis:

Literature has shown that the DT50 is longer in deeper layers than in topsoil layers [63].

Testing of the hypothesis:

The DT50 of the first layer during the rainy period was compared to the one of the second layer (figure 67). In order to prove the hypothesis above, more samples would need to be analysed. The DT50 between the samples 5 and 6 in the second layer was almost twice as long as the DT50 between the same samples in the first layer. By the end of the sampling (sample 10-20), the DT50 of both layers converged.

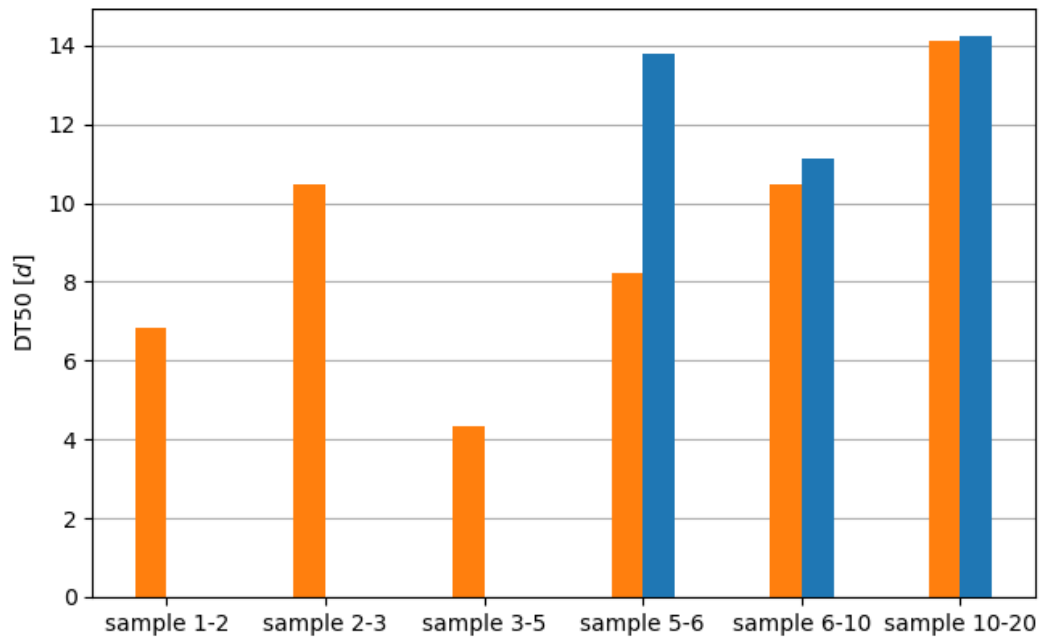


Figure 67: DT50 between two samples of the first (orange) and the second layer (blue)

Explanation:

In literature, the positive correlation between depth and DT50 was explained by a decreasing OC content leading to a slower degradation [23], [63]. Since the OC content in the first and second layer of this soil did not differ markedly (chapter 7.1), the abovementioned effect was minimised. The longer DT50 between samples 5 and 6 of the second layer can be justified by the fact that part of SMOC of the first layer was still leaching into the second layer. In the later stages of the sampling, the leaching into the second layer decreased because adsorption strength increased (chapter 8.1.7).

8.1.9.1 Movement of SMOC in the soil

In order to look at the movement of SMOC in the soil, the masses of SMOC in the first and second layer were compared. The concentrations in the first and second layer could not be directly compared because the second layer was thicker than the first one. The mass of SMOC within the first and second layer per hectare was calculated in the following way:

$$m_{SMOC_{layer1}} = c_{SMOC_{layer1}} \left[\frac{ng}{cm^3} \right] \cdot V_{layer1} [cm^3] = c_{SMOC_{layer1}} \left[\frac{ng}{cm^3} \right] \cdot 5 [cm] \cdot 10^8 [cm^2]$$

$$m_{SMOC_{layer2}} = c_{SMOC_{layer2}} \left[\frac{ng}{cm^3} \right] \cdot 12 [cm] \cdot 10^8 [cm^2]$$

The mass of SMOC in the second layer after the first rainfall was very high. It was about $\frac{3}{4}$ of the mass in the first layer. The question arises as to where this mass has come from. Since SMOC is very immobile, it is unlikely that SMOC was transported during the dry period.

Hypothesis:

SMOC is transported into the second layer by rain.

Testing of the hypothesis:

The trendline was based on the mass of SMOC in the first three samples during the dry period using the same principles as in chapter 8.1.5. The trendline was extended until the sample after the first rainfall. The predicted mass was calculated with the trendline and was compared to the measured mass of SMOC.

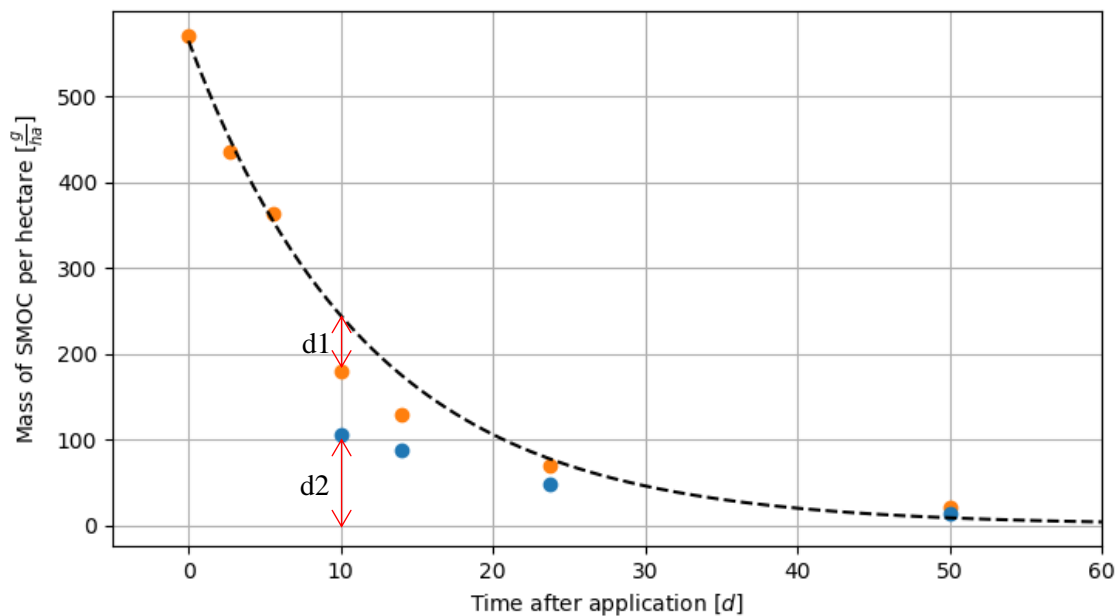


Figure 68: Trendline of the three samples during the dry period (orange: mass of SMOC in the first layer; blue: mass of SMOC in the second layer)

$$\begin{aligned} d_1 &= m_{trendline_{layer1}}(10.03 d) - m_{measured_{layer1}}(10.03 d) \\ &= 564.90 [g] \cdot e^{-0.084 \cdot 10.03} - 179.19 [g] \\ &= 64.63 [g] \end{aligned}$$

$$d_2 = m_{\text{measured}_{\text{layer}2}}(10.03 d) = 105.50 [g]$$

The question of where the mass has come from is not fully answered. d_1 is smaller than d_2 . Only about 60% of the mass of SMOC in the second layer can be explained with this method. A possible explanation is that SMOC diffused into the second layer during the dry period. However, literature provides no evidence for fast diffusion rates of SMOC. Additionally, it should be considered that the difference d_1 could be higher if the degradation slowed down during the first rainfall. However, this is unlikely because the metabolites were detected for the first time after the first rainfall, which even indicates increased degradation.

8.2 Discussion of the metabolites

The concentrations of the metabolites OA and ESA were expected to increase due to the following reasons:

- SMOC is degraded to OA and ESA.
- The concentration of the metabolites in the second layer increases due to leaching of the metabolites out of the first layer.

The degradation of the metabolites is reported to be very slow and was ignored [8]. Consequently, the concentration of the metabolites was expected to decrease mainly due to the following reason:

- The metabolites are mobile and, therefore, leaching can decrease the concentration [8].

8.2.1.1 Kinetics

Hypothesis:

The course of the concentration is a combination of the processes listed above.

Testing of the hypothesis:

The concentration first increased and then decreased (example of ESA in figure 69). Therefore, there had to be significant processes that both increased and decreased the concentration.

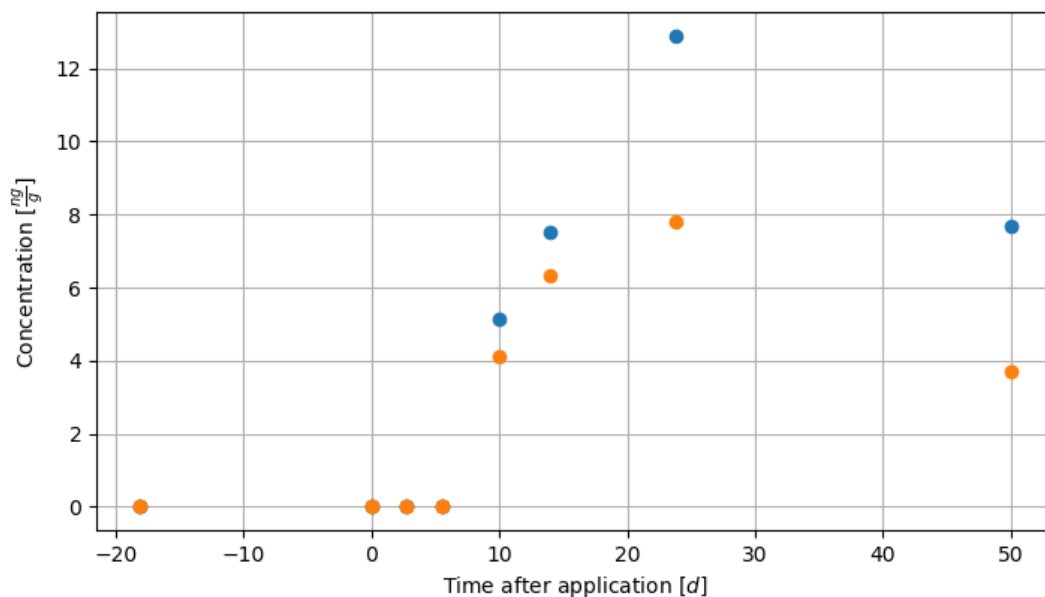


Figure 69: Concentration of ESA in the two layers (orange: layer 0-5 cm; blue: layer 5-17 cm)

Explanation:

The increase was due to the degradation of SMOC because no other source of OA or ESA is conceivable. The increase slowed down because the degradation is an exponential function and the formation is a limited growth function. This means that in the beginning, more metabolites were formed than transported. In the later stages, the transportation outweighed the formation and the concentration decreased. Leaching had to occur in both layers since the concentration decreased in both layers.

8.2.1.2 Mobility**Hypothesis:**

The two metabolites are more mobile than SMOC because ESA and OA are more polar and leach into deeper layers [8].

Testing of the hypothesis:

The mass of the metabolites in the two layers was compared because the concentrations of the two layers could not be directly compared as the second layer was thicker. The mass was calculated the same way as the mass of SMOC in chapter 8.1.9.1. The mass of OA and ESA was higher in the second layer than in the first layer (mass of ESA in figure 70). Assuming that the occurrence fraction was the same in both layers, the high mass of the metabolites in the second layer had to be due to leaching into the second layer since the absolute mass decline of SMOC was higher in the first layer than in the second one.

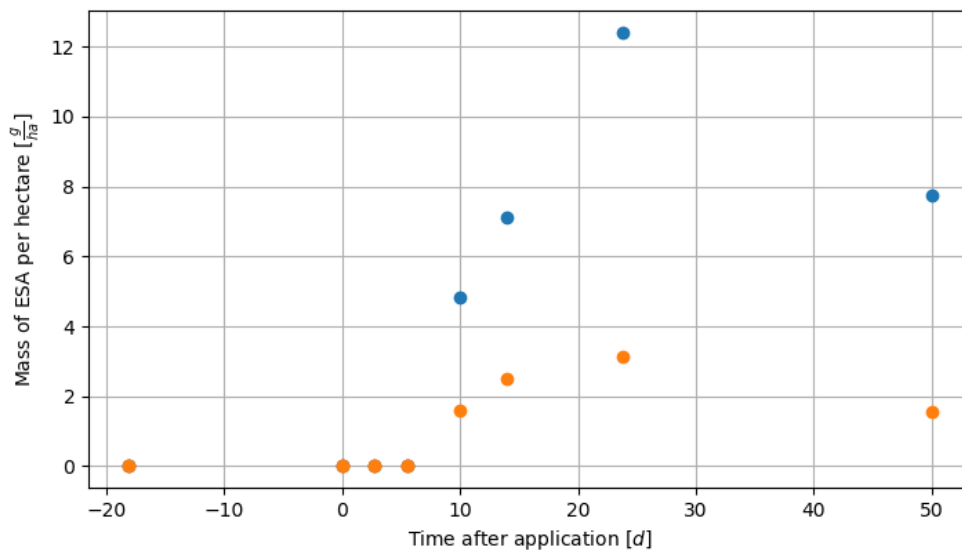


Figure 70: Mass of ESA within the first and second layer per hectare (orange: layer 0-5 cm; blue: layer 5-17 cm)

Hypothesis:

OA is less mobile than ESA due to its lower polarity [8].

Testing of the hypothesis:

The difference between the masses of the metabolites in the first and second layer is higher for ESA than for OA. The more mobile the molecules, the smaller the mass in the first layer and the higher the mass in the second layer (table 26).

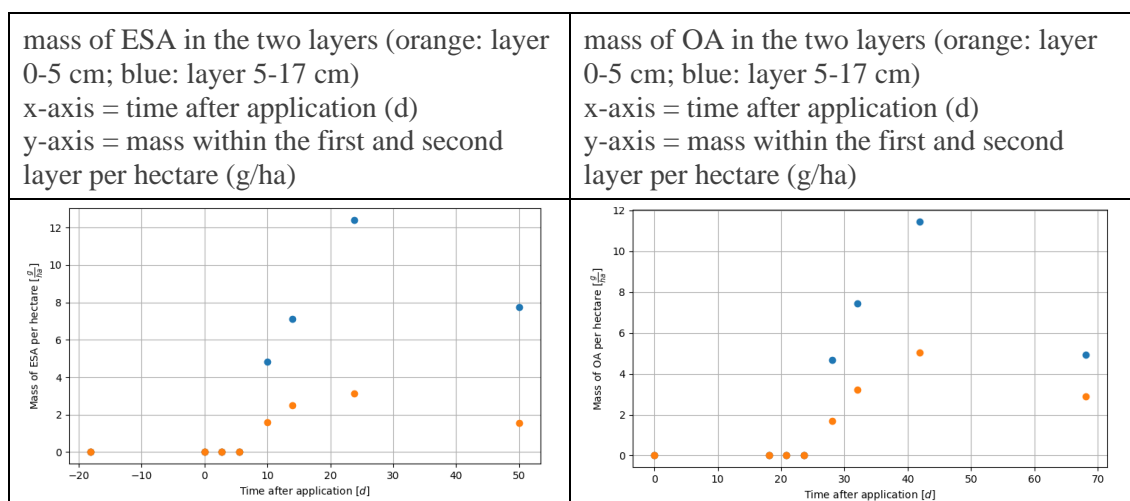


Table 26: Mass of the metabolites in the two layers

8.2.1.3 Occurrence fraction**Hypothesis:**

The occurrence fraction of the metabolites is about 20%, as suggested by literature [8].

Testing of the hypothesis:

The change of the mass of SMOC and its metabolites per hectare was compared in table 27. It transpires that the mass increase of the metabolites is clearly less than 20% of the mass decline of SMOC.

sample interval	absolute mass decline of SMOC in both layers per hectare [g]	absolute concentration increase of OA in both layers per hectare [g]	absolute concentration increase of ESA in both layers per hectare [g]
sample 3-5	$183.39 + x_1$	$6.36 + x_2$	$6.44 + x_3$
sample 5-6	68.31	4.31	3.16
sample 6-10	99.15	5.80	5.94
sample 10-20	83.18	-8.63	-6.21

Table 27: Comparison of the mass decline of SMOC to the mass increase of the metabolites OA and ESA (x_1 : unknown absolute mass decline of SMOC in the second layer; x_2 : unknown absolute mass increase of OA in the second layer; x_3 : unknown absolute mass increase of ESA in the second layer)

Explanation:

It is not possible to measure the occurrence fraction in a field measurement because the formation process of the metabolites cannot be isolated. This means that a big part of the metabolites might have been transported into deeper layers since they are very mobile. Moreover, a big part of SMOC was probably accumulated and transformed in the plants of the field, which were not included in the analysed samples.

8.2.1.4 Formation of degradation products

During the first three samples, no metabolites were detected. This is surprising because the concentration of SMOC decreased during this time and there was no rain to transport SMOC or the metabolites. Only when it started raining, the metabolites were detected.

It is doubtful that the concentration decline of SMOC during the dry period was not due to degradation because it is implausible that SMOC was transported to lower layers without rain. Diffusion rates are usually slow, and literature provides no evidence for fast diffusion rates of SMOC. The metabolites cannot have been degraded faster than they were formed because they are persistent and generally have a higher DT50 than SMOC [8]. There might have been an acclimation period of the microorganisms to SMOC and SMOC might have accumulated in the plants, as explained below:

There might have been a prolonged lag phase after the application. During the lag phase, there was no degradation of SMOC by the microorganisms in the soil because the microorganisms had to adapt to the environmental change. Some microorganisms are more tolerant of SMOC than others [64]. Therefore, the microorganisms that could detoxify and degrade SMOC survived and their number increased. Lag phases can last from hours up to several days [65]. The duration of the lag phase is, for example, dependent on the history of previous field applications [30], [65]. Microbiomes that had been recently exposed to a similar environmental change adapted more quickly. According to the farmer, the field under study has never been treated with SMOC before and, therefore, the lag phase might have been prolonged [65]. The concentration decline of SMOC during the lag phase can be explained by the uptake of the plants, which were not included in the analysed samples. If the plants had metabolised SMOC, they might have released the metabolites in their shoot system because the primary direction of the transportation of SMOC is up to the shoot system [66]. However, it would be a coincidence that ESA and OA were detected for the first time after the first rainfall. It might be that the rainfall increased the adaptation or growth of the microbiome [23].

9 Results of the model calculations

This chapter presents the results of the model calculations. The meaning of the variables used in this chapter can be found in chapter 6.5.

9.1 Parameters

The model used the results of the field measurements, the data provided by literature (chapter 3), and the weather data of three weather stations near the cornfield (Arth, Küssnacht, Cham) [58]. The average rainfall volume of the three weather stations was used because the weather station in Arth was suspected to be broken. The rain volume was multiplied by 0.6 because on average 40% of the rainwater evaporates or is transpired by the plants [67]. Run-off was ignored in the model and, therefore, the rest of the rainwater (60%) leached into deeper layers of the soil.

Δt was 10 min and d was 0.01 m.

The measured concentration in the first layer was 1489.63 ng/g. The starting concentrations in the first five slices, which were part of the first layer of the field, were therefore the following (the formula is taken from chapter 6.4):

In the soil (z ranges from 0 to 4):

$$c_{SMOC_s}(0, z) = \frac{1489.63 \left[\frac{ng}{g} \right] \cdot m_{FS} \cdot K_d}{K_d \cdot m_{FS} + V_w(0, z) + V_{w_{unavailable}}}$$

In the water (z ranges from 0 to 4):

$$c_{SMOC_w}(0, z) = \frac{1489.63 \left[\frac{ng}{g} \right] \cdot m_{FS}}{K_d \cdot m_{FS} + V_w(0, z) + V_{w_{unavailable}}}$$

The background presence (3.56 ng/g) was used for the starting concentrations in the second layer because SMOC was only applied to the surface of the soil. The starting concentrations in the twelve slices of the second layer were therefore the following:

In the soil (z ranges from 5 to 16):

$$c_{SMOC_s}(0, z) = \frac{3.56 \left[\frac{ng}{g} \right] \cdot m_{FS} \cdot K_d}{K_d \cdot m_{FS} + V_w(0, z) + V_{w_{unavailable}}}$$

In the water (z ranges from 5 to 16):

$$c_{SMOC_w}(0, z) = \frac{3.56 \left[\frac{ng}{g} \right] \cdot m_{FS}}{K_d \cdot m_{FS} + V_w(0, z) + V_{w_{unavailable}}}$$

The mobile water volume $V_w(0, z)$ in the slices was set to zero at the beginning.

The DT50 of SMOC during the dry period of the field measurement was used for the degradation rate in the model to exclude the effect of leaching. A trendline was obtained based on the concentration of SMOC in the first three samples during the dry period after the application using absolute minimisation. The obtained DT50 during the dry period was taken for both the first and the

second layer because the DT50 of the second layer converged with the one of the first layer (chapter 8.1.9).

$$c_{layer1_{dry}}(t) = 1474.78 \left[\frac{ng}{g} \right] \cdot e^{-0.0858 [d^{-1}] \cdot t} = 1474.78 \left[\frac{ng}{g} \right] \cdot \left(\frac{1}{2} \right)^{\frac{t}{8.08 [d]}}$$

$$DT50_{SMOC_{dry}} = DT50_{SMOC_{layer1}} = DT50_{SMOC_{layer2}} = 8.08 d$$

Since no concentrations of the metabolites were measured before the first rainfall, the occurrence fraction before the first rainfall was set to zero. The occurrence fraction of OA and ESA was estimated by adjusting the model calculation to the measured concentrations of the metabolites. The occurrence fraction was smaller than the one provided by literature because plants probably took up a substantial part of SMOC.

$$OF_{OA} = 0.1 \left[\frac{g}{g} \right]$$

$$OF_{ESA} = 0.1 \left[\frac{g}{g} \right]$$

The DT50 of OA and ESA were the following (chapter 3):

$$DT50_{OA} = 325 d$$

$$DT50_{ESA} = 235 d$$

$K_{d_{SMOC}}$ was calculated based on the $K_{oc_{SMOC}}$ provided by literature and the measured carbon content in the soil (chapter 3). The OC content was the same in both layers (chapter 5.5).

$$K_{d_{SMOC}} = K_{oc_{SMOC}} \cdot \frac{OC}{100}$$

$$OC = 1.28\%$$

$$K_{d_{SMOC}} = 288.4 \left[\frac{mL}{g} \right] \cdot 0.0128 = 3.69 \left[\frac{mL}{g} \right]$$

$$K_{d_{OA}} = 17 \left[\frac{mL}{g} \right] \cdot 0.0128 = 0.218 \left[\frac{mL}{g} \right]$$

$$K_{d_{ESA}} = 9 \left[\frac{mL}{g} \right] \cdot 0.0128 = 0.115 \left[\frac{mL}{g} \right]$$

The mass of fine soil was calculated using the average of the measured bulk density of the soil in the two Humax samples. The area of a slice was 1 m².

$$m_{FS} = \frac{0.77 \left[\frac{g}{cm^3} \right] + 0.84 \left[\frac{g}{cm^3} \right]}{2} \cdot V_{layer} [cm^3] = 0.81 \left[\frac{g}{cm^3} \right] \cdot A [cm^2] \cdot d [cm] = 8050 g$$

Peter Schwab provided the percentage of the immobile water and the capacity of the whole volume based on a field with a similar soil type as the one of Arth [44].

$$V_{w_{immobile}} = 0.35 \cdot V_{layer}$$

$$capacity = 0.0735 \cdot V_{layer}$$

p , the speed constant, was unknown because the permeability of the soil in Arth was unknown. Therefore, an estimation of p was made based on the following information provided by Peter Schwab [44]:

“Usually, the pores of a 5 cm thick layer, which are fully filled with mobile water, are emptied after one to two days.”

Since the water movement of the model was exponential, there was always a remaining amount of water in the slices. Therefore, emptied was defined as when 1% of the capacity of a slice remains. t_{empty} depends on the grain size distribution and the porosity of the soil [68]. It was assumed that a layer with standard thickness 5 cm was emptied after 1.5 days.

$$p = -\ln(0.01) \cdot \frac{d_{standard}}{t_{empty}} = -\ln(0.01) \cdot \frac{0.05 \text{ m}}{1.5 \text{ d}}$$

9.2 Results

Table 28 lists the measured and modelled concentrations using the parameters from chapter 9.1.

sample	concentration SMOC [ng/g]		concentration OA [ng/g]		concentration ESA [ng/g]	
	measured	calculated	measured	calculated	measured	calculated
sample 1 (0-5 cm)	1489.63	1489.63	0	0	0	0
sample 2 (0-5 cm)	1131.78	1180.10	0	0	0	0
sample 3 (0-5 cm)	936.12	922.71	0	0	0	0
sample 5 (0-5 cm)	458.65	556.82	4.33	13.89	4.14	12.89
sample 5 (5-17 cm)	112.52	32.03	4.98	3.40	5.15	3.80
sample 6 (0-5 cm)	328.28	311.97	8.19	5.92	6.35	4.58
sample 6 (5-17 cm)	92.23	57.95	7.89	14.06	7.52	14.36
sample 10 (0-5 cm)	171.85	73.31	12.55	1.69	7.82	1.37
sample 10 (5-17 cm)	50.18	50.61	11.89	13.99	12.88	10.98
sample 20 (0-5 cm)	47.35	2.21	6.89	0.10	3.70	0.07
sample 20 (0-17 cm)	13.97	7.59	4.89	3.65	7.69	2.57

Table 28: Results of the model calculations compared to the measured concentrations

Figure 71 shows the concentration of SMOC in the first and second layer. The results of the concentrations of SMOC in all slices are illustrated in figure 72.

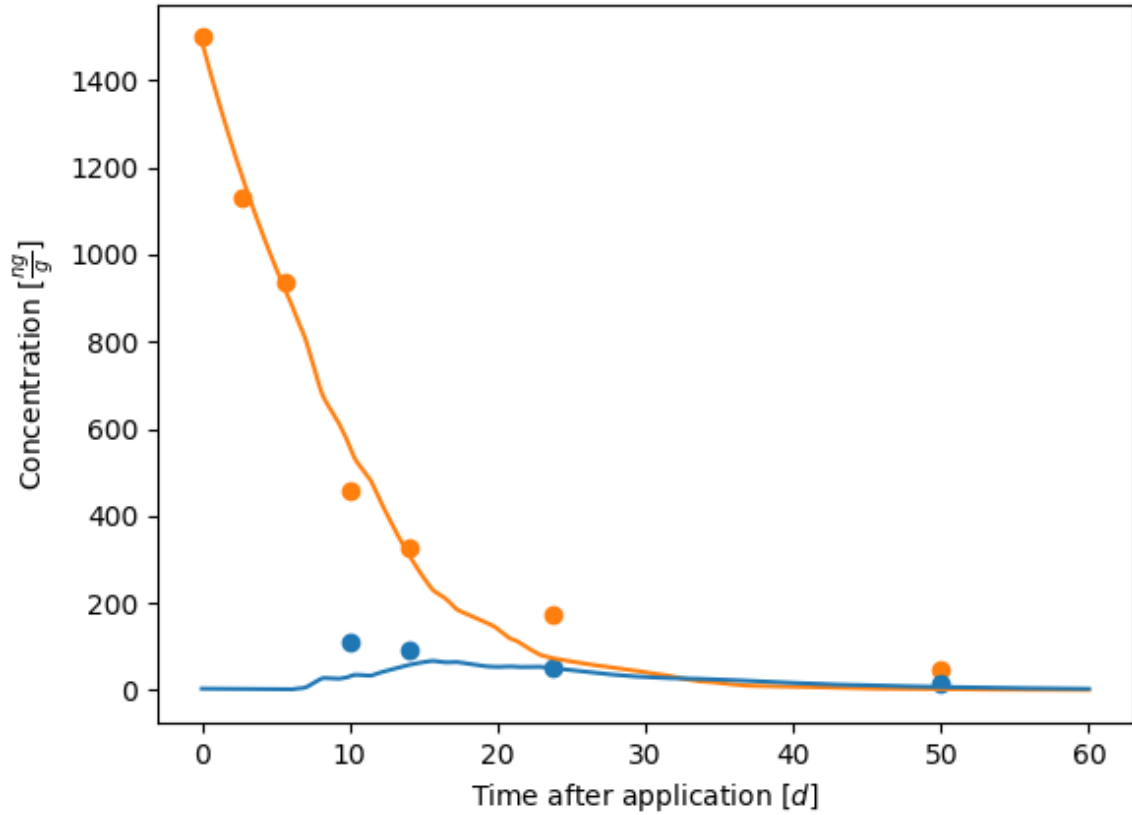


Figure 71: Concentration of SMOC in the first (0-5 cm) and the second (5-17 cm) layer (dots: measurements; lines: calculations; orange: first layer; blue: second layer)

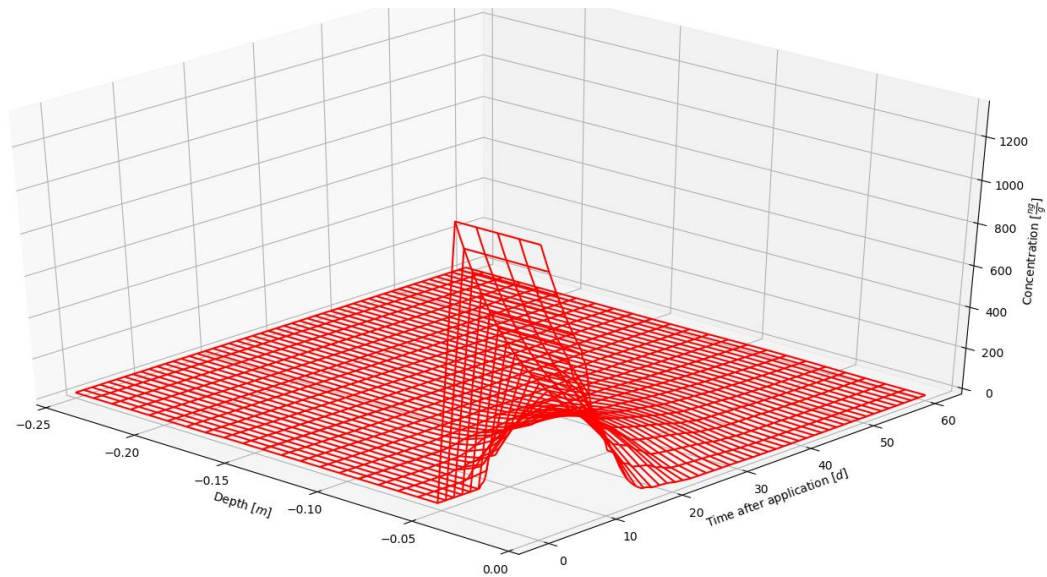


Figure 72: Concentration of SMOC in the slices down to a depth of 0.25 m

Figure 73 shows the concentration of the metabolite OA in the first and second layer and figure 74 shows the concentration in all slices.

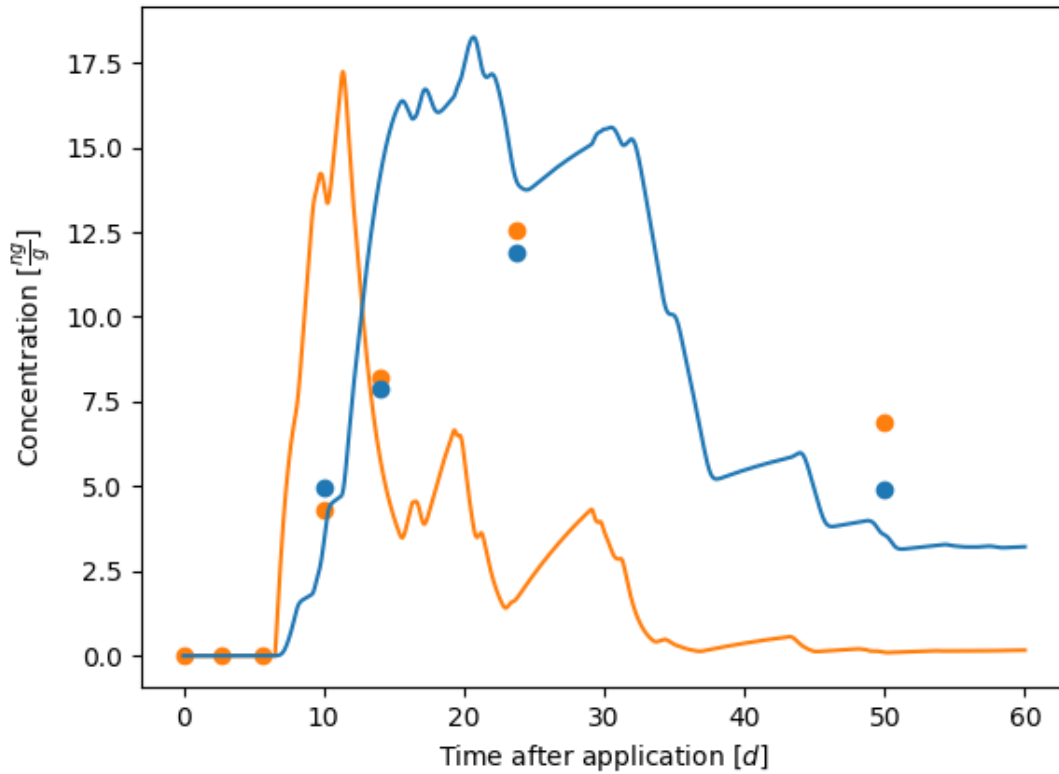


Figure 73: Concentration of OA in the first (0-5 cm) and the second (5-17 cm) layer (dots: measurements; lines: calculations; orange: first layer; blue: second layer)

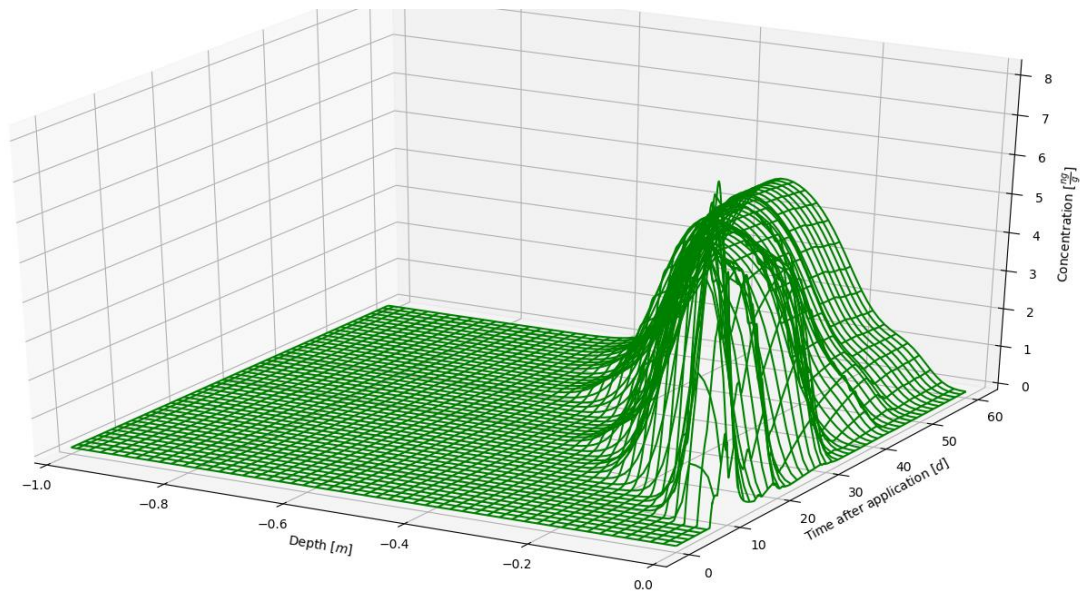


Figure 74: Concentration of OA in the slices down to a depth of 1 m

Figure 75 shows the concentration of the metabolite ESA in the first and second layer and figure 76 shows the concentrations of ESA in all slices.

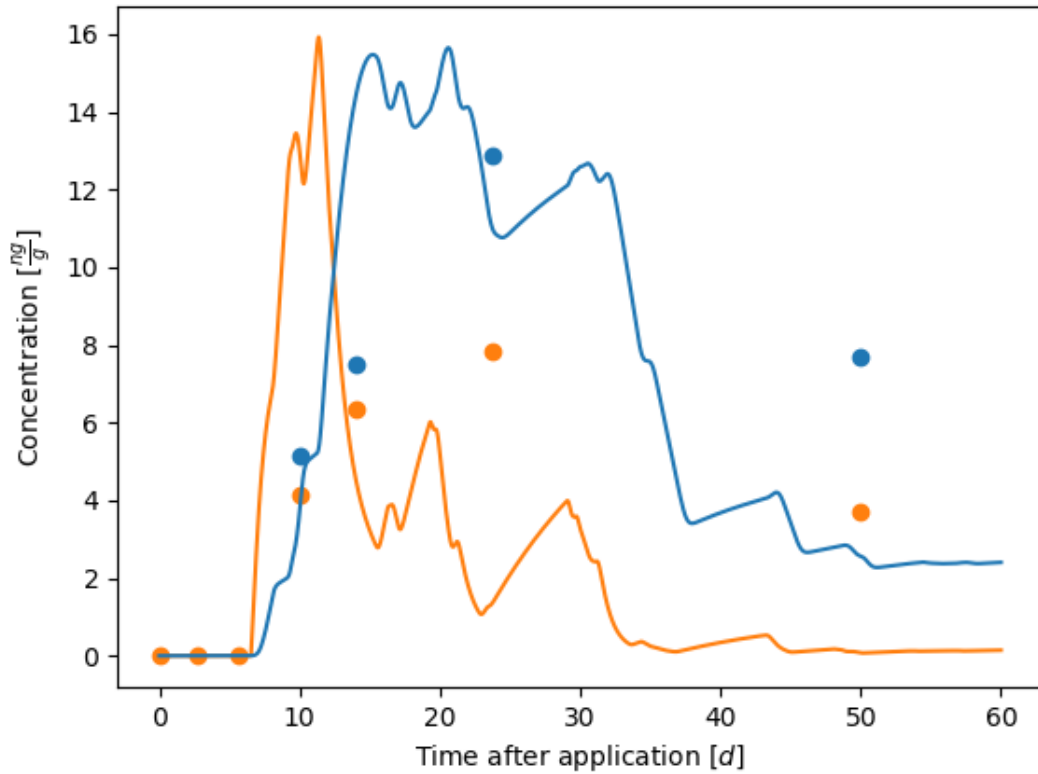


Figure 75: Concentration of ESA in the first (0-5 cm) and the second (5-17 cm) layer (dots: measurements; lines: calculations; orange: first layer; blue: second layer)

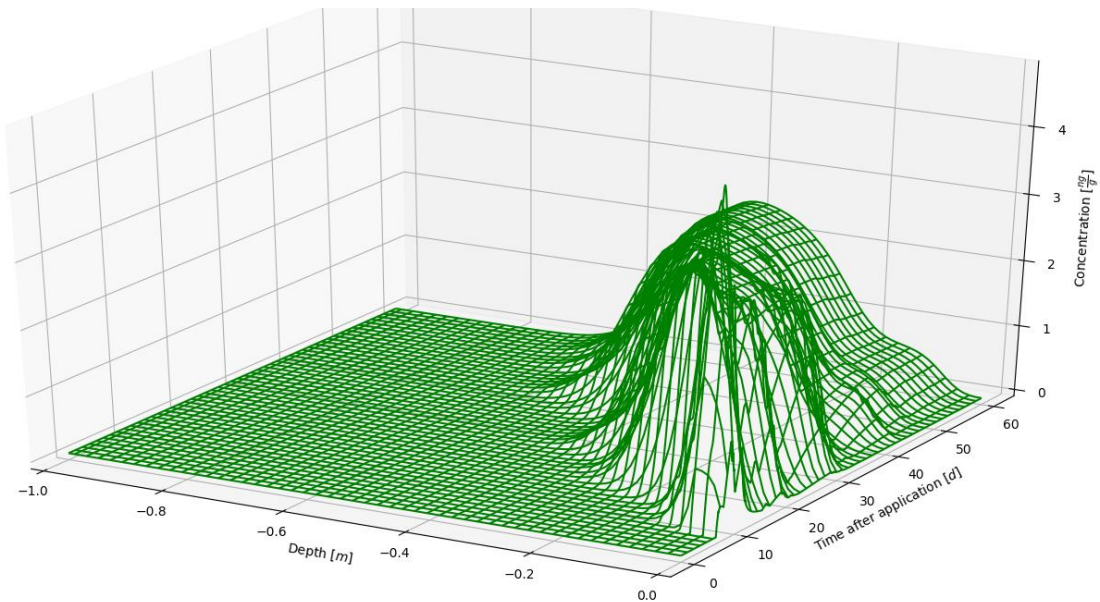


Figure 76: Concentration of ESA in the slices down to a depth of 1 m

The modelled water movement is shown in figure 77.

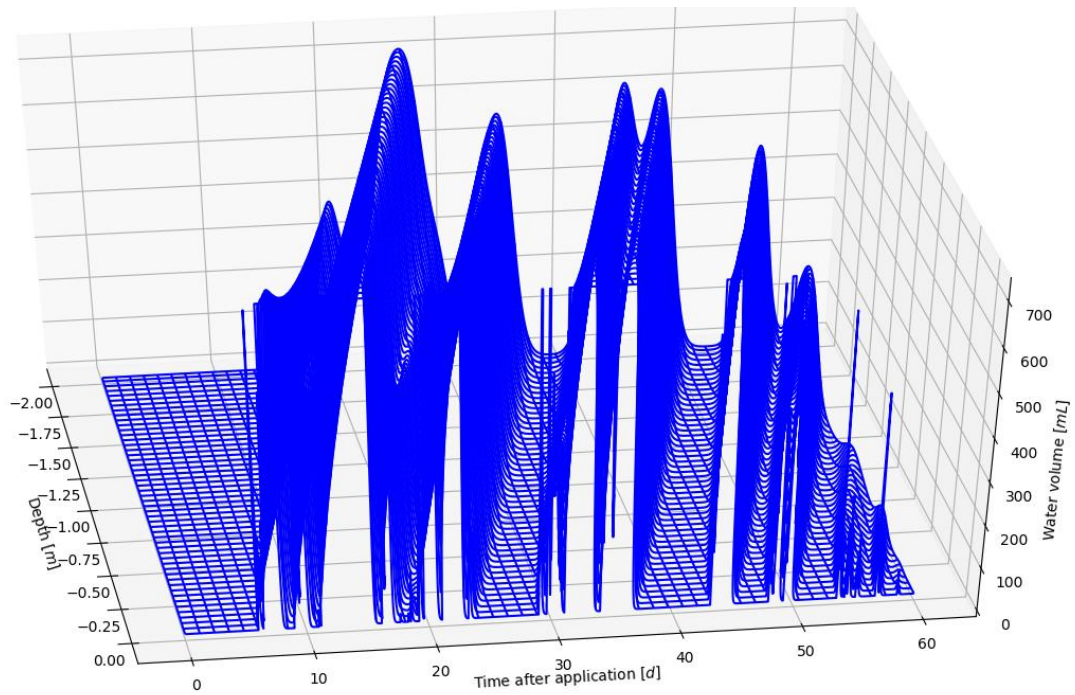


Figure 77: Modelled water movement in the soil

10 Discussion of the model calculations

10.1 Comparison of the model with the field measurement

10.1.1 S-metolachlor

The concentration of SMOC in the second layer was mainly lower than the one in the first layer because the adsorption coefficient of SMOC was set high. Therefore, the rainfall had a marginal impact on the concentration decline of SMOC in the model. This confirmed the hypothesis that the driving force behind the concentration decline of SMOC is degradation and not leaching.

The measured concentration of the first sample after the rainfall was lower than predicted by the model (red circle in figure 78). This is explained by the decisive effect of the first rainfall (chapter 8.1.8.2.2), which was ignored in the model. Meanwhile, the predicted concentration in the second layer did not reach the measured 112.52 ng/g (green circle in figure 78). The model could not fully explain the high concentration in the second layer. Already the qualitative analysis (chapter 8.1.9) has shown that the concentration in the lower level is surprisingly high and the concentrations cannot be explained unless additional key factors (e.g. diffusion) are assumed that have not been modelled.

The last two measured concentrations were higher than the prediction of the model because the model did not consider the increasing adsorption of SMOC and used a constant adsorption coefficient instead. Additionally, the biodegradation rate was assumed to be constant.

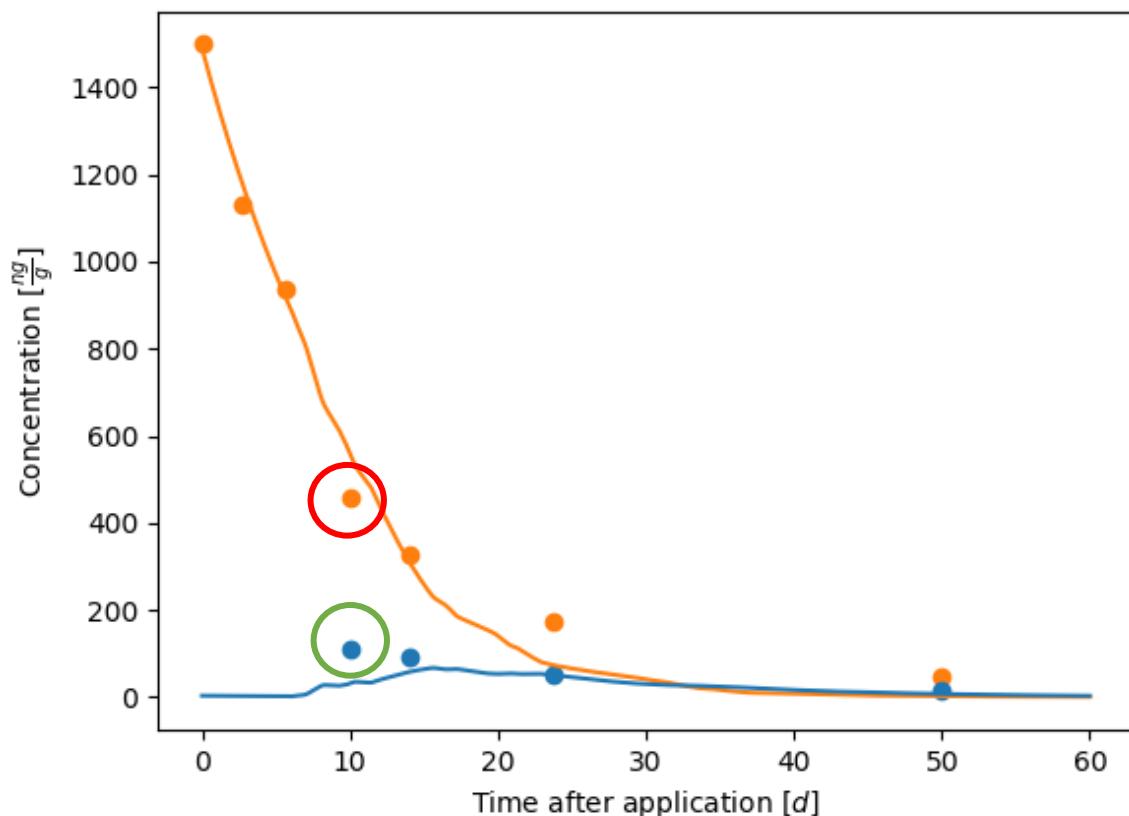


Figure 78: Concentration of SMOC in the first (0-5 cm) and the second (5-17 cm) layer (dots: measurements; lines: calculations; orange: first layer; blue: second layer; red circle: measurement of the sample in the first layer after the first rainfall; green circle: measurement of the sample in the second layer after the first rainfall)

10.1.2 Metabolites

While leaching had a marginal effect on the concentration decline of SMOC, the rain in the model had a decisive effect on the concentration decline of the metabolites OA and ESA. This was noticeable because the concentrations of the metabolites in the second layer were mainly higher than the ones in the first layer and there were abrupt changes in the concentration curve of the metabolites (peaks in figure 79).

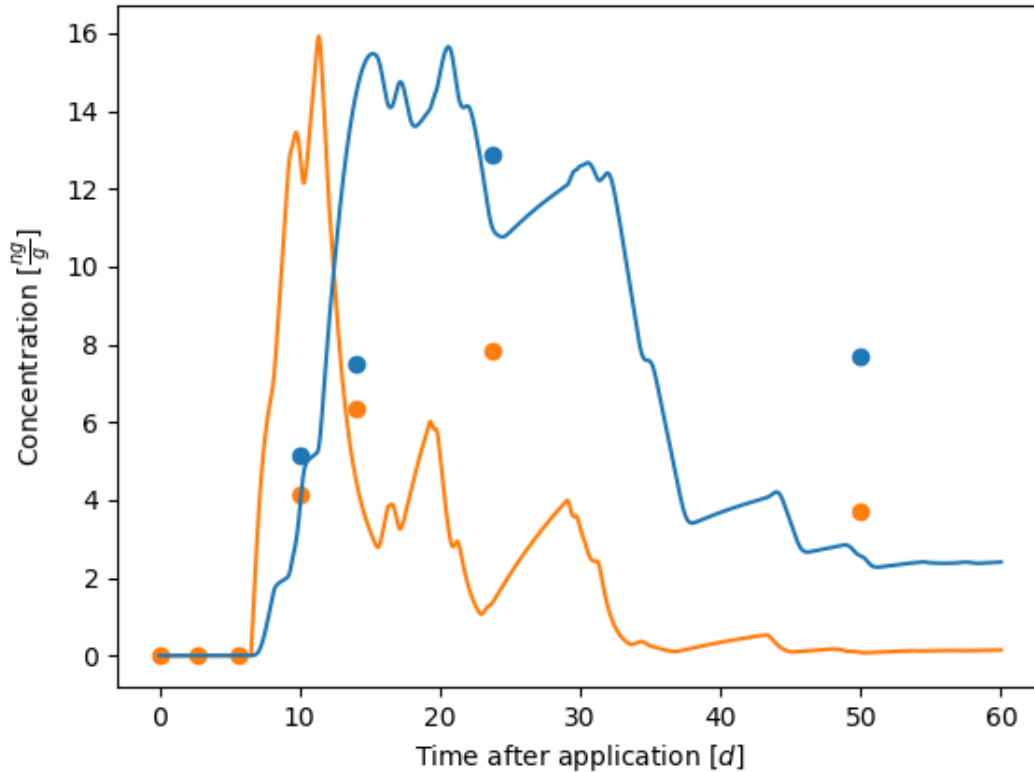


Figure 79: Concentration of ESA in the first (0-5 cm) and the second (5-17 cm) layer (dots: measurements; lines: calculations; orange: first layer; blue: second layer)

Therefore, the model very well reproduced the finding of the field measurement that the metabolites are more mobile than their parent molecule and that the transport of SMOC is of minor importance [1]. The driving forces behind the course of the concentration of the metabolites are therefore probably the degradation of SMOC and leaching of the metabolites. In reality, there are probably more gradual changes in the concentration because soil is inherently heterogeneous and the adsorption equilibrium is not established immediately, as assumed by the model [62].

The calculated concentrations of the first layer were lower than the measured ones. This might be due to a variety of reasons. The occurrence fraction, the adsorption coefficient or the m_{FS} in the first layer might have been higher.

10.2 Comparison of the water movement model with literature

An exponential function approached the water movement in the soil. However, the movement of a liquid in a porous material is much more complicated. Table 29 compares the modelled water movement to the information provided by literature. Richard's equation models the water movement in unsaturated in more detail. Darcy's law models the water movement in saturated soil [53], [52].

literature	model
The capacity of a slice is limited [69].	The capacity of the slices in the model was limited by the limited outflow of the water reservoir into the first slice.
Water in smaller pores is more resistant to emptying and is favoured when the slice is filled due to capillary forces [70], [71].	The capillary forces were imitated by the fact that the outflow of a slice was proportional to the current water volume in the slice. The more water was contained in a slice, the more of the large pores were filled, leading to a faster outflow. Therefore, the outflow slowed down if the water volume decreased.
If it no longer rains, the water keeps flowing into deeper layers. The water is redistributed, which means it is levelled out so that there are no big differences between the water volumes in the slices. Hence, the outflow of a slice depends not only on the current water volume but also on how dry the subsequent slices are [71].	If the inflow into a slice stopped, the water kept flowing out of the slice. However, the model did not consider the dryness of the subsequent slices.
The water can also flow upwards and sideways due to capillary forces and evaporation [72].	The model only considered the downward water movement to the groundwater.
The speed of the water movement depends on the grain size distribution and on the porosity of the soil [68]. The water movement in sandy soils is faster than in clayey soils [71].	The constant "p" in the model determined the speed of the water movement and can be adapted depending on the soil type. The speed constant should be obtained by measuring the speed of the water movement in the soil of Arth.
The speed of the water movement and the capacity changes over depth because there are different layers in the soil, which have different grain size distributions and porosity [73].	The changing capacity and speed over depth were not considered in the model.
If there is heavy rainfall, the water ponds on the surface of the soil. Therefore, the water	The water reservoir imitated ponding on the surface of the soil during heavy rainfall. However, the model ignored run-off from the

literature	model
can run off from fields with steep slopes [24], [60].	field. In order to apply the model to fields with steep slopes as well, the amount of the water in the reservoir that runs off should be reconsidered.
Soil densifies over time. Moreover, the soil aggregates are compacted after the first rainfall leading to slower water movement [22].	The model did not consider compaction of the soil.

Table 29: Comparison between the modelled water movement and literature

10.3 Comparison of the concentration course model with literature

Table 30 compares the model to literature information about the leaching and the degradation of the pollutants.

literature	model
The degradation is not an ideal exponential decline because of changing circumstances such as a growing microbial population, moisture and increasing adsorption over time [23].	The model of the concentration decline assumed an ideal exponential degradation
The biodegradation rate is higher in water because the pollutant is more bioavailable for the microorganisms [23].	The degradation rate was assumed to be the same in soil and water.
The OC content decreases with depth which results in stronger adsorption and faster degradation [63]. Moreover, the bulk density of the soil changes over depth [60].	The model did not consider changes of the OC content or the bulk density.
Some molecules are adsorbed more strongly than others because the soil surface is inhomogeneous [62].	The model assumed a homogeneous soil surface.
The adsorption equilibrium needs time to be established. For this reason, there is often a non-equilibrium in the soil and the water [62].	The model assumed that the adsorption equilibrium is established immediately.

Table 30: Comparison between the modelled concentration decline and literature

10.4 Conclusion

Considerable efforts were undertaken to clarify the premises of the soil water model and to obtain a realistic model of the water flow inside the soil.

The developed model, although highly simplified in essential points, showed a complex behaviour. The model showed a satisfactory qualitative agreement with measured data. By varying the parameters, the effect of those on the concentration decline was examined. In fact, the model helped enormously to clarify the relevance of the various influencing factors and to write the first part of this paper, which can only be poorly reflected in the text.

The model tried to fill the gaps of the measurements by calculating the concentrations in all layers and between the sample measurements. For example, the model showed that the concentration of the metabolites increased significantly in the deeper layers. Nevertheless, the model cannot replace field measurements because the model was still not able to explain the detailed course of the concentrations. Best qualitative agreement with the measured data was achieved with a comparatively fast biodegradation rate, a low leaching rate of SMOC, and higher leaching rates for the degradation products, which is in good agreement with literature data.

The results of the model made it apparent that the fate of the metabolites in nature is much more complicated than the one assumed by the model. They clearly showed that precipitation, water movement, and constant rates of adsorption and biodegradation cannot explain the detailed time course of the chemical concentrations.

The results suggest that the following additional factors are crucial for the exact concentration course of the investigated compounds:

- The model confirmed the hypothesis that degradation and leaching rates must be time-dependent, strongly indicating an increasing adsorption strength over time
- The model showed that in order to understand the initial time course of the degradation products, measurements of the concentration in the lower levels would be indispensable.
- The model suggests that the uptake of the herbicide by plants plays a crucial role, especially during the first days after application of the herbicide.

11 List of abbreviations and glossary

ASE	accelerated solvent extraction
BD	bulk density
ESA	metolachlor ethane sulfonic acid
ESI	electrospray ionisation
FS	fine soil
HPLC-MS/MS	high-performance liquid chromatography coupled to triple quadrupole tandem mass spectrometry
IS	internal standard
K_d	adsorption coefficient
LOQ	limit of quantification
m/q	mass-to-charge ratio
NABO	national soil monitoring
OA	metolachlor oxanilic acid
OC	organic carbon
OF	occurrence fraction
PPP	plant protection product
SMOC	S-metolachlor
SS	solid substance

12 Table of figures

Figure	Source	Page
Figure 1: (α R, 1'S)-metolachlor [5]	[5]	7
Figure 2: (α R, 1'R)-metolachlor [5]	[5]	7
Figure 3: (α S, 1'S)-metolachlor [5]	[5]	7
Figure 4: (α S, 1'R)-metolachlor [5]	[5]	7
Figure 5: Structure of S-metolachlor [11]	[11]	8
Figure 6: Structure of ESA [12]	[12]	9
Figure 7: Structure of OA [13]	[13]	9
Figure 8: Degradation pathways of SMOC (1) to OA (8) and ESA (10) (G: glutathione) [14]	[14]	13
Figure 9: Application method (spraying) of Calado in Arth	-	15
Figure 10: Brown square: 10 x 10 m plot (blue points: tent pegs; red points: Humax samples)	-	16
Figure 11: Distances of the two poles (A, B) of the 10 x 10 m plot to the waypoints (F1, F2)	-	16
Figure 12: Tools: half-pipe drill (1), plastic bag (2), spatula (3), wooden template (4)	-	17
Figure 13: The half-pipe drill is pushed into the soil.	-	18
Figure 14: Half-pipe drill with soil	-	18
Figure 15: Humax drill (5), hammer (6), plastic tube (7)	-	18
Figure 16: Pulling out the Humax drill containing soil	-	18
Figure 17: Overview of the rainfall and the samples (grey: cumulative rainfall; orange: only the sample of the first layer was analysed; blue: the samples of both layers were analysed; black: the samples were not analysed.)	-	19
Figure 18: Overview of the analytical procedure	-	21
Figure 19: Structure of SMOC d11 [35]	[35]	22
Figure 20: The concentration of the analyte (grey) and the IS (yellow) before the analytical procedure ($c_{1analyte}$ and c_{1IS}) and after possible losses ($c_{2analyte}$ and c_{2IS})	-	22
Figure 21: The signal produced by the HPLC-MS/MS over time (grey: area of the peak of the analyte ($A_{analyte}$); yellow: area of the peak of the IS (A_{IS}))	-	23
Figure 22: Example of a calibration curve (blue points: example of concentration ratios and area ratios in calibration samples; $C_{1analyte} / C_{1IS}$: concentration ratio in the first calibration sample; $A_{1analyte} / A_{1IS}$: area ratio in the first calibration sample)	-	23
Figure 23: Average percentual mass decline of the soil samples of the first (orange) and the second layer (blue) during the drying	-	26
Figure 24: Schematic instrumentation of an ASE device [34]	[34]	29
Figure 25: ASE device at Agroscope	-	30
Figure 26: Basic parts of the ASE extraction cell	-	32
Figure 27: Principle of spiked samples (green: the concentration of the background presence; orange: the spiked concentration; yellow: an example of the concentration after the analytical procedure)	-	33
Figure 28: Procedure of scaling the concentration in the extracted samples (1: levelling out volumes; 2: taking an aliquot and adding the IS (blue drop); 3: evaporation; 4: filling of the vials for the HPLC-MS/MS)	-	34

Figure	Source	Page
Figure 29: Spiking three calibration samples with different amounts of SMOC and a constant amount of IS (yellow drop: solvent containing the IS; grey drop: solvent containing the analytes (SMOC, ESA, and OA))	-	36
Figure 30: N2 evaporator	-	36
Figure 31: Method to calculate the area ratio in the samples 1, 2, 3, and 10 (A1analyte: area of the analyte in the undiluted samples; A1IS: area of the IS in the undiluted sample; A2analyte: area of the analyte in the diluted sample; A2IS: area of the IS in the diluted sample)	-	37
Figure 32: HPLC-MS/MS	-	38
Figure 33: Schematic instrumentation of an HPLC device [39]	[39]	39
Figure 34: Schematic instrumentation of an ESI [40]	[40]	40
Figure 35: Schematic instrumentation of an MS/MS with three quadrupoles [34]	[34]	41
Figure 36: Schematic instrumentation of a quadrupole and the illustration of its separation method [43] (DC: direct current; AC: alternating current)	[43]	41
Figure 37: Munsell colour charts with the soil	-	43
Figure 38: Hellige Pehameter	-	43
Figure 39: Water movement according to the first model (blue: water; red: proportional valve)	-	45
Figure 40: Water movement according to the second model during the rainy period and the dry period (The picture on the right shows the water movement during the dry period as soon as slice 0 was empty.)	-	45
Figure 41: Water movement according to the final model (blue: water; red: proportional valve)	-	46
Figure 42: The water volume decline in a slice with a standard thickness $d_{standard}$ as soon as the inflow had stopped (1% of the capacity remains after $t_{emptied}$.)	-	47
Figure 43: Sequence of the calculations of the concentrations of SMOC in a single slice in the soil from t to $t+\Delta t$ (for a description of the variables see chapter 6.5)	-	48
Figure 44: Sequence of the calculations of the concentrations of SMOC in a single slice in the soil water from t to $t+\Delta t$ (for a description of the variables see chapter 6.5)	-	48
Figure 45: Sequence of the calculations of the concentrations of OA in a single slice in the soil from t to $t+\Delta t$ (for a description of the variables see chapter 6.5)	-	51
Figure 46: Sequence of the calculations of the concentrations of OA in a single slice in the water in the soil from t to $t+\Delta t$ (for a description of the variables see chapter 6.5)	-	51
Figure 47: The difference between the measured layers and the first slices with a thickness of 1 cm	-	52
Figure 48: Time course of the concentration of SMOC in two soil layers (orange dots: first layer (0-5 cm), blue dots: second layer (5-17 cm))	-	59
Figure 49: DT50 between two samples of the first (orange) and the second layer (blue)	-	59
Figure 50: Concentration of OA in the two layers (orange: first layer (0-5 cm); blue: second layer (5-17 cm))	-	60

Figure	Source	Page
Figure 51: Concentration of ESA in the two layers (orange: first layer (0-5 cm); blue: second layer (5-17 cm))	-	61
Figure 52: Signal and noise in the LOQ of OA (concentration = 2 ng/g)	-	63
Figure 53: Signal and noise in the LOQ of ESA (concentration = 1 ng/g)	-	63
Figure 54: The difference between accuracy and precision [34]	[33]	64
Figure 55: Concentration of SMOC in the first (orange) and the second (blue) layer with numbering	-	66
Figure 56: Trendlines using different minimisation techniques (dotted: relative minimisation; dashed: absolute minimisation; orange points: measured concentration of the samples in the first layer)	-	69
Figure 57: Trendline of the concentration decline in the first layer using absolute minimisation	-	70
Figure 58: Trendline of the concentration decline in the second layer using absolute minimisation	-	70
Figure 59: DT50 between two samples in the first layer	-	73
Figure 60: Correlation between the concentration and the DT50	-	74
Figure 61: Correlation between the average temperature 2 m above the ground and DT50 in the first layer	-	75
Figure 62: Correlation between time and the DT50. (time after application: the time when sample n was taken; DT50: DT50 between sample n and n+1; blue arrow: impact of the rain; dashed black line: increasing DT50 during the dry period; dotted black line: increasing DT50 during the rainy period)	-	76
Figure 63: DT50 between two samples of the first layer (orange) and the average volume of the rainfall per day between two samples (red)	-	77
Figure 64: Correlation between DT50 and the average volume of the rainfall per day	-	78
Figure 65: DT50 between two samples of the first layer	-	79
Figure 66: Concentration decline in the first layer with the trendline and the cumulative rainfall (dashed: trendline using absolute minimisation; orange: measured samples in the first layer; green: cumulative rainfall since the background sample)	-	79
Figure 67: DT50 between two samples of the first (orange) and the second layer (blue)	-	80
Figure 68: Trendline of the three samples during the dry period (orange: mass of SMOC in the first layer; blue: mass of SMOC in the second layer)	-	81
Figure 69: Concentration of ESA in the two layers (orange: layer 0-5 cm; blue: layer 5-17 cm)	-	82
Figure 70: Mass of ESA within the first and second layer per hectare (orange: layer 0-5 cm; blue: layer 5-17 cm)	-	83
Figure 71: Concentration of SMOC in the first (0-5 cm) and the second (5-17 cm) layer (dots: measurements; lines: calculations; orange: first layer; blue: second layer)	-	89
Figure 72: Concentration of SMOC in the slices down to a depth of 0.25 m	-	89
Figure 73: Concentration of OA in the first (0-5 cm) and the second (5-17 cm) layer (dots: measurements; lines: calculations; orange: first layer; blue: second layer)	-	90
Figure 74: Concentration of OA in the slices down to a depth of 1 m	-	90

Figure	Source	Page
Figure 75: Concentration of ESA in the first (0-5 cm) and the second (5-17 cm) layer (dots: measurements; lines: calculations; orange: first layer; blue: second layer)	-	91
Figure 76: Concentration of ESA in the slices down to a depth of 1 m	-	91
Figure 77: Modelled water movement in the soil	-	92
Figure 78: Concentration of SMOC in the first (0-5 cm) and the second (5-17 cm) layer (dots: measurements; lines: calculations; orange: first layer; blue: second layer; red circle: measurement of the sample in the first layer after the first rainfall; green circle: measurement of the sample in the second layer after the first rainfall)	-	93
Figure 79: Concentration of ESA in the first (0-5 cm) and the second (5-17 cm) layer (dots: measurements; lines: calculations; orange: first layer; blue: second layer)	-	94

Table 31: Source and page of the figures

13 Bibliography

- [1] L. Brückner, H. Kupfersberger, G. Klammler, J. Fank, and M. Kah, 'Sorptions- und Abbau von s-Metolachlor und dessen Metaboliten Metolachlor-OA und Metolachlor-ESA im Boden', p. 6.
- [2] 'ESS5 Pest and pesticide management | Environmental and Social Standards | Food and Agriculture Organization of the United Nations'. <http://www.fao.org/environmental-social-standards/standards/ess5/en/> (accessed Nov. 24, 2020).
- [3] M. Reinhardt, R. Kozel, A. Hofacker, and C. Leu, 'MONITORING VON PSM-RÜCKSTÄNDEN IM GRUNDWASSER', *aqua & gas*, p. 89, Jun. 2017.
- [4] 'Mikroverunreinigungen', *Kanton Zug*. <https://www.zg.ch/behoerden/audirektion/amt-fuer-umwelt/wasser-gewaesser/abwasser/mikroverunreinigungen> (accessed Jan. 12, 2021).
- [5] 'Metolachlor', *Wikipedia*. Jun. 25, 2020, Accessed: Jan. 24, 2021. [Online]. Available: <https://en.wikipedia.org/w/index.php?title=Metolachlor&oldid=964373592>.
- [6] J. Xie, L. Zhang, L. Zhao, Q. Tang, K. Liu, and W. Liu, 'Metolachlor stereoisomers: Enantioseparation, identification and chiral stability', *J Chromatogr A*, vol. 1463, pp. 42–48, Sep. 2016, doi: 10.1016/j.chroma.2016.07.045.
- [7] H. Liu, Y. Xia, W. Cai, Y. Zhang, X. Zhang, and S. Du, 'Enantioselective oxidative stress and oxidative damage caused by Rac- and S-metolachlor to *Scenedesmus obliquus*', *Chemosphere*, vol. 173, pp. 22–30, Apr. 2017, doi: 10.1016/j.chemosphere.2017.01.028.
- [8] K. A. Lewis, J. Tzilivakis, D. J. Warner, and A. Green, 'An international database for pesticide risk assessments and management', *Human and Ecological Risk Assessment: An International Journal*, vol. 22, no. 4, pp. 1050–1064, May 2016, doi: 10.1080/10807039.2015.1133242.
- [9] J. B. Weber *et al.*, 'A Proposal to Standardize Soil/Solution Herbicide Distribution Coefficients', *Weed Science*, vol. 48, no. 1, pp. 75–88, 2000.
- [10] PubChem, 'Metolachlor'. <https://pubchem.ncbi.nlm.nih.gov/compound/4169> (accessed Oct. 14, 2020).
- [11] 'S-Metolachlor | CAS 87392-12-9 | LGC Standards'. <https://www.lgcstandards.com/DE/de/S-Metolachlor/p/DRE-C15171000> (accessed Oct. 11, 2020).
- [12] 'Metolachlor-ESA'. <http://www.neochema-shop.com/pesticides--pharma/pesticides--metabolites/single-substances/metolachlor-esa.php> (accessed Oct. 11, 2020).
- [13] 'Metolachlor OA (152019-73-3) (MET-12478D-10MG)'. https://www.chemservice.com/metolachlor-oa-met-12478d-10mg.html?__SID=U (accessed Jan. 24, 2021).
- [14] D. H. Hutson, *Metabolic Pathways of Agrochemicals*. Royal Society of Chemistry, 1998.
- [15] E. P. Fuerst, 'Understanding the Mode of Action of the Chloroacetamide and Thiocarbamate Herbicides', *Weed Technology*, vol. 1, no. 4, pp. 270–277, 1987.
- [16] 'DUAL GOLD', *Syngenta*, May 10, 2016. <https://www.syngenta.de/produkte/pflanzenschutz/herbizid/dual-gold> (accessed Oct. 10, 2020).
- [17] 'Calado : Produkte : Stähler Suisse SA'. <https://www.staehler.ch/de/produkte/detail/calado%231517> (accessed Nov. 28, 2020).
- [18] J. Stenersen, *Chemical Pesticides Mode of Action and Toxicology*. CRC Press, 2004.
- [19] B. Matthes, 'Die Wirkungsweise herbizidaler Chloroacetamide', *Mode of action of chloroacetamide herbicides*, 2001, Accessed: Oct. 03, 2020. [Online]. Available: <https://kops.uni-konstanz.de/handle/123456789/7958>.
- [20] C. R. Zemolin, L. A. Avila, G. V. Cassol, J. H. Massey, and E. R. Camargo, 'Environmental fate of S-Metolachlor: a review', *Planta Daninha*, vol. 32, no. 3, pp. 655–664, Sep. 2014, doi: 10.1590/S0100-83582014000300022.

- [21] C. Trigo, K. A. Spokas, K. E. Hall, L. Cox, and W. C. Koskinen, 'Metolachlor Sorption and Degradation in Soil Amended with Fresh and Aged Biochars', *J. Agric. Food Chem.*, p. 9, 2016.
- [22] F. Meite, P. Alvarez-Zaldivar, A. Crochet, C. Wiegert, S. Payraudeau, and G. Imfeld, 'Impact of rainfall patterns and frequency on the export of pesticides and heavy-metals from agricultural soils', *Science of The Total Environment*, vol. 616–617, pp. 500–509, Mar. 2018, doi: 10.1016/j.scitotenv.2017.10.297.
- [23] Y. H. Long, R. T. Li, and X. M. Wu, 'Degradation of S-metolachlor in soil as affected by environmental factors', *Journal of soil science and plant nutrition*, vol. 14, no. 1, pp. 189–198, Mar. 2014, doi: 10.4067/S0718-95162014005000015.
- [24] G. I. Patakioutas and T. A. Albanis, 'Runoff of herbicides from cropped and uncropped plots with different slopes', *International Journal of Environmental Analytical Chemistry*, vol. 84, no. 1–3, pp. 103–121, Jan. 2004, doi: 10.1080/03067310310001593747.
- [25] R. J. Rector, D. L. Regehr, P. L. Barnes, and T. M. Loughin, 'Atrazine, S-metolachlor, and isoxaflutole loss in runoff as affected by rainfall and management', *Weed science*, 2003, Accessed: Oct. 11, 2020. [Online]. Available: <https://agris.fao.org/agris-search/search.do?recordID=US201500180513>.
- [26] J. Velisek, A. Stara, E. Zuskova, J. Kubec, M. Buric, and A. Kouba, 'Effects of s-metolachlor on early life stages of marbled crayfish', *Pesticide Biochemistry and Physiology*, vol. 153, pp. 87–94, Jan. 2019, doi: 10.1016/j.pestbp.2018.11.007.
- [27] C. Quintaneiro, D. Patrício, S. C. Novais, A. M. V. M. Soares, and M. S. Monteiro, 'Endocrine and physiological effects of linuron and S-metolachlor in zebrafish developing embryos', *Science of The Total Environment*, vol. 586, pp. 390–400, May 2017, doi: 10.1016/j.scitotenv.2016.11.153.
- [28] P. J. Rice, 'The persistence, degradation, and mobility of metolachlor in soil and the fate of metolachlor and atrazine in surface water, surface water/sediment, and surface water/aquatic plant systems', p. 147.
- [29] P. F. Martins *et al.*, 'Selection of microorganisms degrading S-Metolachlor herbicide', *Brazilian Archives of Biology and Technology*, vol. 50, no. 1, pp. 153–159, Jan. 2007, doi: 10.1590/S1516-89132007000100019.
- [30] L. Alletto *et al.*, 'Sorption and mineralisation of S-metolachlor in soils from fields cultivated with different conservation tillage systems', *Soil and Tillage Research*, vol. 128, pp. 97–103, Apr. 2013, doi: 10.1016/j.still.2012.11.005.
- [31] D. J. Ashworth, S. R. Yates, M. Stanghellini, and I. J. van Wesenbeeck, 'Application rate affects the degradation rate and hence emissions of chloropicrin in soil', *Science of The Total Environment*, vol. 622–623, pp. 764–769, May 2018, doi: 10.1016/j.scitotenv.2017.12.060.
- [32] 'Bundesamt für Landwirtschaft BLW – Pflanzenschutzmittelverzeichnis'. <https://www.psm.admin.ch/de/produkte/5651-2> (accessed Oct. 10, 2020).
- [33] A. Rösch, 'Statement, Agroscope', 2020.
- [34] 'Vorlesungsverzeichnis - ETH Zürich'. <http://www.vvz.ethz.ch/Vorlesungsverzeichnis/lerneinheit.view?lerneinheitId=119957&semkez=2018S&lang=de> (accessed Jan. 16, 2021).
- [35] 'Metolachlor-(2-ethyl-6-methylphenyl-d11) PESTANAL®, analytical standard | Sigma-Aldrich'. <https://www.sigmaaldrich.com/catalog/product/sial/07752?lang=de®ion=CH> (accessed Jan. 24, 2021).
- [36] A. Toubane, S.-A. Rezzoug, C. Besombes, and K. Daoud, 'Optimization of Accelerated Solvent Extraction of *Carthamus Caeruleus* L. Evaluation of antioxidant and anti-inflammatory activity of extracts', *Industrial Crops and Products*, vol. 97, pp. 620–631, Mar. 2017, doi: 10.1016/j.indcrop.2016.12.002.

- [37] B. E. Richter, B. A. Jones, J. L. Ezzell, N. L. Porter, N. Avdalovic, and C. Pohl, 'Accelerated Solvent Extraction: A Technique for Sample Preparation', *Analytical Chemistry*, vol. 68, no. 6, pp. 1033–1039.
- [38] '9. LoD and LoQ'. https://sisu.ut.ee/lcms_method_validation/9-lod-and-loq (accessed Oct. 10, 2020).
- [39] E. Team, 'High Performance Liquid Chromatography (HPLC) : Principle, Types, Instrumentation and Applications', *LaboratoryInfo.com*, Jan. 11, 2020. <https://laboratory-info.com/hplc/> (accessed Nov. 10, 2020).
- [40] L. Konermann, E. Ahadi, A. D. Rodriguez, and S. Vahidi, 'Unraveling the Mechanism of Electrospray Ionization', *Anal. Chem.*, vol. 85, no. 1, pp. 2–9, Jan. 2013, doi: 10.1021/ac302789c.
- [41] P. Bults, M. Meints, A. Sonesson, M. Knutsson, R. Bischoff, and N. C. van de Merbel, 'Improving selectivity and sensitivity of protein quantitation by LC–HR–MS/MS: determination of somatropin in rat plasma', *Bioanalysis*, vol. 10, no. 13, pp. 1009–1021, Jun. 2018, doi: 10.4155/bio-2018-0032.
- [42] E. de Hoffmann, 'Mass Spectrometry', in *Kirk-Othmer Encyclopedia of Chemical Technology*, American Cancer Society, 2005.
- [43] G. Santoiemma, 'Recent methodologies for studying the soil organic matter', *Applied Soil Ecology*, vol. 123, pp. 546–550, Sep. 2017, doi: 10.1016/j.apsoil.2017.09.011.
- [44] P. Schwab, 'Statement NABO', 2020.
- [45] F. Hagedorn, H.-M. Krause, M. Studer, A. Schellenberger, and A. Gattinger, 'Organische Bodensubstanz, Treibhausgasemissionen und physikalische Belastung von Schweizer Böden', p. 98.
- [46] T. Schiller, 'Bodenart und Bodentyp: Bestimmung und Bedeutung für Böden', p. 4.
- [47] D. Neina, 'The Role of Soil pH in Plant Nutrition and Soil Remediation', *Applied and Environmental Soil Science*, vol. 2019, p. 5794869, Nov. 2019, doi: 10.1155/2019/5794869.
- [48] 'Block B: Beschreibung des Humus- und Kohlenstoffgehaltes im Feld'. <https://www.bodenkunde-projekte.hu-berlin.de/carlos/B01feldbeschreibung.html> (accessed Nov. 28, 2020).
- [49] 'Munsell - Charts'. http://www.spectrumcolors.de/cor_munsell_single.php (accessed Sep. 06, 2020).
- [50] D. L. Nätscher, 'Die Bestimmung der Bodenart mittels Fingerprobe', p. 26.
- [51] 'Hellige-pH-indicator - Feldmessgeräte | Eijkelkamp'. <https://de.eijkelkamp.com/produkte/feldmessger-te/hellige-ph-indikator.html> (accessed Nov. 28, 2020).
- [52] M. Allaby, 'Darcy's law', in *A Dictionary of Ecology*, Oxford University Press, 2010.
- [53] Y. Pachepsky, D. Timlin, and W. Rawls, 'Generalized Richards' equation to simulate water transport in unsaturated soils', *Journal of Hydrology*, vol. 272, no. 1–4, pp. 3–13, Mar. 2003, doi: 10.1016/S0022-1694(02)00251-2.
- [54] P. Weisskopf, U. Zihlmann, T. Anken, and M. Holpp, 'Beeinflussen des Wasserhaushaltes von Ackerböden durch Bewirtschaftungsmassnahmen', p. 29.
- [55] B. Magnusson, *The fitness for purpose of analytical methods : A laboratory guide to method validation and related topics (2nd ed. 2014)*. Eurachem, 2014.
- [56] D. A. Armbruster and T. Pry, 'Limit of Blank, Limit of Detection and Limit of Quantitation', *Clin Biochem Rev*, vol. 29, no. Suppl 1, pp. S49–S52, Aug. 2008.
- [57] United Nations Office on Drugs and Crime and Laboratory and Scientific Section, *Guidance for the validation of analytical methodology and calibration of equipment used for testing of illicit drugs in seized materials and biological specimens: a commitment to quality and continuous improvement*. 2009.
- [58] medev, 'agrometeo', *agrometeo*. <https://www.agrometeo.ch/> (accessed Dec. 29, 2020).

- [59] S. Reynolds, 'ANALYTICAL QUALITY CONTROL', p. 46.
- [60] M. Kato *et al.*, 'Influence of Monsoon Regime and Microclimate On Soil Respiration In The Tropical Forests', Mar. 2018, doi: 10.9790/2402-1203026373.
- [61] 'Swiss Geoportal', *geo.admin.ch*. <https://map.geo.admin.ch> (accessed Dec. 12, 2020).
- [62] P. Sidoli, L. Lassabatere, R. Angulo-Jaramillo, and N. Baran, 'Experimental and modeling of the unsaturated transports of S-metolachlor and its metabolites in glaciofluvial vadose zone solids', *Journal of Contaminant Hydrology*, vol. 190, pp. 1–14, Jul. 2016, doi: 10.1016/j.jconhyd.2016.04.001.
- [63] P. Rice, T. Anderson, and J. Coats, 'Degradation and persistence of metolachlor in soil: Effects of concentration, soil moisture, soil depth, and sterilization', *Environmental Toxicology and Chemistry*, vol. 21, pp. 2640–2648, Dec. 2002, doi: 10.1897/1551-5028(2002)021<2640:DAPOMI>2.0.CO;2.
- [64] P. F. Martins *et al.*, 'Effects of the herbicides acetochlor and metolachlor on antioxidant enzymes in soil bacteria', *Process Biochemistry*, vol. 46, no. 5, pp. 1186–1195, May 2011, doi: 10.1016/j.procbio.2011.02.014.
- [65] L. Vermeersch *et al.*, 'On the duration of the microbial lag phase', *Curr Genet*, vol. 65, no. 3, pp. 721–727, Jun. 2019, doi: 10.1007/s00294-019-00938-2.
- [66] P. Böger and B. Matthes, 'Inhibitors of Biosynthesis of Very-Long-Chain Fatty Acids', in *Herbicide Classes in Development: Mode of Action, Targets, Genetic Engineering, Chemistry*, P. Böger, K. Wakabayashi, and K. Hirai, Eds. Berlin, Heidelberg: Springer, 2002, pp. 115–137.
- [67] B. für U. B. | O. fédéral de l'environnement O. | U. federale dell'ambiente UFAM, 'Grundwasser'. <https://www.bafu.admin.ch/bafu/de/home/themen/thema-wasser/wasser--publikationen/publikationen-wasser/grundwasser.html> (accessed Dec. 13, 2020).
- [68] '9. Soil Permeability'. http://www.fao.org/tempref/fi/cdrom/fao_training/fao_training/general/x6706e/x6706e09.htm (accessed Jan. 02, 2021).
- [69] 'Water Holding Capacity', *Agvise Laboratories*, Jul. 31, 2012. <https://www.agvise.com/educational-articles/water-holding-capacity/> (accessed Jan. 21, 2021).
- [70] 'Capillary Forces', in *Theoretical Soil Mechanics*, John Wiley & Sons, Ltd, 1943, pp. 297–308.
- [71] 'Water Movement in Soils — Welcome'. <http://www.soilphysics.okstate.edu/software/water/infil.html> (accessed Jan. 04, 2021).
- [72] B. W. Bache, 'E. C. Childs. An Introduction to the Physical Basis of Soil Water Phenomena. Wiley-Interscience, London, 1969. xiii + 493 pp. Price £6.', *Clay Minerals*, vol. 8, no. 2, pp. 239–240, Dec. 1969, doi: 10.1180/claymin.1969.008.2.13.
- [73] D. Cuadrado and N. Pizani, 'Identification of microbially induced sedimentary structures over a tidal flat', *Latin American journal of sedimentology and basin analysis*, vol. 14, pp. 105–116, Dec. 2007.